

# **Protection Schemes & Optimal Relay Co-ordination for RE Integrated Power Distribution Grid**

A thesis submitted to the  
University of Petroleum & Energy Studies

For the Award of  
**DOCTOR OF PHILOSOPHY  
IN  
ELECTRICAL ENGINEERING**

By  
**Aayush Shrivastava**

**DECEMBER 2020**

**SUPERVISOR (s)**  
**DR. DEVENDER KUMAR SAINI**  
**DR. MANJAREE PANDIT**



**DEPARTMENT OF ELECTRICAL & ELECTRONICS ENGINEERING  
SCHOOL OF ENGINEERING  
UNIVERSITY OF PETROLEUM AND ENERGY STUDIES  
DEHRADUN- 248007: (UTTRAKHAND)**

# **Protection Schemes & Optimal Relay Co-ordination for RE Integrated Power Distribution Grid**

A thesis submitted to the  
University of Petroleum & Energy Studies

For the Award of  
**DOCTOR OF PHILOSOPHY  
IN  
ELECTRICAL ENGINEERING**

Submitted By: -  
**AAYUSH SHRIVASTAVA  
(SAP ID: 500049145)**

**DECEMBER 2020**

Under the Guidance of: -

**Internal supervisor**  
**DR. DEVENDER SAINI**  
**ASSISTANT PROFESSOR- SG**  
**DEPARTMENT OF ELECTRICAL & ELECTRONICS ENGINEERING,**  
**UNIVERSITY OF PETROLEUM & ENERGY STUDIES, DEHRADUN**

**External supervisor**  
**DR. MANJAREE PANDIT**  
**PROFESSOR**  
**DEPARTMENT OF ELECTRICAL ENGINEERING,**  
**MITS, GWALIOR**



**DEPARTMENT OF ELECTRICAL & ELECTRONICS ENGINEERING**  
**UNIVERSITY OF PETROLEUM AND ENERGY STUDIES**  
**DEHRADUN- 248007: (UTTRAKHAND)**

## CERTIFICATE

This is to certify that the thesis titled “Protection Schemes & Optimal Relay Co-ordination for RE Integrated Power Distribution Grid” submitted by Aayush Shrivastava (SAP ID: 500049145) in Partial completion of the requirements for the award of the Degree of Doctor of Philosophy (Engineering) is carried out by him under our joint supervision and guidance. It is certified that this thesis has not been submitted anywhere else for the award of any other diploma or degree of this or any other University.

**DR. DEVENDER KUMAR SAINI**

PROFESSOR

DEPARTMENT OF ELECTRICAL & ELECTRONICS

UNIVERSITY OF PETROLEUM & ENERGY STUDIES, DEHRADUN

**CORPORATE OFFICE:** 210, 2<sup>nd</sup> Floor,  
Okhla Industrial Estate, Phase III,  
New Delhi - 110 020, India.  
T: +91 11 41730151/53, 46022691/5  
F: +91 11 41730154

**ENERGY ACRES:** Bidholi Via  
Prem Nagar, Dehradun - 248 007  
(Uttarakhand), India.  
T: +91 135 2770137, 2776053/54/91, 2776201  
F: +91 135 2776090/95

**KNOWLEDGE ACRES:** Kandoli Via  
Prem Nagar, Dehradun - 248 007  
(Uttarakhand), India.  
T: +91 8171979021/2/3, 7060111775



# MADHAV INSTITUTE OF TECHNOLOGY & SCIENCE, GWALIOR

(A Govt. Aided UGC Autonomous & NAAC Accredited Institute Affiliated to RGPV, Bhopal, M.P.)

Gola ka Mandir, Gwalior (M.P.)- 474 005, INDIA

Ph.: +91-751-2409300, Fax: +91-751-2664684, e-mail: director@mitsgwalior.in, website: www.mitsgwalior.in

## CERTIFICATE

This is to certify that the thesis titled “**Protection Schemes & Optimal Relay Co-ordination for RE Integrated Power Distribution Grid**” submitted by Aayush Shrivastava (SAP ID: 500049145) in Partial completion of the requirements for the award of the Degree of Doctor of Philosophy (Engineering) is carried out by him under our joint supervision and guidance.

It is certified that this thesis has not been submitted anywhere else for the award of any other diploma or degree of this or any other University.

*M. Pandit*  
02/12/2020.

**DR. MANJAREE PANDIT (CO-GUIDE)**

PROFESSOR

DEPARTMENT OF ELECTRICAL ENGINEERING

MADHAV INSTITUTE OF TECHNOLOGY & SCIENCE, GWALIOR

## **ABSTRACT**

In recent years, significant contribution of the renewable power (RP) in power grids has been observed. In fact, it keeps on increasing at a high rate. High contribution of the RP, creates the protection issue in the network due to abrupt change in fault current level. The rise of fault current requires an immediate action of the circuit breaker in order to interrupt the power supply. This fault current surpasses the rated capacity of the circuit breaker which ultimately not able to give the required performance as needed. The circuit breaker (CB) and protection devices of distributed system network needs to get upgrade when RP contribution increases above a threshold. All the critical protection issue initiates as penetration level of DGs increases in the distribution system. Some of these critical issues are; Alter the power flow, Overvoltage on distribution feeders, Power Quality dilemmas, Enhanced Reactive power, Relay miscoordination.

In the present study, a protection scheme has created to deal with all the complex situations that arises on integration of distributed generation power plants and solar PV, into the distribution network.

The analysis of the results obtained show that when solar PV and DGs are integrated, fault current rises whereas the power losses get minimized at the grid. Voltage profile improves at some points while at some buses it decreases. Third harmonic distortion (THD) increases at certain level. The rise of fault current causes mal-functioning of over current relays. To overcome these issues two protection schemes, adaptive protection scheme and hybrid protection scheme are proposed.

There are many different forms by which the DGs are connected to the distribution grid. The aim of the proposed protection schemes is to ensure that if the primary protection scheme is unable to deliver the result, the backup protection scheme would deal with the situation. In the present analysis, non-adaptive protection scheme act as primary protection scheme whereas adaptive protection scheme act as backup protection scheme. This switching from one safety scheme to another often depends upon the maximum and minimum limits of constraints, such as maximum value of fault current, FCL impedance and coordination time interval of relays.

The analysis presented further proved that the proposed adaptive protection scheme for IEEE node 3 system is capable in providing effective results. MATLAB simulation results of

protection schemes are validated using ETAP simulated results. TCC graphs which proves that protection scheme results are capable to handle complex situation when large number of DGs penetrated into the grid.

In the present work four different optimization algorithms are used to adjudge their suitability in getting the appropriate results. The algorithms are GA, PSO, Interior point, SQP algorithms. It is found that SQP algorithm take minimum iteration to reach a feasible solution and PSO take minimum computation time to reaches the feasible results. It is concluded that for relay protection PSO algorithm is more suitable then others.

The hybrid protection scheme is developed and applied to the integration of solar PV with the DG. The results obtained show that this scheme is more versatile as it can handle every complex situation of DGs penetration. This protection scheme tested on IEEE 13 & 33 node test feeders. Testing is carried out in two parts. In first part the testing of non-adaptive protection scheme which is based on optimization of Impedance based fault current limiter. In second part and testing of adaptive protection scheme. The optimization algorithms used during testing are Greywolf optimization (GWO), hybrid Greywolf, particle swarm optimization & Interior point algorithm. The results of protection scheme found that both part of hybrid protection scheme is capable to handle every complex situation of DGs penetration.

The analysis of results obtained using different optimization algorithms, it is found that GWO algorithm is better than all other applied algorithms. GWO takes less computation time which is the vital requirement of fast protection schemes. It is also identified that result obtained through all algorithms are relevant for over-current relay. Results obtained from different optimization algorithms are also validated using the results of reported tools which confirms the authenticity of the results obtained during the course of the present investigation.

### **Plan of the Thesis**

Now a days the use of non-conventional energy is increasing day by day. Through various nonconventional sources are available but the use of solar energy is preferred. This source of energy is available everywhere and can be easily be tapped by an individual. The power generated through solar energy can be coupled with the power available from conventional sources. There are some critical issues comes in picture when the power generated from Renewal sources is coupled with the power available from other sources. This coupling is done at micro grids. How these issues arise and how they are to be tackled when coupling of energy

from two different sources took place at micro grids are discussed in the present investigation. The entire work reported in the thesis is divided in different chapters. There are six chapters in the thesis. The details of each of these chapters are as follows.

**Chapter I** contains the basic *Introduction of the problem* taken into consideration in present investigation. Brief idea of Micro grids, Renewal power sources, Solar PV, DGs, DOCR and FCL are given in this chapter. How the solar PV and DGs are integrated, precaution to be considered in such integration and how the factors affecting the power transmission to be minimized are discussed in this chapter. Earlier work done in this direction is also revived to give firm basis to the problem. The objectives of the thesis are also mentioned at the end of this chapter.

**Chapter two** is devoted to the *Review of Various Algorithms* developed earlier to solve various issues. The applicability and drawbacks of these algorithms are mentioned. It is concluded that each algorithm is developed on the basis of various natural activities of different living entities. Looking at the severity of the problems, these algorithms are modified. A comparative picture of applicability and outcomes of these algorithms are given in this chapter. It is reported that all the algorithms are not suitable for each problem, instead for each problem different algorithms have to be developed.

**Chapter three** contains the details of the proposed *Optimal Relay Coordination Model*. Its objective function, optimization of impedance fault current limiter, constraint for over current and distributed generation protection monitoring index are all beautifully explained in this chapter.

**Chapter four** is devoted to the *Optimization Algorithms* used to solve the problems related to the optimal relay coordination model. These are PSO, GWO, and Hybrid GWO-PSO, Interior point algorithms which are used to solve ORC model. To solve the problems MATLAB *fmincon* function is used.

**Chapter five** contains the *Adaptive Protection Schemes* for obtaining relay coordination for IEEE node 3. The adaptive and hybrid protection schemes are described in this chapter. Considering the flowchart which defines the process of relay setting variation SPV is continuously monitored. The observation process is carried out on 3 node feeders using MATLAB platforms. The setting of the relay is changed as per the SPV status. It is reported

that hybrid protection scheme, being flexible have increased reliability. Various steps are involved in this protection scheme algorithm.

**Chapter Six** is devoted to the *Result & discussion*. Results obtained on implementing the all the four algorithms viz. PSO, GWO, and Hybrid GWO-PSO, Interior point are presented in this **chapter**. These algorithms were applied on IEEE node 3 and IEEE node 13,33. The results related to load flow, impact of solar PV integration on distribution grid, power loss, power factor, THD, voltage and current harmonic distortion with and without filter and impact of solar PV on short circuit current. The Relay coordination solution for IEEE 13 & 33 node solar PV integration distribution grid using DOCR is also described. The impedance fault current limiter optimization using GWO and GWO-PSO for IEEE 13 & 33 node is also measured. It is observed that SQP takes less time to converge and all algorithms is capable to obtain the optimized results for optimal relay Coordination model. GWO algorithm is found superior in all applied algorithms because of less computational time. The hybrid algorithm results are also found effective as they can also be validated using the ETAP results.

**Chapter Seven** is devoted to the *Conclusion* of overall results outcome and future scope of regarding the protection is also discussed.



## ACKNOWLEDGEMENT

I am very much grateful to God Almighty for without his graces and blessings this study would have not been possible. His mercy was with me throughout my student life and ever more in this study. I thank him for giving me the strength and patience to work through all these years so that today I can stand proudly with my head held high.

The work presented in this thesis would not have been possible without my close association with many people. I take this opportunity to extend my sincere gratitude and appreciation to all those who made this Ph.D. thesis possible.

First and foremost, I would like to extend my sincere gratitude to my research *supervisor* **Dr. Devender Kumar Saini, Assistant Professor (SG), UPES, Dehradun (UK)**, for introducing me to this exciting field of electrical engineering and for his dedicated help, advice, inspiration, encouragement and continuous support during the course of my Ph.D. work. I owe him lots of gratitude for having me shown this way of research. I could not have imagined having a better advisor and mentor than him for my Ph.D. study. I am indebted to you sir more than you know.

I record my deep sense of gratitude to my *Co-supervisor* **Dr. Manjaree Pandit**, Professor of Electrical Engineering, MITS Gwalior for her guidance, continuous suggestions in directing me to join the research. I sincerely express my deep sense of gratitude for her affection, support and encouragement during the course of this investigation.

I am grateful to the Vice chancellor, UPES, Dehradun for providing the necessary facilities for completing the work in the department. I am very much thankful to all Professors of the Department of Electrical & Electronics Engineering UPES Dehradun for their valuable suggestions, affection and encouragements that I got during my Ph.D. work.

I also express my sincere thanks to Dr. Kamal Bansal, Dean & Associate Dean SOE, Dr. J. K. Pandey and Dr. Shubhobhan Chowdary, Head, Department of Electrical & Electronics Engineering, UPES for their moral and academic support throughout this investigation. I cannot forget my fellow research scholars Debjoyti Bose, whose all-round help was really a great boon to me in completion of this work. I express my heartfelt thanks to all of them.

I am really thankful to Raj Gaurav Mishra, UPES as it was only him who encouraged me come in the field of research.

I am also thankful to Technical and Laboratory supporting staff of the Department of Electrical & Electronics Engineering, U.P.E.S. Dehradun, especially Mr. Rohit Sharma for their cooperation and facilitating the infrastructure and lab facilities during my stay in the department for this work.

I sincerely acknowledge the financial support provided by University of petroleum and energy studies, Dehradun which was a backbone to me during the course of present investigation.

I am highly indebted to my parents and other family members for extending every possible support with great inspiration and numerous blessings towards me. Finally, I thank one and all, which have contributed and helped me directly or indirectly in bringing this **Thesis** to a successful completion.

(Aayush Shrivastava)

## CONTENT TABLE

<b>Chapter no.</b>	<b>CONTENT</b>	<b>Page no..</b>
	<b>Declaration</b>	<b>i</b>
	<b>Certificate</b>	<b>ii</b>
	<b>Abstract</b>	<b>iii</b>
	<b>Acknowledgement</b>	<b>vi</b>
	<b>Content table</b>	<b>vii</b>
	<b>List of tables</b>	<b>xii</b>
	<b>List of figures</b>	<b>xiv</b>
	<b>List of symbols</b>	<b>xvi</b>
<b>1</b>	<b>Introduction</b>	<b>1</b>
	<b>1.1. Thesis Objectives</b>	<b>5</b>
	<b>1.2. Plan of thesis</b>	<b>5</b>
<b>2</b>	<b>Literature Review</b>	<b>8</b>
	<b>2.1. Optimization techniques used for optimal relay coordination</b>	<b>9</b>
	<b>2.1.1. Firefly algorithm (FFA)</b>	<b>10</b>
	<b>2.1.2. Genetic algorithm (GA)</b>	<b>11</b>
	<b>2.1.3. Differential algorithm (DE)</b>	<b>14</b>
	<b>2.1.4. Modified differential algorithms (MDE)</b>	<b>15</b>
	<b>2.1.5. Ant colony optimization (ACO)</b>	<b>17</b>
	<b>2.1.6. Ant lion optimization (ALO)</b>	<b>19</b>
	<b>2.1.7. Cuckoos search algorithm (CSA)</b>	<b>20</b>
	<b>2.1.8. Modified cuckoos search optimization (MCSO)</b>	<b>21</b>
	<b>2.1.9. Gravitational search optimization (GSO)</b>	<b>23</b>
	<b>2.1.10. Stochastic Fractal search algorithm (SFSA)</b>	<b>24</b>
	<b>2.1.11. Whale Optimization Algorithm (WOA)</b>	<b>24</b>
	<b>2.1.12. Water cycle optimization</b>	<b>26</b>

	2.1.13. Modified Water cycle algorithm (MWCA)	27
	2.1.14. Particle swarm optimization (PSO)	28
	2.1.15. Modified particle swarm optimization (MPSO)	29
	2.1.16. Grey wolf optimization (GWO)	31
	2.2. Fault current limiter along with optimal relay coordination	32
	2.3. Conclusion	35
3	Optimal relay coordination model	36
	3.1. Introduction	36
	3.1.1 Objective function for relay coordination	37
	3.1.2 The constraint for the overcurrent relay coordination model	38
	3.1.3 Optimization of impedance fault current limiter ( $Z_{FCL}$ )	38
	3.1.4 Distributed generation protection monitoring index (DGPMI)	39
4	Optimization algorithms used for solving optimal relay coordination model	40
	4.1 Particle Swarm Optimization for solving ORC	40
	4.2 Grey wolf optimization for solving ORC	42
	4.3 Hybrid GWO-PSO for solving ORC	43
	4.4 Interior point algorithm for solving ORC model	44
5	Adaptive Protection Schemes for obtaining optimal relay Coordination for IEEE node 3	46
	5.1. Adaptive protection scheme	46
	5.2. Hybrid protection scheme for optimal relay coordination	47
6	Result & Discussion	50
	6.1 IEEE node 3 model	50
	6.1.1. IEEE 4 bus system modelling along with SPP integration	50
	6.1.2. Impact of solar PV on distribution grid IEEE node 3 feeder	55
	6.1.2.1. Grid voltage deviation when solar photovoltaic source is connected	55

6.1.2.2. Frequency calculation of solar photovoltaic connected cases in IEEE node 3 network.	57
6.1.2.3. Current Calculation of Solar photovoltaic connected cases	59
6.1.3. Optimal Relay Setting	60
6.1.4. Validation of results for adaptive algorithm for IEEE 4 bus system.	63
6.2. IEEE node 13	69
6.2.1 IEEE 13 node grid parameter variation analysis	69
6.2.1.1 Load flow	70
6.2.1.2. Impact of solar PV DGs on IEEE 13 node distribution grid voltage.	73
6.2.1.3 Impact of solar PV plant on distribution grid power losses.	75
6.2.1.4 Impact on power factor concerning with solar PV.	75
6.2.1.5 THD (Total harmonic distortion)	76
6.2.1.6 Solar PV impact on short circuit current	83
6.2.2. Relay coordination solution for IEEE 13 node Solar PV integration distribution grid	85
6.2.2.1. Impedance Fault current limiter (Zfcl) optimization using GWO & GWO-PSO for IEEE 13 node	86
6.2.3. Results validation for hybrid protection scheme for IEEE 13 node.	93
6.3 IEEE 33 node	96
6.3.1. Impact of solar PV DGs on IEEE 33 node distribution grid	96
6.3.1.1. Impact on fault current of IEEE 33 node distribution grid	97
6.3.1.2. Impact on voltage of IEEE 33 node distribution grid	97
6.3.2. Relay Coordination solution for IEEE 33 node distribution grid using hybrid protection scheme	98

	<b>6.3.2.1. Impedance Fault current limiter (Zfcl) optimization using Grey wolf optimization &amp; Hybrid GWO-PSO</b>	<b>103</b>
	<b>6.3.2.2. Relay TMS optimization using Grey wolf optimization &amp; Hybrid GWO-PSO, Interior point algorithm</b>	<b>106</b>
	<b>6.3.3. Result validation for IEEE 33 node</b>	<b>107</b>
<b>7</b>	<b>Conclusion and recommendation for future work</b>	<b>110</b>
	<b>7.1 Conclusion</b>	<b>110</b>
	<b>7.2 Future scope</b>	<b>112</b>
	<b>References</b>	<b>113</b>
	<b>List of Publications</b>	<b>130</b>

## LIST OF TABLES

Table No.	TABLE NAME	Page no..
2.1	Review of Firefly algorithm for identification of ORC	11
2.2	Review of Genetic algorithm for identification of ORC.	13
2.3	Review of Differential Evolution (DE) algorithms and Modified DE for identification of ORC	16
2.4	Review of ant colony optimization (ACO) algorithms and Modified DE for identification of ORC	18
2.5	Review of Cuckoos search algorithms for identification of ORC	22
2.6	Review of GSA algorithms for identification of optimal relay coordination problem.	23
2.7	Review of Whale optimization algorithms (WAO), Fractal search algorithm & water cycle optimization for identification of ORC	25
2.8	Review of particle swarm optimization and modified particle swarm optimization & Grey wolf optimization for identification of ORC	30
2.9	Review of FCL used for solving the ORC problem	34
6.1	Solar PV parameters used in simulation	51
6.2	List of cases taken for solar photovoltaic integrated 4 buses System	51
6.3	Voltages of each bus for IEEE 4 bus system in Various Cases (RMS)	56
6.4	Current of each bus for IEEE 4 bus system in Various Cases (RMS)	56
6.5	Fault current calculation through Simulink MATLAB	59
6.6	TMS values for various cases (PSO)	61
6.7	Results of primary and backup relay tripping time for various cases.	62
6.8	Result comparison with PSO, GA, SQP, interior point algorithms	63
6.9	Result comparison with ETAP for Case 1	64
6.10	Comparison of results with ETAP for Case 6.	65
6.11	Level of solar PV penetration data for IEEE 13 node	72
6.12	Solar PV panel parameters data for IEEE 13 node	72
6.13	Voltage at each bus of all six cases	75
6.14	Total voltage harmonic distortion (THD) for each level of penetration	79

<b>6.15</b>	<b>Total current harmonic distortion (THD) for each level of penetration</b>	<b>80</b>
<b>6.16</b>	<b>Analysis of fault current for each solar PV penetration case.</b>	<b>83</b>
<b>6.17</b>	<b>Zfcl size optimization for IEEE Node 13 Using GWO for IEEE 13 node</b>	<b>88</b>
<b>6.18</b>	<b>Optimization of Zfcl parameters using GWO-PSO algorithm for IEEE 13 node</b>	<b>89</b>
<b>6.19</b>	<b>Relay TMS optimization for IEEE Node 13 Using Interior point algorithm</b>	<b>90</b>
<b>6.20</b>	<b>Relay TMS optimization for IEEE Node 13 Using GWO algorithm</b>	<b>91</b>
<b>6.21</b>	<b>Relay TDS optimization for IEEE Node 13 Using GWO-PSO algorithm</b>	<b>92</b>
<b>6.22</b>	<b>Result validation of non-adaptive protection scheme result.</b>	<b>93</b>
<b>6.23</b>	<b>Results validation of adaptive protection scheme result.</b>	<b>94</b>
<b>6.24</b>	<b>Optimized Zfcl parameters using GWO-PSO algorithm for IEEE 33 node</b>	<b>99</b>
<b>6.25</b>	<b>Optimized Zfcl parameters using GWO algorithm for IEEE 13 node</b>	<b>101</b>
<b>6.26</b>	<b>Relay TMS parameter optimization using GWO algorithm</b>	<b>104</b>
<b>6.27</b>	<b>Relay TMS parameter optimization using hybrid GWO-PSO algorithm</b>	<b>105</b>
<b>6.28</b>	<b>Relay TMS parameter optimization using hybrid Interior point algorithm</b>	<b>106</b>
<b>6.29</b>	<b>Result validation of non-adaptive protection scheme result.</b>	<b>107</b>
<b>6.30</b>	<b>Results validation of adaptive protection scheme result.</b>	<b>107</b>

## LIST OF FIGURES

Figure no..	Name of figure	Page no..
4.1	Flowchart for PSO	41
5.1	Protection scheme for dynamic relay parameter changes	47
5.2	Hybrid protection scheme (Combination of Adaptive & Non adaptive protection scheme)	49
6.1	Simulation model of solar photovoltaic integrated 4 bus systems	53
6.2	Simulation of solar photovoltaic plant (SPP) with include MPPT	54
6.3	Voltage comparison between case 1 and case 6 at bus 4	55
6.4	Frequency calculation for the solar photovoltaic connected model (Phase A)	57
6.5	Frequency calculation for the solar photovoltaic connected model (Phase B)	58
6.6	Frequency calculation for the solar photovoltaic connected model (Phase C)	58
6.7	Comparison of all optimization algorithms (GA,PSO,Interior point,SQP)	65
6.8	TCC graph for solar connected case (111) with old setting of relay	66
6.9	ETAP time current characteristics of relay (TCC) for result validation of TMS	67
6.10	Relay TCC graph and coordination for fault location at B	68
6.11	Integration of solar PV at node 675,680,634 in IEEE 13 node feeder	73
6.12	Percentage bus voltage rise at bus 634,675,680 when solar PV integrated with the network	73
6.13	Active & reactive power losses for each case of solar PV penetration.	74
6.14	Power factor variation at each line and bus concerning solar PV penetration	76
6.15	voltage waveform for bus 634 when solar PV contribution is 0%	78
6.16	Voltage waveform for bus 634 when solar PV contribution is 80%	78
6.17	Voltage spectrum showing harmonics at a different frequency for bus 634 without using the filter	81
6.18	Voltage spectrum after using the filter at bus 634	81



<b>6.19</b>	<b>Graphical analysis of voltage THD at every penetration level</b>	<b>82</b>
<b>6.20</b>	<b>Graphical analysis of current THD at every penetration level</b>	<b>82</b>
<b>6.21</b>	<b>Fault current analysis for IEEE 13 node distribution feeder</b>	<b>84</b>
<b>6.22</b>	<b>Representation of Zfcl fault current minimization for IEEE 13 node</b>	<b>87</b>
<b>6.23</b>	<b>Zfcl parameter optimization convergence graph for GWO &amp; GWOPSO algorithm (IEEE node 13)</b>	<b>94</b>
<b>6.24</b>	<b>GWO, Interior point &amp; GWO-PSO Convergence graph for TMS optimization (IEEE 13 node)</b>	<b>95</b>
<b>6.25</b>	<b>IEEE 33 node model along with Solar DGs &amp; relay location representation.</b>	<b>96</b>
<b>6.26</b>	<b>Fault current variation at every bus for each PV penetration case</b>	<b>97</b>
<b>6.27</b>	<b>Bus voltage representation for all PV penetration cases</b>	<b>98</b>
<b>6.28</b>	<b>Representation of Zfcl fault current minimization for IEEE 33 node</b>	<b>103</b>
<b>6.29</b>	<b>Representation of Zfcl fault current minimization for IEEE 33 node</b>	<b>108</b>
<b>6.30</b>	<b>GWO, PSO convergence graph for optimizing relay TMS value for IEEE 33 node</b>	<b>108</b>

## LIST OF SYMBOLS & ABBREVIATION

Name of symbols/Abbreviation	Symbols /Abbreviation
Distributed Sustainable Energy Generation	DSEG
Fault Current Limiter	FCL
Directional over current relays	DOCR
Time dial setting	TDS
Coordination time interval	CTI
Plug setting multiplier	PSM
Distributed generation	DGs
Particle swarm algorithm	PSO
Hyper-sphere search algorithm	HSS
Genetic algorithm	GA
Fire fly algorithm	FFA
adaptive modified fire fly algorithm	AMFFA
Improved firefly algorithm	IFA
Inductive fault current limiter	FLC
Modified fire fly algorithm	FFA
Differential algorithm	DE
Modified differential algorithms	MDE
Adaptive differential evolution	ADE
Discrete differential algorithm	IDA
Ant colony optimization	ACO
Ant lion optimization	ALO
Cuckoos search algorithm	CSA
Modified cuckoos search optimization	MCSO
Gravitational search optimization	GSO
Stochastic Fractal search algorithm	SFSA
Whale Optimization Algorithm	WOA

<b>Whale optimization</b>	<b>WAO</b>
<b>Hybrid GWO &amp; whale optimization algorithms</b>	<b>HWGO</b>
<b>Water cycle algorithm</b>	<b>WCA</b>
<b>Modified Water cycle algorithm</b>	<b>MWCA</b>
<b>Modified particle swarm optimization</b>	<b>MPSO</b>
<b>Linear Interior Point Solver</b>	<b>LIPSOL</b>
<b>Hybrid PSO &amp; LP</b>	<b>HPSO</b>
<b>Nelder-Mead PSO</b>	<b>NM-PSO</b>
<b>PSO with inertia weight</b>	<b>PSOG</b>
<b>Local version of PSO with inertia weight</b>	<b>PSOL</b>
<b>Global version PSO with constriction factor</b>	<b>PSOGC</b>
<b>Local version PSO with constriction factor</b>	<b>LPSOGC</b>
<b>chaotic PSO</b>	<b>CPSO</b>
<b>Restore relay coordination using FCL</b>	<b>RRCUF</b>
<b>semiconductor-based fault current limiter</b>	<b>SFCL</b>
<b>Reference</b>	<b>Ref</b>
<b>Number of relays connected</b>	<b>i</b>
<b>Operating time for the relay</b>	<b>t.</b>
<b>cumulative operating time of relays</b>	<b>K</b>
<b>Backup relay operating time</b>	<b>T<sub>b</sub></b>
<b>Operation time of primary relay</b>	<b>T<sub>p</sub></b>
<b>Relay constants</b>	<b>a,b,α</b>
<b>Plug setting multiplier</b>	<b>M</b>
<b>minimum operating time of the relay</b>	<b>T<sub>i</sub></b>
<b>maximum operating time of the relay</b>	<b>T<sub>max</sub></b>
<b>Coordination time interval</b>	<b>TBP</b>
<b>Rain drop</b>	<b>X<sub>1</sub>,X<sub>2</sub></b>
<b>Rain drop cost constant</b>	<b>F</b>

<b>Number of streamers flow</b>	<b>NSn</b>
<b>River position</b>	<b>X<sub>river</sub></b>
<b>Streamer position</b>	<b>X<sub>Streamer</sub></b>
<b>Scaling factor</b>	<b>C</b>
<b>Constant factor</b>	<b>C<sub>1</sub>,C<sub>2</sub></b>
<b>Random population</b>	<b>R<sub>1</sub>,R<sub>2</sub></b>
<b>Best position of swarm</b>	<b>P<sub>best</sub></b>
<b>Global best position of swarm</b>	<b>G<sub>best</sub></b>
<b>Maximum value of time multiplier setting</b>	<b>TMS<sub>MAX</sub></b>
<b>Minimum value of TMS</b>	<b>TMS<sub>Min</sub></b>
<b>Total operation time of relay</b>	<b>K</b>
<b>Weight factor</b>	<b>w</b>
<b>Operating time of relay</b>	<b>t</b>
<b>Relay &amp; Zfcl number</b>	<b>i</b>
<b>Coordination time interval</b>	<b>Δt , CTI</b>
<b>Backup relay tripping time</b>	<b>t<sub>b</sub></b>
<b>Primary relay tripping time</b>	<b>t<sub>p</sub></b>
<b>Time multiplier setting</b>	<b>TMS</b>
<b>Relay constants</b>	<b>a , b , α</b>
<b>Plug multiplier setting</b>	<b>M</b>
<b>Short circuit current</b>	<b>I<sub>SC</sub></b>
<b>Pick up current of relay</b>	<b>I<sub>pickup</sub></b>
<b>Minimum relay tripping time</b>	<b>T<sub>i</sub><sup>Min</sup></b>
<b>Maximum relay tripping time</b>	<b>T<sub>i</sub><sup>Max</sup></b>
<b>Relay tripping time</b>	<b>T</b>
<b>Total impedance of Zfcl connected in network</b>	<b>Z</b>
<b>Impedance of fault current limiter</b>	<b>Z<sub>fcl</sub></b>

<b>Minimum fault current limiter impedance</b>	$Z_{FCL}^{Min}$
<b>Maximum fault current limiter impedance</b>	$Z_{FCL}^{Max}$
<b>Distributed generation protection monitoring index</b>	$DGPMI$
<b>Fault current limiter reactance</b>	$X_{fcl}$
<b>Line to line voltage</b>	$V_{Line\ to\ line}$
<b>Short circuit current after FCL connected</b>	$I_{scA}$
<b>Short circuit current before FCL connected</b>	$I_{scB}$
<b>Represent the vector position of food</b>	$X_{P1}$
<b>indicates the vector position of the grey wolf</b>	$X$
<b>Group of wolves</b>	$\delta, \beta, \omega$
<b>Coefficient vectors</b>	$A \ \& \ C$
<b>Scaling factor</b>	$c$
<b>Constant factor</b>	$C_1, C_2$
<b>Random population</b>	$R_1, R_2$
<b>Best position of swarm</b>	$P_{best}$
<b>Global best position of swarm</b>	$G_{best}$
<b>Lower bond</b>	$LB$
<b>Upper bond</b>	$UB$
<b>Equivalent constraint</b>	$A_{eq}$
<b>Nonlinear constrain</b>	$C_{eq}$

## CHAPTER – 1

### INTRODUCTION

Our country is facing major challenges in different fields. Some of them are (a) To provide energy access to all its citizens, (b) Heavy dependence on fuel imports for energy security, and (c) keeping the economic and social development at foremost priority, to comply the international protocols on climate change mitigations. The increase in energy demand due to growing population, industrialization and depleting fossil fuel resources has stimulated our country's efforts in adopting power generation from renewable energy sources. In 2002, the contribution of power generated from renewal sources was 0.34 GW (2%) out of 17 GW of country's total installed capacity. In 2014 it has reached to 31.7 GW (12.5%) of 250 GW of country's total installed capacity. Today in the field of renewable power generation, our country occupies fifth position. The government policies are steadily encouraging the adoption of renewable energy power generation. In fact there is a need of more vigorous engagement of each individual country to achieve or produce more power to fulfil the need of energy of all citizens along with the countries' economic development. In this context the renewable energy sources (RES) are regarded as an alternative means to fulfil the future energy demand of the world. Now a days, the exploitation of RES is increasing exponentially. As per Ministry of New and Renewable Energy (MNRE) data, the present contribution of RES in the installed capacity of energy is more than 12.5% and the share of RES is expected to increase further in near future [1].

During the last decade, the micro grids have received considerable attention and have become an essential resource in the power industry. One of the main reasons of micro grid success is their ability to integrate sustainable energy generation practices into the distribution network. Solar and wind energy makes the micro-grid feasible in both, grid and island connection and in reducing the power loss. In order to exploit the full potential of micro grids, various technical challenges are to be tackled. The security is one of them.. Conquering the

protection problems, adaptive protection strategy is one of the most effective solutions for micro grid protection. FCL and relay coordination that minimizes the current of the fault, is also used for protection [1].

Inverse time overcurrent relays are widely used for detecting faulty current values and current directions. These relays are designed to provide a robust redundant safety framework while reducing load interruption[2]. This form of protection scheme made for distribution systems make easy to detach the faulty portion from the remaining healthy portion of the power system. The main goal of various security schemes is to limit the spread of faults. Primary relays protects the distribution lines and feeders [3]. Over current relays are used as main and backup relays for distribution networks. However, their slow operating speed to use as primary protection schemes for sub-transmission systems is not desirable. Distance relays are the preferred alternative, as primary protection for sub-transmission systems and over-current relays are used for back-up relays [4][2]. Such relays uses current and voltage signals to evaluate the magnitude and direction of short-circuit currents, simultaneously. In terms of the clearance time of main and backup relays, the appropriate synchronization of Directional over current relays (DOCR) have always been a dilemma in power systems. Optimum DOCR coordination is typically needed to establish the appropriate relay settings, including the time dial setting (TDS) and plug setting multiplier (PSM). For a given failure, a coordination time interval (CTI) should be considered to eliminate the void between primary and backup relays. Different scientists have examined DOCRs ‘ optimal coordination problem and proposed multiple optimization methods to seek appropriate relay configurations [5]. In some papers, it is suggested to use FCL for restoring relay coordination, instead of disconnecting Distributed Generation (DGs) and re-coordination of the relay [2].

DGs ‘penetration into the power system shifts the degree of fault current seen by the OCRs. This may deteriorate OCRs ‘coordinated behaviour. The time difference between backup and main relays may be below the standard threshold or even the backup OCR can operate improperly before the main OCR. For all countries resetting OCRs is especially tedious in large systems,

the original coordinated process cannot be restored alone in the presence of DGs. Elmitwally *et.al* have used the Fault Current Limiters (FCLs) to keep the directional OCRs synchronized without resetting OCRs, irrespective of DG status [5]. Hamid Javadi *et.al* [2] have proposed a new approach is to restore over-current directional relay coordination using three types of Fault Current Limiters (FCLs). The suggested restoration solution is carried out without modifying the initial relay settings or separating DGs from the distributed system in the case of a fault [2].

High value of RP, creates the protection issue in the network due to abrupt change in fault current level. The rise of fault current requires an immediate action of the circuit breaker in order to interrupt the power supply. This fault current surpasses the rated capacity of the circuit breaker, which ultimately not able to give the required performance as needed. The circuit breaker (CB) and protection devices of distributed system network needs to get upgrade when RP contribution increases above a threshold [6]. The complete renewal and replacement of protection devices are very costly process. Therefore, utilities tend to install fault current limiter (FCL) inside the system, which helps to decrease the transient fault current value at permissible level [7]. All the critical protection issue initiates as penetration level of DGs increases in the distribution system [8] [9][10]. These critical issues are;

- Alter the power flow,
- Overvoltage on distribution feeders,
- Voltage control issue,
- Phase imbalance,
- Power Quality dilemmas,
- Enhanced Reactive power and
- Islanding recognition problem
- Relay malfunctioning

Power quality is a vital factor in the distribution system, which should remain within bounds. The lousy power quality might lead to below ranked and may affect the lifespan of the system equipment. Extensive penetration of RP is a



bonus for higher power demand but might result problematic towards power high-quality issues [11][12].

Intermittent nature of PV and its integration inside a circulation network, creates wavering of voltage and voltage unbalance which are of capricious nature. The significant variation between PV output voltage and bus voltage creates the issues of voltage rise, unbalance loading, flicker in the working system and poor power quality. Therefore, distribution system operator plays a vital role to maintain the grid performance, especially when the massive penetration of solar PV get injected into the system [11][13][14][15][16]. Moreover, extensive integration of PV generators increases the short circuit capacity of the system and total harmonic distortion. The increase in short circuit current & harmonic variations have the straight impact on coordination of protection devices. PV invertors being semiconductor devices are the chief culprits to increase the total harmonics distortion (THD) [17][14]. As per IEEE 519 standards [18] [19], the permissible limit of THD is 20% in the network. If the THD exceeds the permissible value, it can damage the protection device and malfunctioning may occur.

Protection is vital part of the power network and is essential to maintain system healthy. The rise in short circuit level leads to change in the performance of directional over current relay (DOCR) which causes protection mis-coordination. Many techniques are developed to bring down the short circuit current level within the proper functioning limit of the protection scheme. FCL technique is one of them which help to reduce the amount of short circuit current and also to maintain the lifespan of gears [20].

DOCRs are the simplest and cheapest. They are the most difficult to apply as they need quick re-setting as system changes. They are mostly implemented in the distribution network, which is the most dynamic part of the whole power system. Consequently, these dynamic changes affect their sensitivity and selectivity, which cause inappropriate operations. However, as DOCRs need to meet some fundamental requirements of sensitivity, selectivity, reliability and speed, in the present study coordination on a real time basis is proposed. Moreover, the idea is to coordinate DOCRs online which as a result enhances

in meeting the fundamental requirements mentioned above. The use of dynamic algorithm first updates data from the latest changes of the system and then computes load flow and fault analysis in order to obtain input data for the optimization of algorithms. The fault extinction time, correct/false tripping operations of each relay directly impacts the fundamental requirements of sensitivity, selectivity, simplicity and reliability. To maintain the fundamental requirement of dynamic complex network re- setting of relay and fault current limiter is also implemented to achieve the desired relay coordination..

The dynamic online re-setting of DOCRs & fault current limiter parameter as per the need of distribution grid, when DGs penetration impact is becoming high on distribution grid. To maintain the distribution grid healthy, online setting of DOCR and FCL re-setting plays the vital role in network protection due to malfunctioning of the relays.

### ***1.1.Research objectives***

- 1) To analyze the effect of Penetration of renewable DG on protection system of distribution systems.
- 2) To design the hybrid protection scheme with “fault current limiter” for RE integrated power distributed system.
- 3) Enhancement of co-ordination index for design of protection scheme using Con/Eve (Conventional & Evolutionary) technique.
- 4) Validation of the Results on numeric relay protection panel.

### ***1.2.Plan of the Thesis***

Now a days the use of non-conventional energy is increasing day by day. Through various nonconventional sources are available but the use of solar energy is preferred. This source of energy is available everywhere and can be easily be tapped by an individual. The power generated through solar energy can be coupled with the power available from conventional sources. There are some critical issues comes in picture when the power generated from Renewal sources is coupled with the power available from other sources. This coupling is done at micro grids. How these issues arise and how they are to be tackled when coupling

of energy from two different sources took place at micro grids are discussed in the present investigation. The entire work reported in the thesis is divided in different chapters. There are six chapters in the thesis. The details of each of these chapters are as follows.

**Chapter one** contains the basic *Introduction of the problem* taken into consideration in present investigation. Brief idea of Micro grids, Renewal power sources, Solar PV, DGs, DOCR and FCL are given in this chapter. How the solar PV and DGs are integrated, precaution to be considered in such integration and how the factors affecting the power transmission to be minimized are discussed in this chapter. Earlier work done in this direction is also revived to give firm basis to the problem. The objectives of the thesis are also mentioned at the end of this chapter.

**Chapter two** is devoted to the *Review of Various Algorithms* developed earlier to solve various issues. The applicability and drawbacks of these algorithms are mentioned. It is concluded that each algorithm is developed on the basis of various natural activities of different living entities. Looking at the severity of the problems, these algorithms are modified. A comparative picture of applicability and outcomes of these algorithms are given in this chapter. It is reported that all the algorithms are not suitable for each problem, instead for each problem different algorithms have to be developed.

**Chapter three** contains the details of the proposed *Optimal Relay Coordination Model*. Its objective function, optimization of impedance fault current limiter, constraint for over current and distributed generation protection monitoring index are all beautifully explained in this chapter.

**Chapter four** is devoted to the *Optimization Algorithms* used to solve the problems related to the optimal relay coordination model. These are PSO, GWO, and Hybrid GWO-PSO, Interior point algorithms which are used to solve ORC model. To solve the problems MATLAB *fmincon* function is used.

**Chapter five** contains the *Adaptive Protection Schemes* for obtaining relay coordination for IEEE node 3. The adaptive and hybrid protection schemes are described in this chapter. Considering the flowchart which defines the process

of relay setting variation SPV is continuously monitored. The observation process is carried out on 3 node feeders using MATLAB platforms. The setting of the relay is changed as per the SPV status. It is reported that hybrid protection scheme, being flexible have increased reliability. Various steps are involved in this protection scheme algorithm.

**Chapter Six** is devoted to the *Result & discussion*. Results obtained on implementing the all the four algorithms viz. PSO, GWO, and Hybrid GWO-PSO, Interior point are presented in this **chapter**. These algorithms were applied on IEEE node 3 and IEEE node 13,33. The results related to load flow, impact of solar PV integration on distribution grid, power loss, power factor, THD, voltage and current harmonic distortion with and without filter and impact of solar PV on short circuit current. The Relay coordination solution for IEEE 13 & 33 node solar PV integration distribution grid using DOCR is also described. The impedance fault current limiter optimization using GWO and GWO-PSO for IEEE 13 & 33 node is also measured. It is observed that SQP takes less time to converge and all algorithms is capable to obtain the optimized results for optimal relay Coordination model. GWO algorithm is found superior in all applied algorithms because of less computational time. The hybrid algorithm results are also found effective as they can also be validated using the ETAP results.

**Chapter Seven** is devoted to the *Conclusion* of overall results outcome and future scope of regarding the protection is also discussed.

## CHAPTER - 2

### LITERATURE REVIEW

In the optimal relay setting for distribution grid, many optimization techniques are used for calculation of over current relay THD. Atteya *et.al* have solved the problem of relay coordination and proposed *particle swarm algorithm* (PSO). The obtained result were compared with the results obtained using the traditional procedure. It was found that constant variable modification helped to keep all particles with a feasible solution. It is also reported that the PSO is capable of providing the feasible solution and optimal coordination along with satisfying the constraints [21]. S.A Ahmadi *et.al* have used *Hyper-sphere search algorithm* (HSS) and *Genetic algorithm* (GA) to solve the optimal relay coordination model. They compared HSS and genetic algorithm results and finds that HSS coordination results are better than that of genetic algorithms. They have used six bus models to test the coordination [22] . Mohamed Awaad *et.al* have taken into account both adaptive and non-adaptive methods. In adaptive approach, they used different topologies of PG (power grid), PG + All DGs (Distributed generations), islanded, islanded + (n-1) DGs) relay on adaptive relay setting based on the system. It requires multiple SGF (switch group factor) relays. Relay settings can be modified either through communication or without communication [23].

In non-adaptive approach it is necessary to insert an external device such as FCL. Waleed et al have inserted the FCL with the main utility to limit the utility contribution to the fault –when it is connected and thus adjust the relay setting for the fault values of the insulated mode. They have also considered the insertion of FCL with the DG to limit the contribution of DG to the fault by keeping the relay setting without modifications as in the traditional system without DGs. Finally, the purpose of FCL insertion is not to change the relay setting with different configurations [24][9].

### ***2.1. Optimization techniques used for optimal relay coordination***

In the last six decades since the 1960s, many strategies and methods for organizing current relays have been suggested by different workers. These methods can be divided into three groups: trial and error, topological analysis and optimization methods [25][26][27][28][29]. Due to large number of iterations necessary for the appropriate relay setting, the trial and error approach has slow convergence rate [30]. A technique for breaking all loops called breakpoint. It is strongly recommended to locating the beginning of relays at these points to minimize the number of iterations required for the coordination process. Here the crucial part is the starting of coordination process. To evaluate break points, topological methods like functional as well as graph methodologies are used [30]. The solution obtained using this framework is the best alternative settings but is not strictly optimal. In other words, the time setting multiplier (TSM) or time dial (TDS) configurations of the relays are high. In addition, due to the process complexity, the methodology of trial and error and topological analysis takes time. When the distribution system is linked to even more than one source, directional overcurrent relays are the convenient option. Birla et al. in [31] have studied the problem of directional overcurrent relays and proposed solution on the bases of three classifications: Technique in curve fitting, Conceptual graph technique and Technique of optimization. The curve fitting techniques are being used to evaluate the finest data structure where relay element is mathematically designed in polynomial form with curve fitting [32][25]. The second category is the theoretical graphical techniques as defined in [33]. In this technique system structure is used in the analysis of minimal breakpoint data, relay sequence and all primary and backup relays.

Various scientists have proposed the coordination theory of circuit breaker, fuse and relays [34][35]. The outcome of this proposed theory is validated through the curve fitting graph solution. This proposed technique is competent in solving many optimization problems and may outperform other conventional algorithms; where the statistic performance of the firefly algorithm has measured using various stochastic standard test functions against other well-known optimizing algorithms [36][37][38].

### 2.1.1. Firefly algorithm (FFA)

Firefly algorithm is newly established technique of optimization based on the fireflies flashing behaviour, proposed by Xin-She [37]. The FFA has many similarities, both in theory as well as in implementation, with other algorithms that are based on so-called swarm intelligence. The authors have noticed that the firefly algorithm is able to provide optimal results for the best coordination between relays. In comparison to other evolutionary algorithms, the researcher found that the results obtained using this firefly algorithm are the best [39] [40].

In FFA, the main attractiveness function  $\beta$  can be expressed as monotonically decreasing functions as given in equation 2.1, [40]:

$$\beta(r) = \beta_0 e^{-\gamma \cdot r^{pq}} \quad \therefore n \geq 1 \quad (2.1)$$

$$r_{ij} = |X_i - X_j| = \sqrt{\sum_{d=1}^d (x_{id} - x_{jd})^2} \quad (2.2)$$

Where,  $\beta_0$  represents attractiveness at  $r=0$ . The movement of firefly “i” is always towards the brighter firefly “j”,

Here  $d = 1, 2 \dots D$ ;  $D$  is the problem dimension,  $X_i$  and  $X_j$  are the position of firefly,  $r_{ij}$  is the distance between  $X_i$  and  $X_j$ . Kurshaid *et.al.* have proposed an improved version of Improved Firefly Algorithm (IFA) [39]. In this two strategies: self-adaptive weight and learning experience of searching fireflies were added to improve the trade-off between exploitation and exploration. Simulation results clearly depicts that IFA outperforms other metaheuristic algorithms in terms of convergence speed.

An Adaptive Modified Firefly Algorithm (AMFFA) for solving the relay coordination problem was also proposed in literature [41]. The main aim of AMFFA is to overcome the drawback of MFFA & FFA that has slow convergence rate. AMFFA has high convergence behaviour for identification of optimal relay coordination. This modification is done by including the random movement factor of fire fly, controlled by self-adaptive method in the

iterations while running the algorithm. The random movement factor is defined by  $\alpha$ , which changes dynamically as per the equation 2.3.

$$\alpha^F = \alpha^F * \left(\frac{1}{2} * F_{max}\right)^{\frac{1}{F_{max}+1}} \quad (2.3)$$

Here F is defining the iteration value and  $F_{max}$  is defined its maximum iteration value.

**Table 2.1. Review of Firefly algorithm for identification of ORC**

Ref	Bus model	Optimization Techniques	Outcome
[39]	IEEE 6,9 & 30 bus	Firefly algorithm, Improved firefly & whale optimization algorithm	Firefly results found better in terms of convergence speed as well as reaching to an optimal value.
[40]	IEEE 8 bus system	Firefly algorithm	Optimization relay coordination in the presence of Inductive fault current limiter (IFLC) devices. It has found that FFA is capable of obtaining satisfactory results within the define iterations.
[41]	IEEE 2,3,4 bus	Adaptive modified firefly algorithm (AMFFA), Modified firefly algorithm (MFFA), firefly algorithm (FFA), particle swarm optimization (PSO)	The convergence graph of each proposed algorithms validates that AMFFA algorithm gives superior results to among all applied algorithms.

### 2.1.2. Genetic algorithm (GA)

GA is a technique of optimization based on genetics and natural selection principles. GA helps is gathering information about the population of many individuals to develop into a state that maximizes fitness in compliance with unique selection standards. The classical optimization methods have limitations in the search for an optimal global point and are sometimes caught at optimal



local point. In fact the GA is not the conventional single point search method but it is a multipoint search method. Moreover, GA promises to provide the global optimal point [42][43][44]. Philosophically, GA is based on Darwin's theory of "survival of the fittest". In the first phase of GA initial population is generated randomly. Here, the preliminary variables for each relay are chosen randomly. The next step involves the assessment of the fitness benefit in the current generation for each chromosome. The value of fitness, based on the objective function of the primary relay equation (2.4) is described. The GA chooses certain chromosomes and uses them for next generation in order to increase the current population and find an optimum solution proportional to fitness values. Crossover and mutation operators are added to the pair of selected chromosomes in the decision-making space. The cycle is completed after a certain number of decades. The number of generations required varies between systems and depends on the complexity and size of the genetic population of the system.

The problem of malfeasance of current methods requires a rewrite of the simplified objective function ( $K$ ) equation 2.4 [45];

$$K = \alpha_1 \sum_{i=1}^n t_i^2 + \alpha_2 \sum_{i=1,2}^n \Delta t_{BP}^2 \quad (2.4)$$

$$\Delta t_{BP} = t_b - t_p \quad (2.5)$$

Modified objective function for discrete and continuous TMS value can be

written as. 
$$K = \alpha_1 \sum_{i=1}^n t_i^2 + \alpha_2 \sum_{i=1,2}^n (\Delta t_{BP} - \beta_1 (\Delta t_{BP} - |\Delta t_{BP}|))^2 \quad (2.6)$$

**Table 2.2. Review of Genetic algorithm for identification of ORC.**

<b>Ref</b>	<b>Bus model</b>	<b>Optimization techniques</b>	<b>Outcome</b>
[44]	IEEE-4 bus ring main system	Genetic algorithms	GA is capable to obtain the optimized results
[26]	IEEE-8 bus model	Genetic algorithm with Linear programming algorithm	Successfully applied hybrid GA & LP algorithm for solving the ORC model and found this is capable to give the finest results.
[46]	IEEE-4 bus system	Continuous genetic algorithm	Different systems including multi-loop systems have been tested for the continuous GA method, and in all cases, satisfactory results are found.
[45][47]	IEEE-6 bus model	Genetic algorithm	The simple genetic algorithm applied for solving the ORC model and six different GA coefficients used for solving the ORC and found the finest results in all setting of GA.
[48]	IEEE-6 bus	Genetic algorithm	The lowest batter value was given by the GA method compared to the Quasi-Newton method.

[49]	IEEE-6 bus	genetic algorithm	This method enhances the relay coordination and relay operation which help to enhance the efficiency of the relay.
[50]	5 bus ring model	Genetic algorithm	The time coordination approach has been applied effectively to organize the backup relay settings, in violation of the operating principles. GA optimizes the relay setting margins efficiently and minimizes coordination constraint violations.

### 2.1.3. *Differential algorithm (DE)*

Storn has introduced another algorithm known as DE algorithm. This has inspired evolutionary computing, and has proved to be an efficient global optimizer in the field of continuous search [51]. Because of its elegance, robustness and high-speed convergence in algorithm, DE has effectively been applied in several fields of technology, such as power systems, mechanical engineering, communication and trend recognition [52]. DE begins with the random generation of many test vectors, of which some may be enough to solve a specific problem. There are three parameters of control that have a significant effect on the DE optimization performance are population size, scaling factor and crossover frequency. The steps of DE algorithm working are defined in [53].

#### ***2.1.4. Modified differential algorithms (MDE)***

Since it is not possible to overcome all the drawbacks of various optimization algorithm and therefore, stochastic algorithms such as DE must be tailored to solve the given problem [52]. The modern DE has its own drawbacks because DE regulation parameters need to be calibrated. It is assumed that the parameters  $F$ ,  $F1$  and  $F2$  (Scaling factors) remain constant during the entire iterative process. The nature of the problem being discrete in the field. The decision variables need more exploratory ability to perform search effectiveness in the search space. The mutations in the decision variables are strongly influenced by the parameters of control. The adaptive design of the control parameters controls the mutation process so that mutation between random vectors become more prevalent in magnitude when the person shows less change with respect to its previous objective function value. When the individual vectors show progressive habits to reduce, more weightage is given to the mutation regarding the best vector [54]. Unlike traditional DE algorithms, each person in the population (or search space) has its own unique set of control parameters ( $\pi$  and  $F$ ). Therefore, space-varying control parameters contribute to the proposed ADE algorithm's exploration capabilities. This prevents stopping local optima decision variables. Otherwise, stalling is most certain because every single feasible hyperspace search point is densely surrounded by infeasible solutions in the problem of relay coordination [54].

**Table 2.3. Review of Differential Evolution (DE) algorithms and Modified DE for identification of ORC**

<b>Ref</b>	<b>Bus model</b>	<b>Optimization techniques</b>	<b>Outcome</b>
[54]	IEEE 4,3,6 bus system	Adaptive differential evolution (ADE) algorithm, Modified the DE with varying scaling factor. In conventional DE scaling factors consider constants.	ADE algorithm gives better optimum relay time and without the miscoordination compared to other algorithms.
[47]	IEEE 9 bus and 30 bus system	differential algorithm with self-adaptive re-clustering technique and discrete differential algorithm (IDA)	For an optimizing relay coordination problem, IDA with self-adaptive re-clustering technique provides optimum value for the objective function which is comparable to the value obtained by the hybrid GA–NLP.
[55]	IEEE 3,4,6 bus models	Modified differential evolution (MDE) algorithms and five different ways of mutation process used in the research paper.	The absolute weighted disparity between the individual with the highest fitness value and a randomly chosen individual is considered in one MDE scheme. In comparison with all other algorithms, this scheme found the best result.
[56]	IEEE 3,4,6 bus model	chaotic differential evolution algorithm	The scaling factor according to the user's defined probability is generated in this algorithm. The results showed that the proposed algorithms would find superior TDS and PS settings in the IEEE models tested
[57]	IEEE 5 bus system	Differential algorithms	The researcher used the DE algorithm to overcome mixed variables and constraints optimization problems and the tests for effective relay

			coordination have been found to be feasible.
[58]	IEEE 3 & 4 bus model	DE along with new mutation method.	The two main differences between the fundamental DE transformation operation and the schemes proposed are first, Use the absolute difference of the two points as opposed to a simple vector difference and second, Use of the scaling factor Laplace distribution instead of the predefined value. The author found that up to 50 percent improvement in the convergence rate compared to the basic DE

### 2.1.5. *Ant colony optimization (ACO)*

Ant Colony Optimization (ACO) algorithms are used to construct solutions for constraint-based optimization problems by using the so-called pheromone model. A pheromone model is a set of numeric values, called pheromones, that depend on the algorithm's search experience [59]. Pheromone model serves as a basis for the solution development of high-quality solutions for the search areas. The advantage of a mixed ACO approach for the model coordination problem is that it provides better solutions for the actual systems.

The Ant Colony Optimization (ACO) algorithm uses ant forging actions to find the optimal solution to a problem. Food forages tend to spread throughout a region to speed up the process. When travelling, every ant secretes pheromones to show that this route was investigated. If the ant sees the source of the food the trails overlap thus increasing the concentration of the pheromones for that trajectory. As further ants pursue the track with the highest concentration of the pheromone, the pheromone on the other tracks evaporates over the time. So, the best direction is clearly seen. Thus, ACO was used for discrete problems in the traditional way. Work is carried out in order to optimize constrained equations in the continuous sector. In order to address problems in the continuous domain, the ACO algorithm was developed.

The following are the functional steps of ACO [60][61];:

- 1) Codification
- 2) Construction of a solution
- 3) ACOMV Parameters
  - A. Continuous variable
  - B. Categorical variable

**Table 2.4. Review of ant colony optimization (ACO) algorithms and Modified DE for identification of ORC**

Ref	Bus model	Optimization techniques	Outcomes
[61]	IEEE 14 bus	Ant colony optimization	ACO-based adaptive safety strategy was suggested by the author & Identified the improvement of the operating time, sensitivity and relay selectivity.
[61]	IEEE- 3 and 8 bus	Colony Ant optimization for problems of mixed variable optimization	ACO cable to finding high-quality solutions for relay coordination.
[62]	IEEE radial 2 bus	Ant colony & firefly optimization algorithms	In finding the best options for the setting of time and running time of relays, ACO and Firefly. Firefly is found to be better than an ACO algorithm for the optimum solution.
[63]	IEEE 13 & 30 bus	ACO optimization, DE, GA	By considering all three algorithms, the DE is the most suitable for online coordination for the relay.
[64]	IEEE 3,6 & 8 bus	ACO- LP hybrid optimization	The hybrid approach has shown surprisingly promising results in improved response time and the number of function evaluations.

Angel Esteban et al, have suggested a methodological procedure to organize directional overcurrent relays [61]. This causes number of equipment used to increase in order to overcome this nonlinear problem. The use of ACO algorithm allows the probabilistic approach to implement if the number of

function evaluations is commensurate with the chance of finding the optimum value. ACO demonstrates the ability to solve problems using the same Algorithm parameters for all iterative processes with different characteristics variables. The value of a new restart mechanism linked to the elitism ACOR parameter to increase the solution efficiency. The experimental results for the real problems of coordination of the IEEE shows that ACO can robustly assume different types of variables but also, more significantly, find high-quality solutions.

Meng Yen Shih *et.al.* have used three, *GA, ACO and DE* algorithms and shown that the tested system is able to produce reasonable results [63]. Due to the need for pace in online communication, however, the number of people and ant agents for the complicated problem was reduced to only 500. This has resulted poor results for GA & ACO. On the other hand DE's demonstrates exceptional performance. For 500 individuals, DE is fastest and gives best results among the three algorithms. The excellent work efficiency, result consistency, robustness and convergence capability were demonstrated by DE. Consequently, DE is the most appropriate online coordination candidate for the implementation . Angel Esteban Labrador Rivas *et.al* have proposed a hybrid ACO-LP (traditional ACO integrated with a Linear Program (LP) solution) algorithm [64]. In order to find a better response time and improved function evolution, they have found the hybrid technique surprisingly promising.

#### ***2.1.6. Ant lion optimization (ALO)***

Antlion optimisation algorithm forms a computer search that is biologically inspired. This algorithm imitates the Antlion insect's natural behaviour. Two main stages of Antlion's life cycle are larvae, adult and larvae.

It can take 3 years, mostly in larvae, to complete the life cycle. Usually, the adult is 25-45 days old. The Antlion adulthood period is taken for reproduction, and larvae for hunting [48][65].

The larvae of Antlion excavate a conic trap through a revolving path in the sand and cast the sand off with its large shovel-shaped head [65],[66]. The larvae buried in the centre of the conical trap under sand and waited after they



excavated the trap to be caught in the pit [67]. The trap is a conical and steep shape with a sharp border to allow the ants to descend into the pit [66]. When the ant falls into the pit, it tries to get away by climbing up the walls of the trap. The Antlion is trying to catch it by pushing the sand to the bottom of the pit. Antlions, after they have pulled and taken the ant, throw the remains and sand from the box and make a trap for the next search[27]. Author A. Y. Hatata *et.al.* identifies that ALO manages the lowest operating time successfully. The comparative results demonstrate the highest accuracy of the proposed ALO [27].

The step ALO follows to determine the optimal results which described in [27].

- 1) Read the inputs
- 2) Generation the initial populations
- 3) Evaluation of fitness function
- 4) Evaluation of antlion solutions
- 5) Selection process
- 6) Update the positions
- 7) Creation of random walk
- 8) Update the position
- 9) Evaluation of the best solution
- 10) Storing results

#### **2.1.7. Cuckoos search algorithm (CSA)**

G.U.Darji *et.al.* have applied the cuckoos search algorithm (CSA) for determining the optimal TDS value. They have found the better optimum solution for relay coordination as compared to the solutions obtained using GA and GA-NLP hybrid CSA with tuned parameters. They have also identified that the obtained results using CSA indicate that this method is powerful, robust and provide high degree of precision [68].

The CSA is a new technique for meta-heuristic optimisation which fills the eggs with nests from other host birds or sometimes of other species by making the necessary progeny parasites of a few cuckoos. If the host birds discover an

alien egg in the nest, they either abandon their nest or throw away an alien egg and build another. The CSA optimizes the reproduction behaviour of certain birds and fruit flies in conjunction with leys flight behaviour for application to a multiple constraint optimization problem.

Almost all modern metaheuristics are strong because they imitate nature's best features, especially the biological systems which have formed through natural choice for millions of years. Fitness range or environmental adaptation are two important features. They can mathematically be translated into two essential elements of modern metaheuristics: Intensification and diversification [69]. Intensification is aimed at finding the best possible solutions and selecting the best candidates or solutions. Diversification, o the other hand ensures that the algorithm is searched efficiently. Similarly, the algorithm of the cuckoo search is also the algorithm of existence. Following the cuckoo bird breeding strategy, CS algorithm based on the following three principles:

- That cuckoo puts one egg at a time and throws it into a randomly selected nest.
- In the next generation, the best egg nests (main fitness) should pass for next process.
- The host nests are built, and the egg laid by a cuckoo is found by a host bird with a probability  $p_a \in [0, 1]$ . The host bird will throw away the egg or leave the nest for the construction of a new nest.

#### ***2.1.8. Modified cuckoos search optimization (MCSO)***

CSO is not a perfect method, as the key problem is easily dropped towards the local solution and has slow convergence rate. Thus another algorithms, an improved version of CS, named as Modified Cuckoos Search Optimization, (MCSOs), was used as independent adjustable approach. In MCSO, the adaptive mutation technique has used with two changes to the original search algorithm mutation [70].

The first offers two more equations, added to the original mutation model to update new solutions. Nonetheless, depending on the solution fitness value, only one of the three equations needs to be determined to apply the

adaptive mutation technique to each given solution [74]. Therefore, it is suggested that the best equation can be used for each solution by comparing each solution's fitness function index to the best solution's fitness and the mean fitness indices in comparison with the best solution. The second modification is used to help efficiently the first one, so that high-quality solutions can be made. The proposed method will diversify the search by combining local search and global search from small to larger areas through adaptive mutation technique.

**Table 2.5. Review of Cuckoos search algorithms for identification of ORC**

<b>Ref</b>	<b>Model</b>	<b>Optimization techniques</b>	<b>Outcomes</b>
[68]	IEEE 8 bus & 15 bus	Cuckoos search optimization	Compared to the CA and the GA-NLP hybrid, the CSA with tuned parameters offers the best solution to the relay coordination problem.
[70]	IEEE 4 bus	Modified Cuckoo search optimization	Modified Cuckoo search algorithm (MCSO) updated for the best setting of relays for effective relay coordination and fault isolation on a microgrid network.
[71]	Radial, parallel & distributed fedder	Cuckoss search	The results obtained indicate the promising results of the Cuckoo Search algorithm.
[72]	IEEE 8, 9 bus model	Hybrid CSA & Firefly algorithms	The CSA-FFA Hybrid proves its effectiveness in converging with a small gap in results and increased application performance to a global best solution.
[73]	4-bus Model	cuckoos search and pso algorithms	Authors found in contrast to PSO algorithms, the Cuckoos search algorithm had better performance.

### 2.1.9. Gravitational search optimization (GSO)

Adhishree Srivastava *et.al.* have used GSA and PSO hybrid algorithm for the identification of TDS values for the wind and photovoltaic source models, The 13-bus distribution system used to simulate the model and several cases were analysed. The optimal relay setting was created, including wind speed shift, penetration changes, cell temperature changes and photovoltaic insulation. They have reported that, GSA- PSO is capable to find the precise results. They have further used GSA & PSO to identify the optimal TDS value for IEEE 4 bus model. The analyses were done for various DG penetration level and found that in all cases GSA is superior [75]

**Table 2.6. Review of GSA algorithms for identification of optimal relay coordination problem.**

Ref	Model	Optimization	Outcomes
[75]	IEEE 13 bus	GSA, PSO, Hybrid GSA & PSO	Hybrid GSA & PSO result found better and precise.
[76]	IEEE-3,9,30 bus	PSO, GSA, Hybrid GSA & SQP	The hybrid GSA-SQP algorithm is suitable to address the DOCR coordination issues as a global optimal solution and GSA-SQP results were more reliable than PSO & GSA results.
[77]	IEEE 4 bus	GSA, PSO	Authors found that GSA is superior from PSO.
[78]	IEEE 8,15,30 bus	GSA	GSA found the feasible results for relay coordination problem.
[79]	IEEE 4 bus	GSA	Authors found that adaptive relay coordination based on GSA is a very effective tool for restoring the relay coordination of microgrid operating modes. The relay settings are optimized by implies of a quick and robust gravitational search algorithm in this method.

#### **2.1.10. Stochastic Fractal search algorithm (SFSA)**

Attia A. El-Ferganyey *et.al.* have applied SFSA algorithm for the identification of optimal relay coordination. The fractal search is a complex algorithm in which the algorithm modifies the number of agents. In the SFSA, the diffusion process and the updating process are two primary processes. Each agent or particle spreads in their current position to satisfy the process of exploitation during the diffusion process, which surpasses the probability of global minimum. It stops local minimums from stagnating. In this algorithm the diffusion mechanism is static, where the strongest particle is taken into account and the other particles are overlooked. The particle position, based on the position of other particles in the group in the updating process, is updated. The update process in the SFSA involves exploration process. The final outcome of this algorithm shows a high speed of convergence, requires less parameters and excellent results. SFSA is a popular algorithm that can also be used for other energy system optimization problems [80]

#### **2.1.11. Whale Optimization Algorithm (WOA)**

Mirjalili has created the whale optimizing algorithm (WOA) in 2016. Abdul Wadood had applied whale optimization algorithm for obtaining the optimal TDS value for directional overcurrent relay. This heuristic technique was used to solve engineering problems and various issues of mathematical optimisation. WOA is based on the common behaviour of buckling whales. The bubble-net hunting method of squash whales encourages this optimization strategy as they adopt a circular shaped course for hunting small fish close to the surface. This feeding process is a distinguishing behaviour, making this optimization unique among other methods of optimization inspired by nature. The bubble-net hunting process is followed in three phases. The first step is to surround the prey, the second step is to shift the spiral bubble nets and the third step is to locate the prey[81]. They have concluded that WOA simulation results minimize the problems of six models (IEEE 3, 8, 9,15,30,14 bus models). The obtained results confirm that the proposed WOA offers an efficient and reliable method for coordinating overcurrent directional relays.

**Table 2.7. Review of Whale optimization algorithms (WAO), Fractal search algorithm & water cycle optimization for identification of ORC**

<b>Ref</b>	<b>Model</b>	<b>Optimization technique</b>	<b>Outcomes</b>
[80]	IEEE 8,9,15 bus	SFSA	SFSA provide high speed of convergence, requires fewer parameters and excellent results for ORC problem.
[81]	IEEE 3,8,9,14,15,30 bus model	Whale optimization (WAO)	whale optimization algorithm capable of obtaining the optimal TDS value for direction overcurrent relay. The WOA results are an efficient and reliable method for coordinating overcurrent directional relays.
[82]	IEEE 8,9,15,30 bus model	Hybrid GWO & whale optimization algorithms (HWGO)	The HWGO algorithm will converge to the best possible solution, preserving the validity and satisfying the co-ordination margin.
[83]	IEEE 15, 30 bus	Water cycle algorithm (WCA)	The WCA method has been effective in solving the problem of coordination of such systems. It concluded from the results that WCA is superior from the other methods for optimization in the managing of the coordination problem.
[84]	IEEE 8,9,15,30 bus	Modified water cycle algorithm (MWCA), GA,GA-NLP,FFA,GSA, GSA-SQP	The author found that MWCA identified the best relay setting.

### 2.1.12. Water cycle optimization

Attia A. El-Fergany *et.al.* have used water cycle algorithms to identify the optimal relay coordination. Rivers are created in our life by falling rain and snow on mountains. The river runs through the mountains. All the water branches are combined to create a river that flows into the sea from mountains. Based on the environmental conditions, the water of the rivers evaporates into the atmosphere to create clouds in the sky. The steam is condensed in the winter season and returns to earth forming rain. These statements actually represent the nature of the water cycle. WCA starts with the raindrops triggered randomly between the lower and the upper limits as per equation (6), (7) and (8). The best raindrop that has the minimum objective function is chosen as a sea and the good raindrops are chosen as a river. The remaining raindrops are collected as streams. In the search area population is generated randomly.

$$Rain_{Drops} = [x_1, x_2, \dots, x_i] \quad (2.7)$$

$X_1, X_2 \dots X_i$  represents the raindrop

Calculating the Cost value of raindrop:

$$Cost \text{ function} = [x_1, x_2, \dots, x_i] * f \quad (2.8)$$

$N_{pop}$  streams are developed in the first step (population). Then a selection of the best are chosen as the sea and rivers  $N_{sr}$  (minimum values). Amongst the others, the stream with the minimal value is known as the sea. However,  $N_{sr}$  is the sum (defined by the user) of rivers and one single sea. The other population ( $N_{stream}$ ) is known as streams that flow into the rivers or may flow straight into the sea. [85].

$$Ns_n = round \left( \frac{Cost_n - Cost_{N_{sr}+1}}{\sum_{n=1}^{N_{sr}} C_n} * N_{stream} \right) \quad (2.9)$$

$$n = 1, 2, 3, \dots n$$

where  $N_{Sn}$  is the number of streams flowing into particular rivers and the sea [85]. The exploitation and exploration process define in the reference [83]& [85].

A stream flow to the rivers or sea. Also, rivers flow to the sea. The new position for streams and rivers may be given as equation (17) & (18):

$$x_{stream}^{i+1} = x_{stream}^i + rand * C(x_{river}^i - x_{stream}^i) \quad (2.10)$$

$$x_{river}^{i+1} = x_{river}^i + rand * C(x_{sea}^i - x_{river}^i) \quad (2.11)$$

### **2.1.13. Modified Water cycle algorithm (MWCA)**

The phases of exploitation and exploration are two contradictory milestones and are needed for population-based algorithms. The global minima could be ensured by a correct balance between exploration and exploitation. The exploitation process seeks to find local solutions while the exploration phase offers the opportunity to search for space solutions [83][84][85]. In WCA algorithm, balance can be established in between the exploration and exploitation phases through a parameter  $C$  (parameter constant). The ‘ $C$ ’ value makes it possible for streams to flow to the rivers in different directions when it is bigger than one [84]. In the traditional WCA algorithm the  $C$ -value is selected as 2 as per equation (18) [85][84]. In MWCA the value of ‘ $C$ ’ is allowed to increase gradually from 1 to 2. This amendment improves the balance between exploration and exploitation to find the optimum global solution by increasing the exponential of ‘ $C$ ’ value over the iteration cycle instead of just being picked as a constant value.

$$C^i = 2 - \left(1 - \frac{i}{Max\ iteration}\right) \quad (2.12)$$

In the same way, the position equation 2.10 & 2.11 also updated in a modified water cycle.



#### 2.1.14. Particle swarm optimization (PSO)

M. R. Asadi had used the PSO algorithm to identify the ORC [86]. Effective stochastic optimisations have taken place in the last three decades. In contrast to conventional adaptive stochastic search algorithms, evolutionary computational (EC) techniques leverage a number of possible solutions, which identify the population and provide the best solution by cooperating and competing with the observed population. In difficult optimisation problems, these techniques often detect optimum faster than conventional methods. Kennedy and Eberhart have proposed a new technique of Evolutionary Computation (EC), called PSO [87]. PSO is actually a new AI strategy that can be viewed as an essential part of a broad variety of swarm intelligence [88]. PSO has a number of common features related to evolutionary computing techniques. The PSO algorithm initializes the problem with a randomly feasible population solutions and find the best possible solution through an update of a certain number of generations. The PSO algorithm's potential solutions called particles are traveling across the problem area by following the most suitable existing particles. These particles exchange information. Each element changes its position on the basis of its own and neighbouring experience.

Suppose the “F” is the dimension of search space, Then a F dimensional vector can represent the *i*th swarm particle  $X_i = \{X_{i1}, X_{i2}, \dots, X_{iF}\}$ . The velocity of particles represents another F Dimension vector  $V_i = \{V_{i1}, V_{i2}, \dots, V_{iF}\}$ . The best previously visited position is represented as  $P_i = \{P_{i1}, P_{i2}, \dots, P_{iF}\}$ . The swarm is manipulated according to two equations by defining ‘g’ as the index of the best particle in the swarm

#### Velocity Update Equation:

$$V_{if} = V_{if} + C_1 R_1 (P_{if} - X_{if}) + C_2 R_2 (P_{gf} - X_{if}) \quad (2.13)$$

#### Position Update Equation:

$$X_{if} = X_{if} + V_{if} \quad (2.14)$$

Where  $f = 1, 2, \dots, F$ ;  $i = 1, 2, \dots, N$ , and  $N$  is swarmed size;  $c_1$  and  $c_2$  are constants, defined respectively and generally as cognitive and social scaling parameters,  $C_1 = C_2$ ;  $R_1, R_2$  are random numbers, Distributed equally in  $\{0, 1\}$ .

### 2.1.15. Modified particle swarm optimization (MPSO)

Mohamed M. Mansour had proposed the modified particle swarm optimization for solving the ORC problem [31]. In the modified PSO algorithm the coordinated constraints of the relays are tackled while searching for the optimum configuration. Furthermore, instead of random initialization, another technique for initializing PSO is proposed. Once the location of each particle is changed, a position check is conducted to ensure the number of the particles flowed out of the search area limits or violated the constraints, all the solutions generated are feasible. A repair algorithm will be employed to push the offending particle into the viable region if a violation is detected. Many particles fly outside the search space in high constrained optimization problems. In this scenario, the particle is moved back to its pbest location and in the next iteration, it is possible to explore again the search space at its velocity to refine the quest in pbest's.

**At first constraint violation:**

$$V_i^{K+1} = C_1 * rand(C) * \frac{P_{best_i} - S_i^k}{\Delta t} + C_2 * rand(C) * \frac{g_{best_i} - S_i^k}{\Delta t} \quad (2.15)$$

**At second constraint violation:**

$$V_i^{K+1} = C_2 * rand(C) * \frac{g_{best_i} - S_i^k}{\Delta t} \quad (2.16)$$

**At third constraint violation:**

$$S_i^{K+1} = P_{best_i} \quad (2.17)$$

$$V_i^{K+1} = 0 \quad (2.18)$$

**Table 2.8. Review of particle swarm optimization and modified particle swarm optimization & Grey wolf optimization for identification of ORC**

<b>Ref</b>	<b>Model</b>	<b>Optimization technique</b>	<b>Outcomes</b>
[86]	IEEE 8 bus	PSO	PSO solves the issues as discreet and continuous TSM 'S and PSM 'S and is able to tackle the problem of miscoordination.
[31]	IEEE 3,6,8 bus	MPSO, Linear Interior Point Solver (LIPSOL)	MPSO can find a viable setting while the LIPSOL algorithm does not reach a fissile outcome. With regard to computational speed, in an acceptable time, MPSO is able to achieve a very good result.
[89]	IEEE 5 bus	MPSO	The PSO algorithm is able to achieve a solution that is nearly optimal. According to the author one configuration is not possible for relays to satisfy the connected grid case and micro-grid functions of DGs. Therefore, a central protection unit is necessary to change the relay's settings depending on the device setup.
[90]	IEEE 5 bus	Hybrid PSO & LP (HPSO)	HPSO capable to provide fissible result along with coordination constraints are satisfied when microgrid operates in the grid connected mode and islanded mode.
[91]	IEEE 13 bus	PSO, GSA, Hybrid PSO-GSA	PSO-GSA results for ORC problem found superior from GSA & PSO
[92]	IEEE 6 bus	MPSO	MPSO is shown to solve both linear and non-linear programming problems.
[93]	IEEE 8,14 bus	Nelder-Mead PSO( NM-PSO), MPSO	The results found through the MN-PSO and MPSO validate that MN-PSO result is better.

[94]	IEEE 3,4 bus	PSO with inertia weight (PSOG), local version of PSO with inertia weight (PSOL), global version of PSO with constriction factor (PSOGC), local version of PSO with constriction factor (PSOGC) and chaotic PSO (CPSO)	CPSO is found to be a robust technique for such type of constrained nonlinear optimization problems.
[95]	IEEE 4 bus	GWO, PSO,GA,CSO, CSA+LP	GWO is capable to work for grid connected case and islanding case & capable to find the optimal solution and CSA+LP & GWO results found superior in all applied algorithm.
[82]	IEEE 8,9,15,30 bus	WHO,GWO, HWGO	HWGO found superior from PSO, DE,GA,FFA,GA-NLP, CSA,GSO.

#### 2.1.16. Grey wolf optimization (GWO)

Jiang Yi *et.al.* have used GWO for solving the relay coordination problem. Grey wolves are usually gregarious and the population is strictly socially hierarchical. By priority a wolf pack may be split into 4 grades: alpha (ours), beta(s), delta(s), omegas ( $\omega$ ), etc. The entire process of optimisation is essentially carried out with ' $\omega$ '. The other three high-level search groups must determine the direction of  $\omega$ . Only  $\alpha$ ,  $\beta$  and  $\delta$  will decide if they are upgrading to their position after the information obtained by  $\omega$  is returned to the top groups. The positions  $\alpha$ ,  $\beta$  and  $\delta$  are optimal and the sub-optimal, respectively. The third best solution is obtained when the GWO reaches the maximum number of Iterations [95][82]. Ahmed Korashy *et.al.* have proposed the HGWO algorithms. This algorithm is hybridisation of whale optimization and grey wolf optimization. This concept is also based on the exploration and exploitation process of algorithms. The concept which follows in this algorithm is "Use of the hierarchy of GWO to change the position of whale" [82].

## 2.2. Fault current limiter along with optimal relay coordination

Distribution Generation (DG) can be used to minimize network failure, to increase dependency or isolate space and to provide backup power during utility shutdown. The architecture of the protection system poses challenges in this dual configuration capability. Depending on the operating mode, the fault current amounts can differ. DG grid protection system based on the optimum size of fault current limits and optimal placement of directional overcurrent relays is of prime importance. The protection system is optimally built with respect to both operating modes viz. grid-connected and islanding. Restoration of DORC coordination is the big challenge for system operator when DG fault occurs.

In these special cases FCL play vital role for restoration of DORC Coordination. In the running condition change in the relay setting for each and every DGs condition, makes the system more complex. The FCL is the only easy option which can easily decrease the  $I_F$  (Fault current) as per the relay CTI (coordination time interval).

The benefit of resistive & inductive FCL are:

- 1) Less maintenance required
- 2) Low cost
- 3) Easy implementation

The drawback of FCL

- 1) Voltage drop
- 2) It causes lagging power factor
- 3) Bulky in nature.
- 4) Harmonics introduced in line due to switching.

Due to these drawbacks semiconductor-based fault current limiter (SFCL) are used for limiting the fault current and relay restoration. The drawback of this SFCL is high cost but this will overcome the drawback of simple resistive and inductive FCL.

Walid El-Khattam *et.al.* have proposed FCL based relay coordination restoration solution without altering the existing relay settings (technology

replacement) or disconnecting DGs. They have reported result which proved that resistive FCL is found to achieve the required relay coordination with lower impedance value than that of the inductive FCL [96]. W. El-khattam have also discussed two different solution of ORC named as adaption and non-adaptive solution [97]. Adaptive solution based on “change the relay setting for every case” and non-adaptive solution based on FCL value change as per relay CTI”. In achieving relay coordination for the reported scenarios, the proposed approaches shows their effect within the parameters described in the study. R.M. Chabanloo et *et.al.* have proposed the overcurrent relay coordination solution by considering the transient behaviour of fault current limiter [98]. Fault current limit (FCL) is applied in order to limit fault current levels and the effect of DGs on overcurrent (O/C) during relay coordination failures. In distribution networks the use of DG and FCL contributes to certain transient currents in faulty conditions. The proposed method is based on the genetic algorithm (GA) and use the dynamic O/C characteristic model instead of fixed coordination curves. The proposed approach is capable of determining the precise setting of relays in the transient state of FCL. Meng Yen Shih *et.al.* have proposed another method which is based on FCL [99]. They a have proposed FCL based adaptive protection technique where FCL value changes as per the distributed generation (DGs) status. They found that in this protection system are FCLs can restore network failure without making any change in the relay settings. The proposed scheme is found robust for intermittency of DGs and various network contingency operating conditions.

The optimization techniques are based on nature’s creation provides results which are relevant to the performance of the power system. Various bus models are considering for the application of these techniques. It is reported that almost all the techniques, give outcomes, which clear the picture of effect of DSEG on distribution grid. The outcome of various optimization techniques applied on different models are given in different tables numbered from 2.1 to 2.9.

**TABLE 2.9. Review of FCL used for solving the ORC problem**

Refer- Ence	Objective	Method used	Outcome
[96]	Restore relay coordination using FCL (RRCUF)	Using genetic algo for obtaining the optimal relay setting and optimal value of FCL.	Resistive and inductive FCL found economical for restoring the relay settings and capable to work for multiple cases of DGs.
[97]	Overcome the impact DGs	Proposed two method one is adaptive and one non adaptive which based of FCL	Author found the Non adaptive method is more affective because it is less complex and No limitation DGs connections in non-adaptive method.
[98]	Restore relay coordination with consideration of transient behaviour of FCL	To evaluate the precise setting of relays in a transient state, GA proposes to implement a dynamic relay model in coordination, instead of steady state relay characteristics.	This method gives the accurate values of TSMs which satisfy all coordination constrains and leads to a minimum objective function value in transient conditions.
[99]	Overcome the impact of DGs and FCL on DOCR	Adaptive protection scheme which based on DE algorithm. DE is used for identification of optimal FCL and Optimal relay setting.	Results have shown that the proposed adaptive protection scheme can simultaneously and adequately mitigate impacts of both DGs and FCL.
[100]	Optimal placement and sizing of FCL	GSO is used for identification of optimal placement of FCL and optimal sizing of FCL.	GAO is shown that it has good accuracy for this both purposes.

There has been a thorough review of ongoing relay coordination. Mathematical tools including AI and “Nature inspired algorithm”-based optimization methods, seem to be accurate and quick to meet modern demands during the past decades. In the overall review, it is found that Water cycle optimization and hybrid whale-GWO, GSA-SQP algorithms results are found very impressive for solving the ORC problem. Adaptive protection methods based on nature optimization method for solving ORC in cases of DGs, FCL play the vital role but transient effect of FCL can mitigate the relay setting. This transient effect come due to the switching process of FCL. So, instead of resistive and inductive FCL, semiconductor based FCL are preferred to overcome the DGs effect. In fact, the main factor needs to be considered are optimal sizing of FCL, before implementation of FCL for solving the ORC.

### **2.3. Conclusion**

The review presented above clearly indicates that various algorithms were proposed by different workers to tackle the issue of optimal relay setting for distribution grid. All these algorithms are based on various phenomenon we encounter in nature. Each algorithm has its limitations and looking at these limitations these algorithms were modified to get the optimal solution of the problems. The use of FCL has come out to be a possible mean to provide the solution of ORC problems. The adaptive and non-adaptive protection schemes simultaneously and adequately mitigate impacts of DGs.



## CHAPTER- 3

### OPTIMAL RELAY COORDINATION MODEL

#### 3.1. Introduction of optimal relay coordination model

The main aim of proposed model is to identify TMS relay with respect to pick up current. TMS and plug setting multiplier (PSM) decides the operating time of implemented relay. RES integrated system needs updating the protection relay parameters as per dynamic changes in system behaviour. Most important constraint in relay coordination is CTI. CTI is difference between operating time of primary and secondary relay in protection network and defined if operating time of primary is high as compare to secondary. This is also called as mis-coordination. Miscoordination occurs due to sudden increase in fault current level. Proper coordination need to setup for a reliable protection scheme. DOCR relay's plug setting (PS) ranging from 50 to 200 % in steps of 25%. The PS defines the current setting of the relay while the TMS defines the operating time of relay in steps of 0.1, 0.2, 0.3 to 1.0 seconds [101][102][103][80]. For any over current relay, the plug setting is defined by two parameters: the fault current during the unsymmetrical fault and the pick-up relay current [104]. Inverse definite minimum time relay (IDMT) operates when the current exceeds a normal value and follow an inverse characteristic between operating time and PSM. The main feature of the IDMT relay is that it takes least time to operate which is based on the value of fault current [104][105][106][107]. To find the optimized operating time of the relay (back up relay) objective functions are desired.  $\alpha$  and  $\beta$  are the two constants for determining the shape of the curve between operating time and PSM given by IEEE standard. The standard value of  $\alpha$  is 0.02 and value of  $\beta$  is 0.14. PSM is defined as the ratio of fault current ( $I_f$ ) and pick-up current ( $I_p$ ). The PSM and constants  $\alpha$  and  $\beta$  correcting to operating time of relays were calculated. Hence the optimized operating time of the relay calculated through optimizing the main function with respect to constraints [108][109][110][111][112].

### 3.1.1. Objective function for relay coordination:

The objective function for optimal relay coordination can be expressed as;

$$\min K = \sum_{i=1}^n w_i t_i \quad (3.1)$$

The number of relays is expressed by 'i' and the operating time for the relay is shown by 't'. K is the cumulative operating time of relays of the faulty portion isolated from the network.  $W_i$  the weight depends on the probability of a given failure occurring in each protective area and is typically set to one.

CTI is the relay time interval of coordination that defines the difference between the primary and backup relay operating time intervals. This is very important for maintaining a healthy system. Equation (2) describes the relay CTI that was working in the event of a fault.

$$\Delta t = t_b - t_p \quad (3.2)$$

$\Delta t$  =CTI (Coordination time interval)

The operating time of overcurrent is defined in equation (3.3). TMS is the time multiplier setting which lies between 0 to 1 and this value which define the delay in operating time of the relay,

$$t = TMS \left( \frac{a}{M^\alpha - 1} + b \right) \quad (3.3)$$

$t$  = Operating time interval of overcurrent relay

$a, b, \alpha$  = Relay constants

$M$  = Plug setting multiplier

$$M = \frac{I_{SC}}{I_{pickup}} \quad (3.4)$$

Plug setting multiplier, M forms an important part of the relay setting. M's value lies between 0 and 1. M can be expressed as given in equation (3.4). Thus **M** is the ratio of short circuit and picks up current of the relay.

### 3.1.2. The constraint for the overcurrent relay coordination model

If  $t_b$  and  $t_p$  are backup relay and primary relay operating time then we have;

$$t_b - t_p \geq CTI \quad (3.5)$$

Where CTI is coordination time interval. Equation (3.5) describes the relationship at the time of operation between the primary relay and the backup relay.

The operating time of the relay is the function of the current pickup and the current deviation perceived by the relay. Based on the type of relay, the operating time is calculated by generic characteristic curves or analytical equation. The equation expressed as [113][40];

$$T_i^{Min} \leq T \leq T_i^{Max} \quad (3.6)$$

Here,  $T_i^{Min}$  &  $T_i^{Max}$  is the minimum and maximum operating time of  $I^{th}$  relay.

$$TMS_i^{Min} \leq TMS_i \leq TMS_i^{Max} \quad (3.7)$$

$$Max(I_{load}^{Max} I_{set}^{Min}) \leq I_{set_i} \leq Min(I_{fault}^{Min} I_{set_i}^{Max}) \quad (3.8)$$

The least pickup current setting of the relay is the maximum  $I_{set}^{Min}$  value among the minimum available tap settings on the relay and maximum load current  $I_{load}^{Max}$  passes through it. In a similar manner, the maximum pickup current setting is chosen less than the minimum value between the maximum available tap settings  $I_{set_i}^{Max}$  on the relay and minimum fault current  $I_{fault}^{Min}$  which passes through it.

### 3.1.3. Optimization of impedance fault current limiter (ZFCL)

$$Min(z) = \sum_{i=1}^n Z_{fcl} \quad (3.9)$$

In FCL impedance optimization, we have the constraint are:

$$z_{FCL}^{Min} \leq \sum z \leq z_{FCL}^{Max} \quad (3.10)$$

The FCL optimal sizing and implementation, impact the impedance values of the system and also affected the fault current value. “z” represents the FCL impedance value and  $Z_{FCL}^{Min}$  &  $Z_{FCL}^{Max}$  are the lower and upper values of FCL.

$$X_{FCL}^{Min} \leq X \leq X_{FCL}^{Max} \quad (3.11)$$

The FCL optimal sizing and implementation impact the impedance values of system and also affected the fault current value. “X” is representing the FCL reactance value and  $X_{FCL}^{Min}$  &  $X_{FCL}^{Max}$  is represent the lower and upper bonds of FCL.

#### **3.1.4. Distributed generation protection monitoring index (DGPMI)**

DGPMI is defined as the impact of DGs on power grid. The calculation of DGPMI makes it easy to identify the impact on relay coordination due to DG power integration.

$$DGPMI = \frac{- (Change\ on\ DGs\ power\ integration)}{Change\ in\ relay\ coordination\ time\ interval\ of\ relays} \quad (3.12)$$

Equation (3.10) clearly indicates that the positive value of DGPMI refers to an increase in DGs penetration and thus effecting the coordination time interval of relay.

# CHAPTER 4

## OPTIMIZATION ALGORITHMS USED FOR SOLVING OPTIMAL RELAY COORDINATION MODEL

### 4.1. Particle Swarm Optimization for solving ORC

Particle swarm optimisation was introduced in 1995 by Kennedy and Eberhart. This algorithm is inspired by the social activities of birds. In this particle swarm optimization, each individual particle searches for the best solution in a search space by succeeding the previous best position of the neighbours and best position of own. Every particle is characterised by its own velocity and position which are changed as given equation (4.1).

$$S_i^{K+1} = S_i^k + V_i^k \quad \backslash \quad (4.1)$$

$$V_i^{K+1} = wV_i^k + C_1 * rand_1 * (Pbest_i - S_i^k) + C_2 * rand_2 * (gbest - S_i^k) \quad (4.2)$$

$S_i^k$  &  $S_i^{K+1}$  is represented the previous and current position of “I” particle,  $V_i^k$  &  $V_i^{K+1}$  are the previous and current velocity of particle of “i<sup>th</sup>” particle,  $P_{best}$  &  $G_{best}$  are individual best positions and best global best position identified in the whole swarm.  $C_1$  &  $C_2$  are the acceleration constants,  $W$  is inertia weight of PSO which lies between 0 to 1 & defined that how much previous velocity is preserved. Each particle of PSO share information with neighbors, updated equation (4.1) & (4.2) show PSO associate the cognition component of every particle with social component of every particle in group. The social component advises that individuals overlook their own experience and alter their behaviour according to the prior best particle in the neighbourhood of the group.

In equation (4.2)  $w$  and  $c_j$  shows the weighting operator and weighting factor (acceleration factor) correspondingly.  $rand$  represents a uniformly distributed random range between zero and one. Provides present position of  $i_{th}$  individual at iteration. In equation (4.3) Where, “iter” represents the rate of  $i_{th}$

individual at iteration. Weight operates varies iteratively in PSO. Here,  $w_1$  and  $w_2$  are 0.9 and 0.4 respectively.

$$w = (w_1 - w_2) \times \frac{(\max it - iter)}{\max it} + w_2 \quad (4.3)$$

Where  $w_1$  and  $w_2$  represent first and last weight respectively, matrix and iter show largest current iteration number. Flowchart shown that procedure of optimizing the objective function using particle swarm optimization (PSO) shown in figure 4.1.

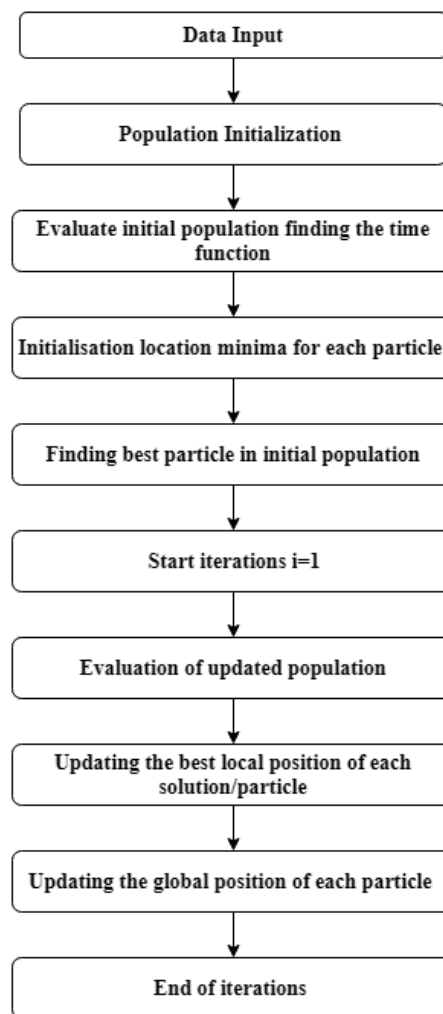


**Figure 4.1. Flowchart for PSO**

## 4.2. Grey wolf optimization for solving ORC

Mirjalili et al., have proposed the Grey Wolf Optimizer Algorithm (GWO) in 2014 [27]. GWO is one of the most recent bio-inspired algorithms. Grey Wolf Optimizer (GWO) algorithm is based on Swarm Intelligence (SI) algorithms based on social behaviour and the grey wolves hunting strategy. The grey wolves residing collectively in teams known as a package and the hierarchy management in the package is separated as alpha, beta, delta as well as omega. Alpha wolf ( $\alpha$ ) is based on the first level in public hierarchy where it is considered the best expert and the other wolves in the package adhere to his guidelines. Beta wolf ( $\beta$ ) is to be the 2nd levels of management where the beta wolf supports the alphas for the tasks of the package. The third member at public hierarchy is based on the delta ( $\delta$ ) wolves that follow  $\alpha$  as well as  $\beta$  wolves. The rest of the wolves tend to be omegas ( $\omega$ ). The GWO algorithm structured in three steps which are: (1) Searching, following and approaching the food (2) Surrounding and harassing the food (3) assaulting the food [114][115][116]. Surrounding the food by a grey wolf can be mathematically modelled as follows:

$$D_1 = C \cdot X_{p1}(t) - X(t) \quad (4.4)$$

$$X(t+1) = X_{p1}(t) - A \cdot D_1 \quad (4.5)$$

Here,  $t$  represents the current iteration,  $X_{p1}$  represent the vector position of food and  $X$  indicates the vector position of the grey wolf.  $A$  &  $C$  are coefficient vectors. These can be calculated through given equation:

$$A = 2b - r_1 - b \quad (4.6)$$

$$C = 2r_2 \quad (4.7)$$

Here, value of  $b$  is decrease from linearly two to zero within iteration. Value of  $r_1$  and  $r_2$  are value random number between 0 to 1. In the process of hunting wolf recognize the position of food. In the hunting process the package effected by  $\alpha$ ,  $\beta$ ,  $\delta$ . The best generated results saved by the best agents and remaining agents update the positions. The identification of best first, second, third hunting agents can be given by using equation 4.8 to 4.13 equation given as follows:

$$D_\alpha = |C_1 \cdot X_\alpha - X| \quad (4.8)$$

$$D_{\beta} = |C_2 \cdot X_{\beta} - X| \quad (4.9)$$

$$D_{\delta} = |C_3 \cdot X_{\delta} - X| \quad (4.10)$$

$$X_1 = X_{\alpha} + (A_1 \cdot D_{\alpha}) \quad (4.11)$$

$$X_2 = X_{\beta} + (A_2 \cdot D_{\beta}) \quad (4.12)$$

$$X_3 = X_{\delta} + (A_3 \cdot D_{\delta}) \quad (4.13)$$

Reintroduce the position of the current hunt agent as per equation 4.13.

$$X(t+1) = \frac{X_1 + X_2 + X_3}{3} \quad (4.14)$$

The grey wolves tend to finishing the hunting process by attacking the food. The grey wolf attacks correctly when the food stops moving forward. The grey wolves tend to be finishing the hunting process by attacking the food. The grey wolf attacks correctly when the food stops moving forward. It can be accomplished mathematically by decreasing the value slowly from 2 to 0. Therefore, A is changed arbitrarily with the variation of alpha, and it will be in the range [-1, 1], hence the upcoming location of search agents might be around its current position as well as around the position of the food.

### 4.3. Hybrid GWO-PSO for solving ORC

In GWOPSO, first three agents' position is updated in the search space by the proposed mathematical equations (4.15–4.17). Instead of using usual mathematical equations, we control the exploration and exploitation of the grey wolf in the search space by inertia constant. The modified set of governing equations are

$$D_{\alpha} = |C_1 \cdot X_a - w \cdot X_1| \quad (4.15)$$

$$D_{\beta} = |C_2 \cdot X_{\beta} - w \cdot X_2| \quad (4.16)$$

$$D_{\delta} = |C_3 \cdot X_c - w \cdot X_3| \quad (4.17)$$

In combination of GWO and PSO the updated velocity and updated equation as follows



$$V_i^{K+1} = w(V_i^K + (C_1 \times rand_1 \times (pbest_i - S_i^K)) + (C_2 \times rand_2 \times (gbest - S_i^K)) + (C_3 \times rand_3 \times (gbest - S_i^K))) \quad (4.18)$$

$$S_i^{K+1} = S_i^K + V_i^{K+1} \quad (4.19)$$

$S_i^K$  and  $S_i^{K+1}$  represent the previous and current position of “i” particle,  $V_i^K$  &  $V_i^{K+1}$  are the previous and current velocity of “i<sub>th</sub>” particle, best & gbest are individual best positions and best global best position found in the whole swarm.  $C_1$  &  $C_2$  are the acceleration constants, “w” is inertia weight of PSO which lies between 0 to 1 & defined as how much previous velocity is preserved. Each particle of PSO share information with neighbors. The updated equation (4.18) & (4.19) show PSO associate the cognition component of every particle with the social component in the group. The social component advises that individuals overlook their own experience and alter their behavior according to the prior best particle in the neighborhood of the group.

In equation (4.20) Where “iter” represents the rate of i<sub>th</sub> individual at iteration. Weight factor varies iteratively in PSO. Where w1 and w2 represent first and last weight respectively, matrix and iter show largest current iteration number. Here, the value of w1 and w2 are taken as 0.9 and 0.4 respectively. Weight operates of the matter as.

$$w = (w1 - w2) \times \frac{(\max it - iter)}{\max it} + w2 \quad (4.20)$$

#### 4.4. Interior point algorithm for solving ORC model

The MATLAB framework provides a very simple implementation of different non - linear optimization algorithms. Constraint mapping and problem definition are provided in a very user - friendly environment using the powerful 'fmincon' library function. The 'fmincon' function finds a constrained minimum of a function specified over a number of variables [117]. "fmincon" attempts to solve type problems:

$$\min_x f(x) \text{ s.t. } : A * X \leq B, A_{eq} * X = B_{eq} \quad (4.21)$$

$$c(x) \leq 0, c_{eq}(x) = 0 (\text{Nonlinear constraint s}) \quad (4.22)$$

Where

$$LB \leq x \leq UB \text{ (Bounds)} \quad (4.23)$$

The 'fmincon' function implements four different algorithms; i) Interior point ii) Sequential quadratic programming (SQP) iii) Active Set and iv) Trust Reflective Area. Any of those four algorithms can be selected by specifying the choice below:

$$options = optimset('Algorithm', 'interior-point') \quad (4.24)$$

The above options set are then passed to 'fmincon' for the implementation of the interior point algorithm. The following instructions, as equation (34), are used to launch the optimization process.

$$x = fmincon(fun, x0, A, b, Aeq, beq, lb, ub, nonlcon, options) \quad (4.25)$$

## CHAPTER 5

### ADAPTIVE PROTECTION SCHEMES FOR OBTAINING OPTIMAL RELAY COORDINATION

In this chapter various protection schemes for obtaining optimal relay coordination are described. The protection schemes used in the present schemes are;

- Adaptive protection scheme relay coordination
- Hybrid protection scheme for optimal relay coordination

The description of each of these schemes are described below.

#### 5.1. Adaptive protection scheme for relay coordination

In the relay protection scheme used adaptive methodology which used for IEEE node 3 distribution grid. The adaptive relay methodology is shown in fig 5.1 as flow chart. This flow chart defines the process of relay setting variation. Here, SPV is continuously observed, this observation process is carried out on MATLAB platform with the help of function block. The decision of changing setting of relay is taken as per SPV status. Here “0” is used to denote the “not connected” mode and “1” denote the connected mode of SPP on grid e.g. 000” shows that no SPP is integrated over grid and “111” indicates that all three SPP are integrated over grid.

The flow chart of relay setting is shown in fig 5.1. This flow chart defines the process of relay setting variation. Here, SPV is continuously observed, this observation process is carried out on 3 node feeders on Matlab platform with the help of function block. The decision to change the setting of relay is taken as per SPV status. This protection scheme continuously monitored the DGs status and as per DGs connection, relay setting dynamically changes.

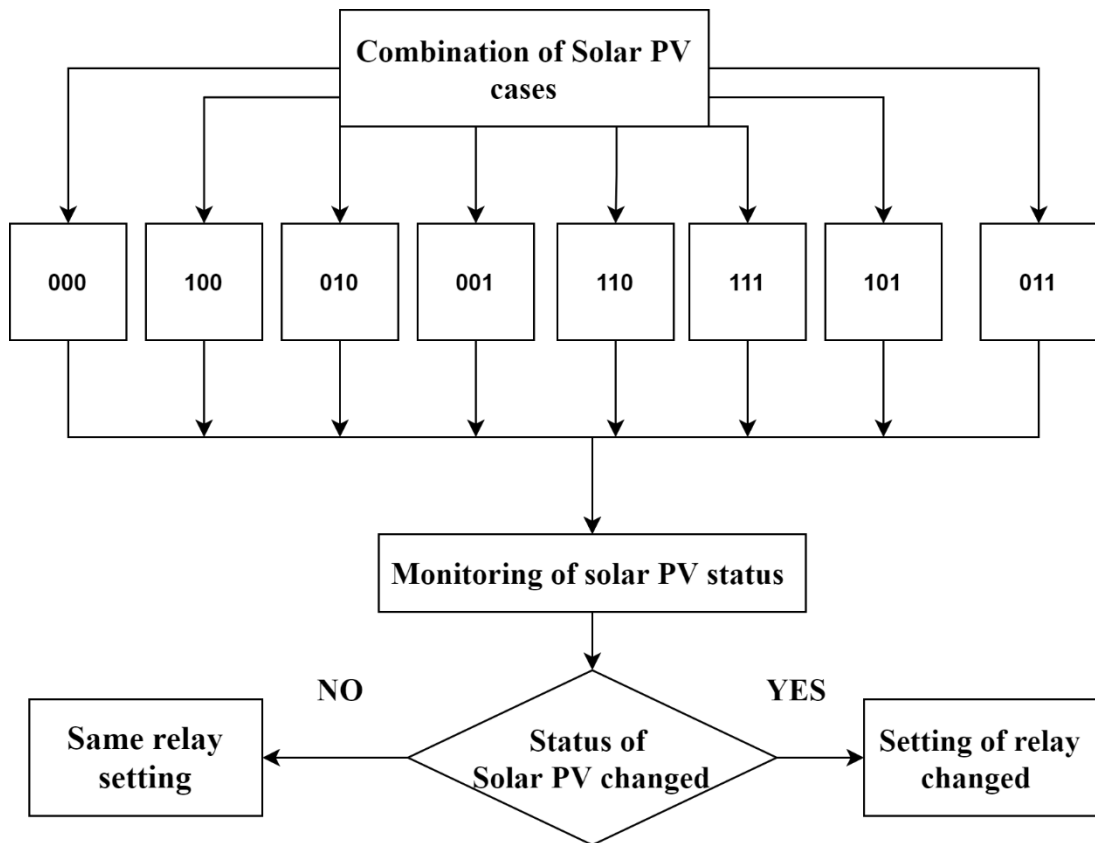


**Fig 5.1. Protection scheme for dynamic relay parameter changes**

## **5.2. Hybrid protection scheme for optimal relay coordination for IEEE 13 & 33 node**

In hybrid protection scheme is a combination of adaptive and non-adaptive algorithms. This algorithm increases reliability and flexibility, as algorithms are flexible. Here, Step 1 to Step 7 offers a non-adaptive protection scheme, and Step 8 to Step 11 offers an adaptive protection scheme. Figure 1 describes the complete protection scheme showing all measures of identification for optimum relay setting and optimum setting of  $Z_{fcl}$ .

In protection scheme algorithm is defined in the following steps:

Step 1: Study of the load flow for the full network.

Step 2: Fault analysis and CTI calculation of DG penetration cases.

Step 3: DGPMI is measured that determines the effect of DGs on the distribution grid.

Step 4: Identification of the affected protection zones, due to the penetration by DGs.

Step 5: Calculation of the  $X_{fcl}$  value for the location affected by the DGs penetration level.

$$X_{fcl} = \frac{V_{Line\ to\ line}}{\sqrt{3}} \left( \frac{1}{I_{scA}} - \frac{1}{I_{scB}} \right) \quad (5.1)$$

Where;

$I_{scA}$  = Short circuit current after the  $X_{fcl}$

$I_{scB}$  = Short circuit current before the  $X_{fcl}$

The  $Z_{FCL}$  can be expressed as;

$$Z_{FCL} = \sqrt{R^2 + X^2} \quad (5.2)$$

Here resistance **R** is taken as a variable optimized by using an optimization algorithm.

Step 6: Measurement of the total of all optimized  $Z_{fcl}$  values, within maximum & minimum defined limits. The measurement of CTI is also within the defined limits of the parameters.

Step 7: If the  $Z_{fcl}$  limits are not satisfied or the CTI limits are not satisfied, then the algorithm shifts to the adaptive protection scheme and the network load flow process occurs again.

Step 8: Calculation of optimized relay settings using optimization techniques.

Step 9: Optimized relay configuration applied to all connected relays.

Step 10: Checking the CTI of all relays & if CTI did not satisfy the limits then Step 7 to Step 9 repeated and reset the relay.

The flow chart of relay setting is shown in fig 5.2. This flow chart defines the process of relay setting variation. Here, SPV is continuously observed, this observation process is carried out on 13 & 33 node ETAP. The decision to change the setting of relay is taken as per SPV penetration level. This protection scheme continuously monitored the DGs status and  $Z_{fcl}$  limiter value as per DGs connection and keeps same relay setting.  $Z_{fcl}$  seen in this algorithm if the  $Z_{fcl}$  value not satisfied the constraint. Then, adaptive protection scheme take care of the relay setting in distribution network.

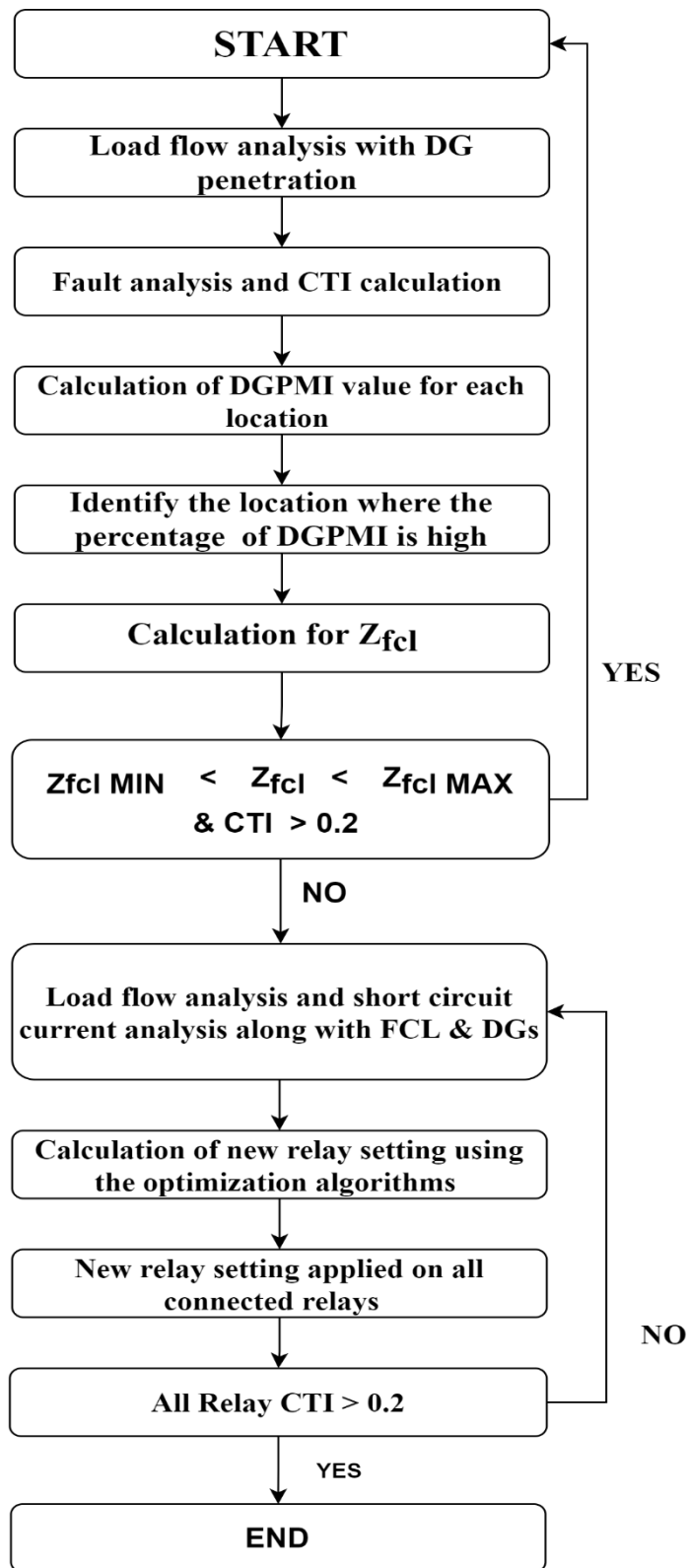


**Fig 5.2. Hybrid protection scheme (Combination of Adaptive & Non adaptive protection scheme)**

## CHAPTER 6

### RESULT & DISCUSSION

In this chapter various IEEE bus system taken to study the optimal relay coordination model. The IEEE standard model used in the study are mentioned below;

- IEEE node 3 (4 bus)
- IEEE node 13
- IEEE node 33

The results obtained using these above models are discussed here;

#### **6.1. IEEE node 3 model**

##### **6.1.1. IEEE node 3 system modelling along with SPP integration**

Here, three SPP are used for the analysis of solar PV penetration for IEEE node 3 system. This simulation model of SPP integrated with IEEE node 3 system on MATLAB platform is shown in figure 6.3. The thirty-two different cases have taken for the study and their status are shown in table 6.2. Here “0” is used to denote the “not connected” mode and “1” denote the connected mode of SPP on grid e.g. “000” shows that no SPP is integrated over grid and “111” indicates that all three SPP are integrated over grid. The simulation of IEEE node 3 distribution feeder on MATLAB Simulink model [118][119][120], is shown with location of three various fault cases indicated by A, B, and C. The position of directional over current relays (DOCR) (R1, R2, R3, R4, R5) at various positions on IEEE 4 bus feeder system is also shown in figure 6.1. Simulink model of solar photo voltaic is given in figure 6.2. Numerical values of various parameters used in modelling of solar PV are tabulated in table 6.1.

**Table 6.1. Solar PV parameters used in simulation**

<b><u>Solar PV Parameters</u></b>	<b><u>Values</u></b>
Cell in module	96
Module short-circuit current (Isc)	5.96 A
Module open-circuit voltage (Voc)	64.2 V
Module voltage and current at maximum power (Vmp , Imp)	54.7 V, 5.58 A
sun irradiance (MAX)	1000 W/m <sup>2</sup>
DC- DC boost converter	273 V to 500-volt DC
3 phase Inverter	500 v DC to 260 V AC
No of series connected string	5
No of parallel connected string	66
Transformer rating	100 KVA, (260 V to 12.47, 4.16KV)

**Table 6.2: List of cases taken for solar photovoltaic integrated in IEEE node 3 fedder System**

<b>Case number</b>	<b>Fault location</b>	<b>Solar Connection Type</b>
1	No fault	000
2	No fault	100
3	No fault	010
4	No fault	001
5	No fault	011
6	No fault	111
7	No fault	101
8	No fault	110
9	A	000
10	A	100
11	A	010



12	A	001
13	A	011
14	A	111
15	A	101
16	A	110
17	B	000
18	B	100
19	B	010
20	B	001
21	B	011
22	B	111
23	B	101
24	B	110
25	C	000
26	C	100
27	C	010
28	C	001
29	C	011
30	C	111
31	C	101
32	C	110

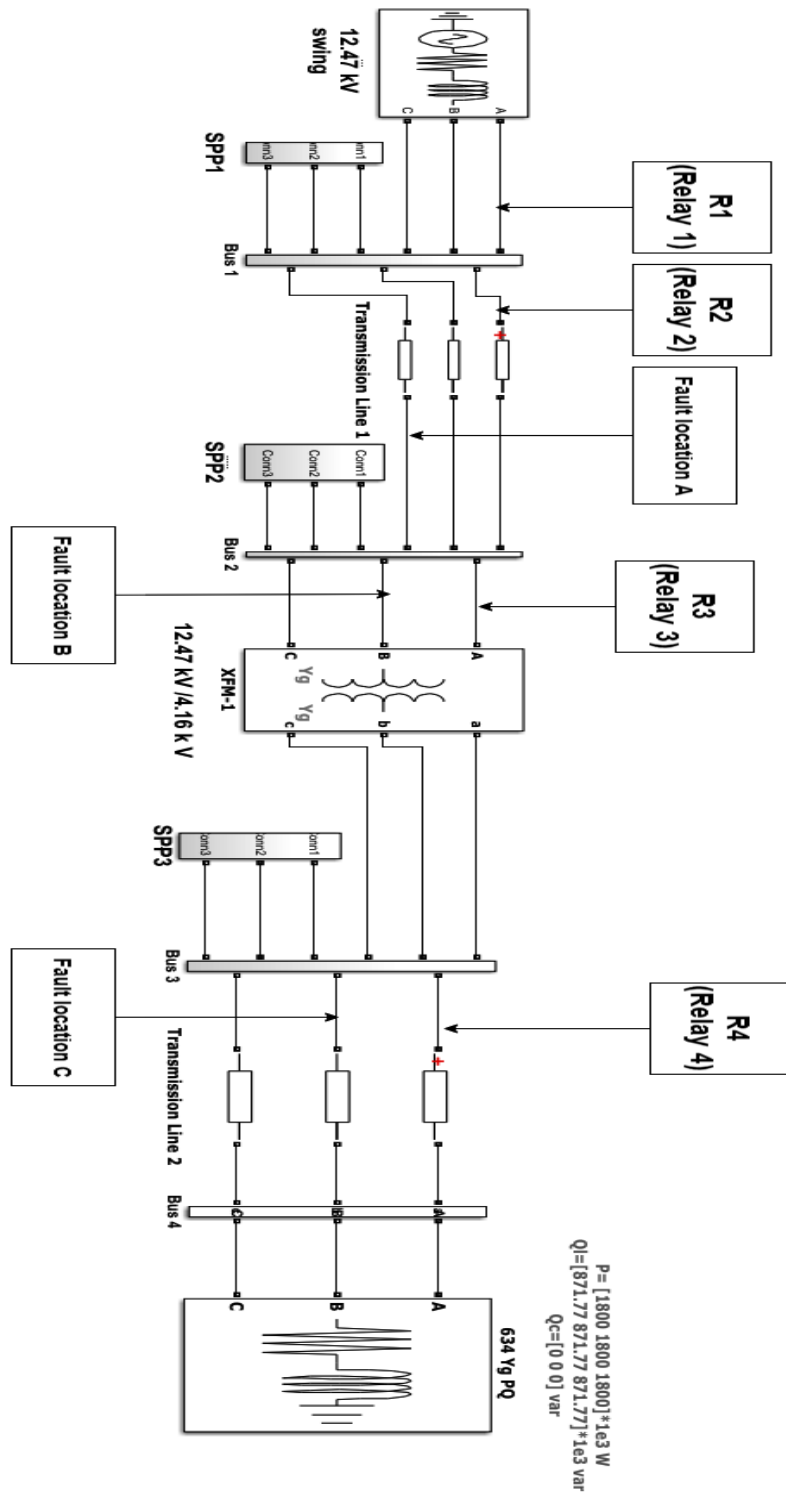


**Fig 6.1. Simulation model of solar photovoltaic integrated in IEEE node 3 systems**

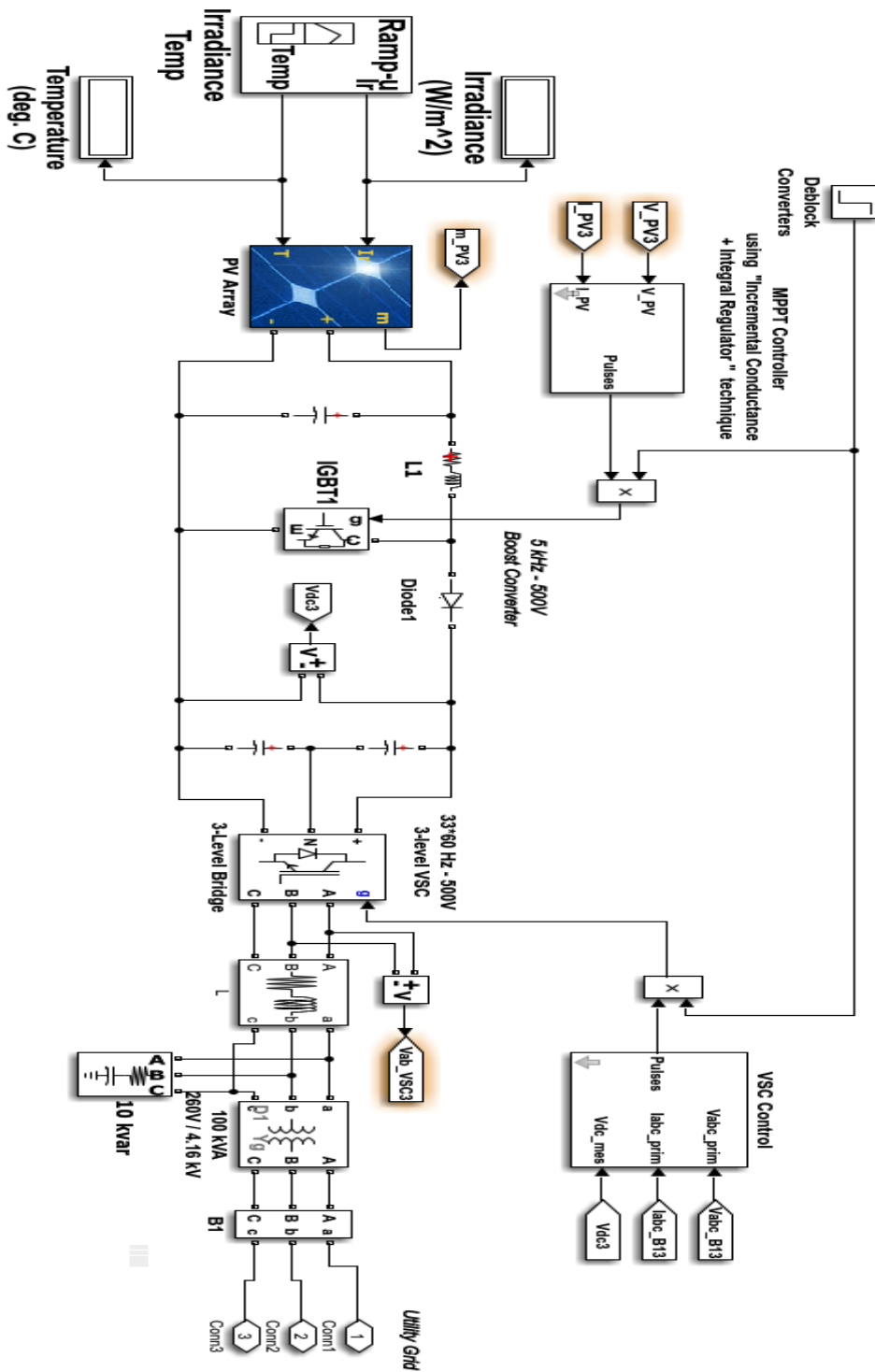


**Fig. 6.2 : Simulation of solar photovoltaic plant (SPP) with include MPPT**  
 [118][119]

### 6.1.2. Impact of Solar PV on Distribution grid IEEE node 3 feeder.

Here different situations of grid voltage deviation are considered. The details of each one is described in detail as follows.

#### 6.1.2.1. Grid voltage deviation when solar photovoltaic source is connected

Grid voltage variation in different cases, when a single SPP is connected on grid are tabulated in table 6.3. It is clear from these results that for case number 2, negligible deviation in voltage has noticed. For case number 3, it is clear that the voltage dropped to 1.5% at load bus for phase c. Similarly, for case number 6 the results indicate a voltage drop by 1.1%. Analysis of the grid voltage variation is considered only for the integration of grid and SPP as shown in figure 6.3.

CTI in equation (3.5) is taken from the literature[121], which means that the difference between backup relay tripping and primary relay tripping should always be more than or equal to 0.3 second. The fault crated on three location A, B and C are mentioned in figure 6.1. When fault is created on phase C to ground on three different buses, the maximum magnitude of fault tabulated in table 6.5. When fault occur at site A then maximum current flows in case 16 (110) and second maximum for case 6 (111), similarly result has been recorded for fault location B & C.

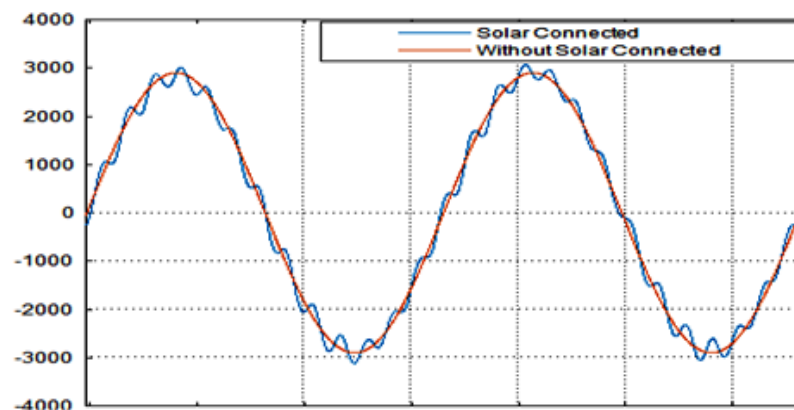


**Fig 6.3. Voltage comparison between case 1 and case 6 at IEEE node 3 feeder.**

**Table.6.3. Voltages of each bus for IEEE node 3 fedder system in Various Cases (RMS)**

CASE NUMBER	CASE TYPE	Va1 (Volts)	Vb1 (Volts)	Vc1 (Volts)	Va2 (Volts)	Vb2 (Volts)	Vc2 (Volts)	Va3 (Volts)	Vb3 (Volts)	Vc3 (Volts)	Va4 (Volts)	Vb4 (Volts)	Vc4 (Volts)
1)	000	7157.382	7159.601	7153.6176	7083.495	7085.692	7079.7392	2305.7988	2306.043	2305.0755	2051.4036	2051.7116	2050.7948
2)	100	7156.08	7158.296	7152.3098	7082.394	7084.558	7078.6506	2305.422	2305.6676	2304.7008	2051.0132	2051.3228	2050.406
3)	010	7157.5815	7159.8497	7153.7371	7077.6883	7080.1865	7073.9816	2298.2932	2298.8577	2297.7295	2020.665	2022.2039	2020.7811
4)	001	7157.5573	7159.7769	7153.7918	7083.9464	7086.1489	7080.1931	2306.4	2306.6495	2305.6827	2058.3899	2058.7268	2057.836
5)	011	7157.717	7159.7208	7153.6796	7077.8345	7080.0766	7073.4553	2298.5968	2299.1647	2297.4296	2027.2775	2029.1556	2025.2306
6)	111	7156.5675	7158.6283	7152.7747	7077.5504	7079.3029	7073.4323	2298.9998	2298.9477	2297.8807	2029.5925	2028.9573	2027.4881
7)	101	7156.273	7158.4816	7152.5294	7082.8692	7085.0878	7079.218	2305.9921	2306.3327	2305.3521	2057.891	2058.5653	2057.4058
8)	110	7156.199	7158.392	7152.4632	7076.5334	7078.5735	7072.77	2297.9399	2298.0514	2297.1604	2020.4985	2020.298	2019.6572

**Table 6.4. Current of each bus for IEEE 4 bus system in Various Cases (RMS)**

CASE NUMBER	CASE TYPE	Ia1 (Ampere)	Ib1 (Ampere)	Ic1 (Ampere)	Ia2 (Ampere)	Ib2 (Ampere)	Ic2 (Ampere)	Ia3 (Ampere)	Ib3 (Ampere)	Ic3 (Ampere)	Ia4 (Ampere)	Ib4 (Ampere)	Ic4 (Ampere)
1)	000	239.440	239.4786	239.3519	239.4157	239.4938	239.3636	711.1819	711.4033	711.0269	711.185	711.4072	711.0308
2)	100	245.215	245.3050	245.1732	239.3562	239.4312	239.3043	711.0049	711.2274	710.8508	711.008	711.2313	710.8547
3)	010	254.019	252.9440	252.6363	254.0324	252.9566	252.648	755.1349	751.9382	751.0443	700.5210	701.1724	700.6287
4)	001	238.589	238.6589	238.5357	238.6018	238.6708	238.5476	708.7413	708.9460	708.5804	708.7451	708.9498	708.5842
5)	011	255.623	254.0766	255.7258	255.6364	254.0893	255.7386	760.177	755.3371	760.3194	697.7052	698.4608	697.0274
6)	111	257.949	256.8355	257.2302	252.6768	251.4210	251.9214	751.3651	747.3316	748.8347	698.4414	698.3549	697.6963
7)	101	244.094	244.4603	244.1121	238.5231	238.6769	238.4536	708.5071	708.9656	708.2999	708.5109	708.9694	708.3037
8)	110	259.1673	260.22446	260.06861	253.8183	254.8491	254.73995	754.53472	757.58557	757.33313	700.42092	700.47033	700.18662

### 6.1.2.2. Frequency calculation of solar photovoltaic connected cases in IEEE node 3 network.

Figure 6.4, 6.5, and 6.6 shows the frequency variation after integration of SPP with the grid. It is clear from this table that the observed frequency deviation at phase A is (+) 0.24, at phase B (-) 0.12 and at phase C it is (+) 0.53. Thus, it stays in limits i.e.  $\pm 1\%$ . The standard frequency for system is taken to be 60 Hz. Moreover, no change in the sinusoidal variation is observed.

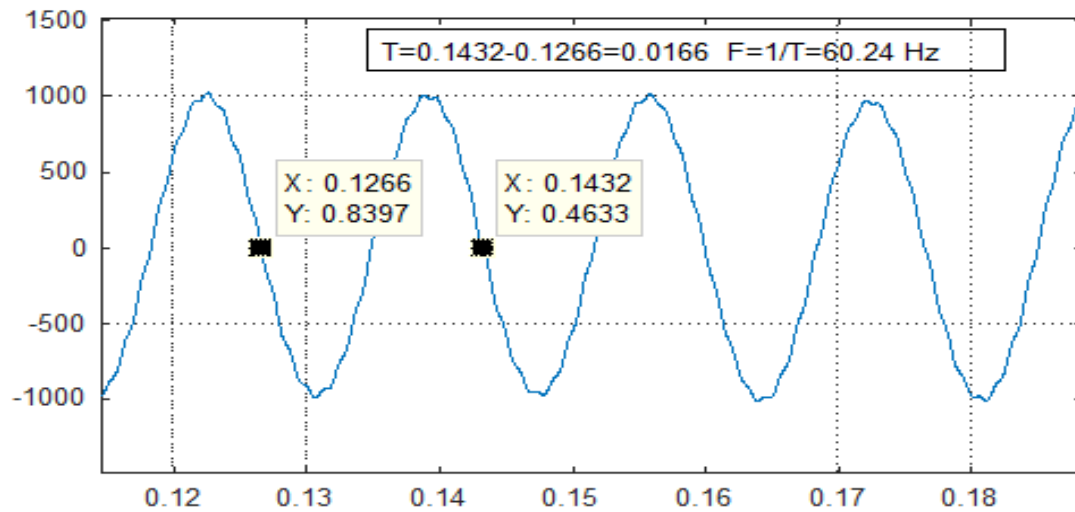


**Fig 6.4. Frequency calculation for the solar photovoltaic connected model (Phase A)**

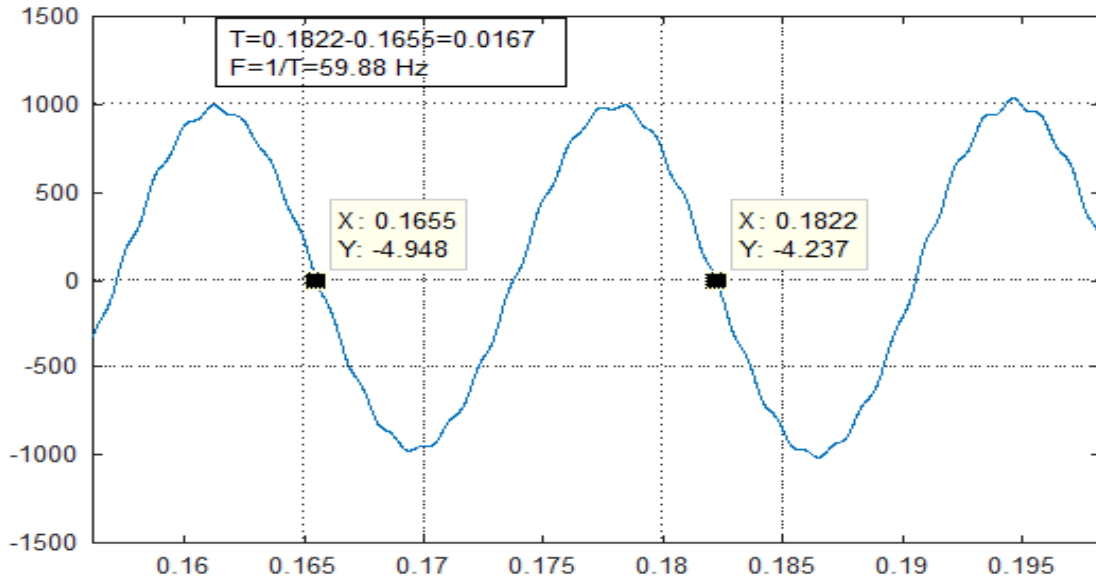


**Fig 6.5. Frequency calculation for the solar photovoltaic connected model  
(Phase B)**

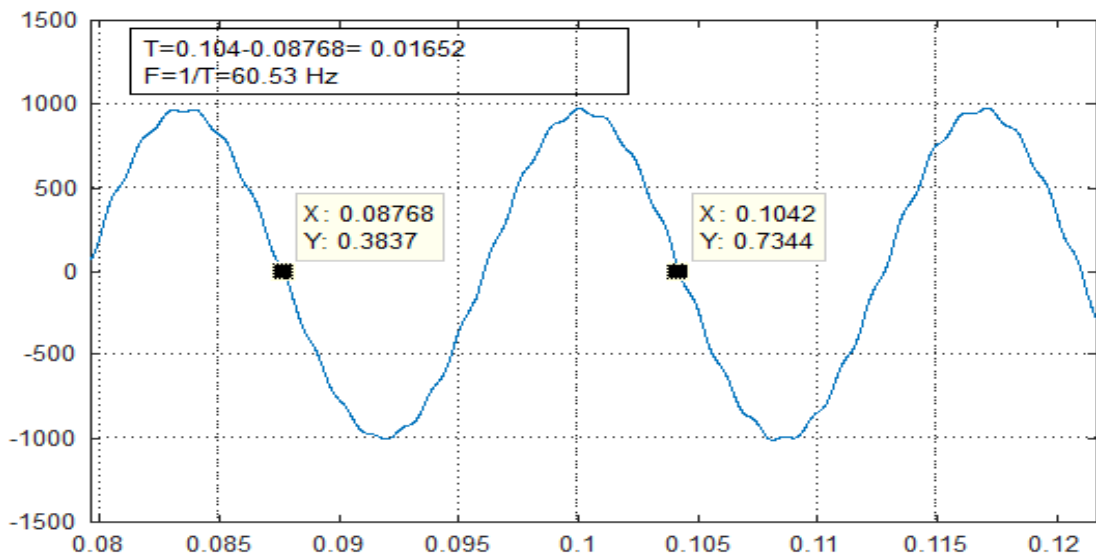


**Fig 6.6. Frequency calculation for the solar photovoltaic connected model  
(Phase C)**

### 6.1.2.3.Current Calculation of Solar photovoltaic connected cases

Table 6.5 shows the current calculation for each bus and SPP connected without any fault. The results show that when the solar is connected the level of the current at buses increase to certain level and it also reflects when fault occurs in the case of solar connected circumstances, the level of fault current also increased shows in table 6.5.

**Table 6.5. Fault current calculation through Simulink MATLAB**

<b>S.no</b>	<b>Case number</b>	<b>Case Type</b>	<b>Fault location</b>	<b>Fault current (RMS) Ampere</b>
1	9	000	A	9670.4757
2	10	100	A	9702.0893
3	11	010	A	9673.7574
4	12	001	A	9670.3311
5	13	011	A	9673.6584
6	14	111	A	9705.0517
7	15	101	A	9701.9266
8	16	110	A	9705.3782
9	17	000	B	9670.4869
10	18	100	B	9737.5177
11	19	010	B	9673.7687
12	20	001	B	9670.3426
13	21	011	B	9673.6701
14	22	111	B	9740.5222
15	23	101	B	9737.4719
16	24	110	B	9740.6155
17	25	000	C	1598.018
18	26	100	C	1597.6294
19	27	010	C	1654.9082



20	28	001	C	1642.111
21	29	011	C	1720.9479
22	30	111	C	1720.2336
23	31	101	C	1641.7186
24	32	110	C	1656.3535

### 6.1.3. Optimal Relay Setting

For optimal relay setting, an objective function has been modelled, equation (3.1), to minimize the operating time of the relay while satisfying CTI (coordination time interval) of the relay equation (3.5). The issue of relay mal operation sometimes happens for integrated SPP-DG grid, because unstable SPP increases the fault current level. To analyse and overcome above mentioned issue, PSO (Particle Swarm Optimization) algorithm is used to optimize the single objective nonlinear constrained function. Single line diagram of IEEE-4 bus system and locations of five relays, R1 – R4 are shown in Figure 6.1. As per the fault current value and the state of connected SPP proper coordination in between these relays is desired. For fault location “A”, R2 behaves as a primary relay and R1 as a working backup relay. For fault location, “B”, R3 acts as a primary relay and R2, R1 as a backup relay. Similarly, for fault location “C”, R4 is primary relay and R3, R2 are backup relays. Limit of TMS is taken 0.01 to 1 for relay setting ( $0.01 \leq TMS \leq 1$ ). Table.6.6 & 6.7. shows the optimal relay tripping time and TMS for the primary as well as for backup relays. Coordination of relay setting is justified through the CTI calculation which is more than or equal to 0.3. It has been found that in case number 32, when a fault occurs at C location, backup relay takes more time to clear fault but satisfied the CTI constraint [122]. The result shown in table 6 shows that the relay setting is automatically changed as per the condition, because SPP never generates power for 24 hours. Thus as per the condition prevails, relay setting will be changed and the decision of this change is decided by PSO. The tripping time of relay for the fault occurrence at various locations is depicted in

Table 6.7. The results indicates that the tripping time of relay satisfy all the constraints.

**Table.6.6. TMS values for various cases (PSO)**

S.no	Type	TMS				
		R1	R2	R3	R4	R5
1	000	0.99	0.7653	0.5257	0.2534	0.01
2	100	0.99	0.7435	0.4854	0.2373	0.0104
3	010	0.99	0.7589	0.5048	0.2621	0.01
4	001	0.99	0.7505	0.4935	0.232	0.01
5	011	0.99	0.7562	0.4921	0.2376	0.01
6	111	0.99	0.749	0.4928	0.2621	0.01
7	101	0.99	0.7503	0.5161	0.2764	0.01
8	110	0.99	0.7519	0.4939	0.2539	0.01

The flow chart of relay setting is shown in figure 5.1. This flow chart defines the process of relay setting variation. Here, SPV is continuously observed, this observation process is carried out on MATLAB platform with the help of function block. The decision to change the setting of relay is taken as per SPV status. The setting of relay as per SPV status is given in table 6. The results obtained using different techniques viz. GA, interior point and SQP techniques are compared and tabulated in table 8. These results shows that, PSO gives better-optimized tripping time for the primary and backup relay. The convergence graph of relevant optimization algorithm is shown in figure 6.7. Here it is clear that PSO takes 35 iterations to reach best value. On the other hand GA and interior point algorithm takes 20 and 11 iteration, respectively.

**Table.6.7. Results of primary and backup relay tripping time for various cases.**  
 ((FL =Fault Location, PR= Primary Relay, BR= Backup Relay)

Cases	FL	PR	BR1	BR2	Tripping Time (PR) (sec)	Tripping Time (BR1) (sec)	Tripping Time (BR2) (sec)
9	A	R2	R1	-	1.0049	1.3131	-
10	A	R2	R1	-	0.9756	1.3122	-
11	A	R2	R1	-	0.9964	1.313	-
12	A	R2	R1	-	0.9855	1.3131	-
13	A	R2	R1	-	0.9929	1.313	-
14	A	R2	R1	-	0.9828	1.3121	-
15	A	R2	R1	-	0.9845	1.3122	-
16	A	R2	R1	-	0.9997	1.3295	-
17	B	R3	R2	R1	0.6954	1.0175	1.3295
18	B	R3	R2	R1	0.6421	0.9886	1.3296
19	B	R3	R2	R1	0.6687	1.0097	1.3305
20	B	R3	R2	R1	0.6537	0.9985	1.3305
21	B	R3	R2	R1	0.6524	1.0025	1.3258
22	B	R3	R2	R1	0.6504	0.9936	1.3265
23	B	R3	R2	R1	0.6734	0.9845	1.3122
24	B	R3	R2	R1	0.6533	0.9997	1.3295
25	C	R4	R3	R2	0.7901	1.6432	2.3921
26	C	R4	R3	R2	0.74	1.5174	2.3414
27	C	R4	R3	R2	0.8248	1.5921	2.3935
28	C	R4	R3	R2	0.7131	1.5209	2.3129
29	C	R4	R3	R2	0.7384	1.5327	2.3553
30	C	R4	R3	R2	0.809	1.5246	2.3339
31	C	R4	R3	R2	0.8496	1.5904	2.33
32	C	R4	R3	R2	0.8018	1.5631	2.3955

#### 6.1.4. Validation of results for adaptive algorithm for IEEE 4 bus system.

The difference in between the result obtained from ETAP, Typhoon hill and MATLAB are shown in table 6.9 & 6.10. Bus current for each bus, when no SPP connected, for case number 1, is listed in table 6.9. A close comparison of these results indicates that MATLAB simulation results shows a deviation of (0.079 to 1.01) % from ETAP results. Thus MATLAB results are practicable within a very small deviation. Similarly, the results of bus voltage variation for case number 6 when all three SPV are connected is shown table 6.10. These results shows that the percentage variation of simulation results are within 0.073 to 1.3%.

**Table.6.8: Result comparison with PSO, GA, SQP, interior point algorithms**

	TMS (Case 111)					
Relay \ Algorithm	R1	R2	R3	R4	R5	Iteration taken to reach optimal result
PSO [31]	0.990	0.7562	0.4921	0.2376	0.01	35
GA[32]	0.997	0.708	0.434	0.349	0.081	20
Interior point [33]	0.9273	0.7011	0.4774	0.1069	0.0100	11
SQP [34]	0.9272	0.7010	0.4773	0.1069	0.0100	4

**Table 6.9: Result comparison with ETAP for Case 1.**

<b>Bus</b>	<b>Phase</b>	<b>MATLAB RESULTS (Current in RMS) (Ampere)</b>	<b>ETAP RESULTS (Current in RMS) (Ampere)</b>	<b>Typhoon Hill RESULTS</b>	<b>Difference in %</b>
<b>Bus 1</b>	A	239.40∠-34.115	239.6∠ - 29.6	240.6∠ - 30.6	0.083
	B	239.40∠-154.17	239.6∠ - 149.6	240.6∠ - 148.6	0.083
	C	239.40∠-85.83	239.6∠ - 90.4	240.6∠ - 90.4	0.083
<b>Bus 2</b>	A	239.41∠ - 34.16	239.6∠ - 29.6	240.6∠ - 29.6	0.079
	B	239.46∠ - 154.18	239.6∠ - 149.6	240.6∠ - 149.6	0.079
	C	239.36∠ - 85.82	239.6∠90.4	240.6∠90.4	0.079
<b>Bus 3</b>	A	711.18∠ - 34.04	718.3∠ - 29.6	719∠ - 29.6	1.01
	B	711.18∠ - 154.06	718.3∠ - 149.6	719∠ - 149.6	1.01
	C	711.03∠85.94	718.3∠90.4	719∠90.4	1.01
<b>Bus 4</b>	A	711.18∠ - 34.04	718.3∠ - 29.6	719∠ - 29.6	0.991
	B	711.18∠ - 154.06	718.3∠ - 149.6	719∠ - 149.6	0.991
	C	711.18∠85.94	718.3∠ - 90.4	719∠ - 90.4	0.990

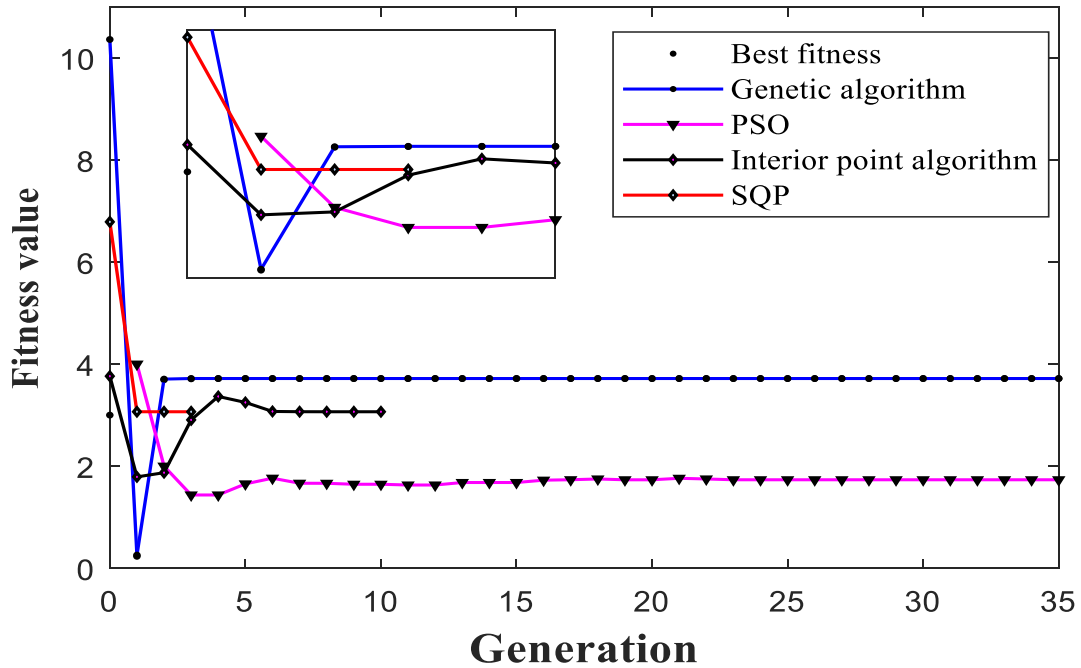


**Fig 6.7: Comparison of all optimization algorithms (GA,PSO,Interior point,SQP)**

**Table 6.10: Comparison of results with ETAP for Case 6.**

	Phase	MATLAB Voltage RMS	ETAP Voltage RMS	Difference in %
<b>Bus 1</b>	A	7156.55 $\angle$ 0.21	7200 $\angle$ 0	0.603472
	B	7159.55 $\angle$ - 119.79	7200 $\angle$ - 120	0.561806
	C	7153.56 $\angle$ 120.21	7200 $\angle$ 120	0.645
<b>Bus 2</b>	A	7077.5504 $\angle$ - 0.27	7122 $\angle$ - 0.257	0.624117
	B	7079.3029 $\angle$ - 120.27	7139 $\angle$ - 120.3	0.836211
	C	7073.4323 $\angle$ 119.72	7132 $\angle$ 119.65	0.821196
<b>Bus 3</b>	A	2298.9998 $\angle$ - 1.77	2269 $\angle$ - 3.16	1.32216
	B	2298.9477 $\angle$ - 121.80	2275 $\angle$ - 123.19	1.052646
	C	2297.8807 $\angle$ 118.20	2272 $\angle$ 116.75	1.139115
<b>Bus 4</b>	A	2029.5925 $\angle$ - 8.22	2023 $\angle$ - 7.82	0.325877
	B	2028.9573 $\angle$ - 128.24	2030 $\angle$ - 127	0.051365
	C	2027.4881 $\angle$ 111.76	2026 $\angle$ 112.13	0.07345

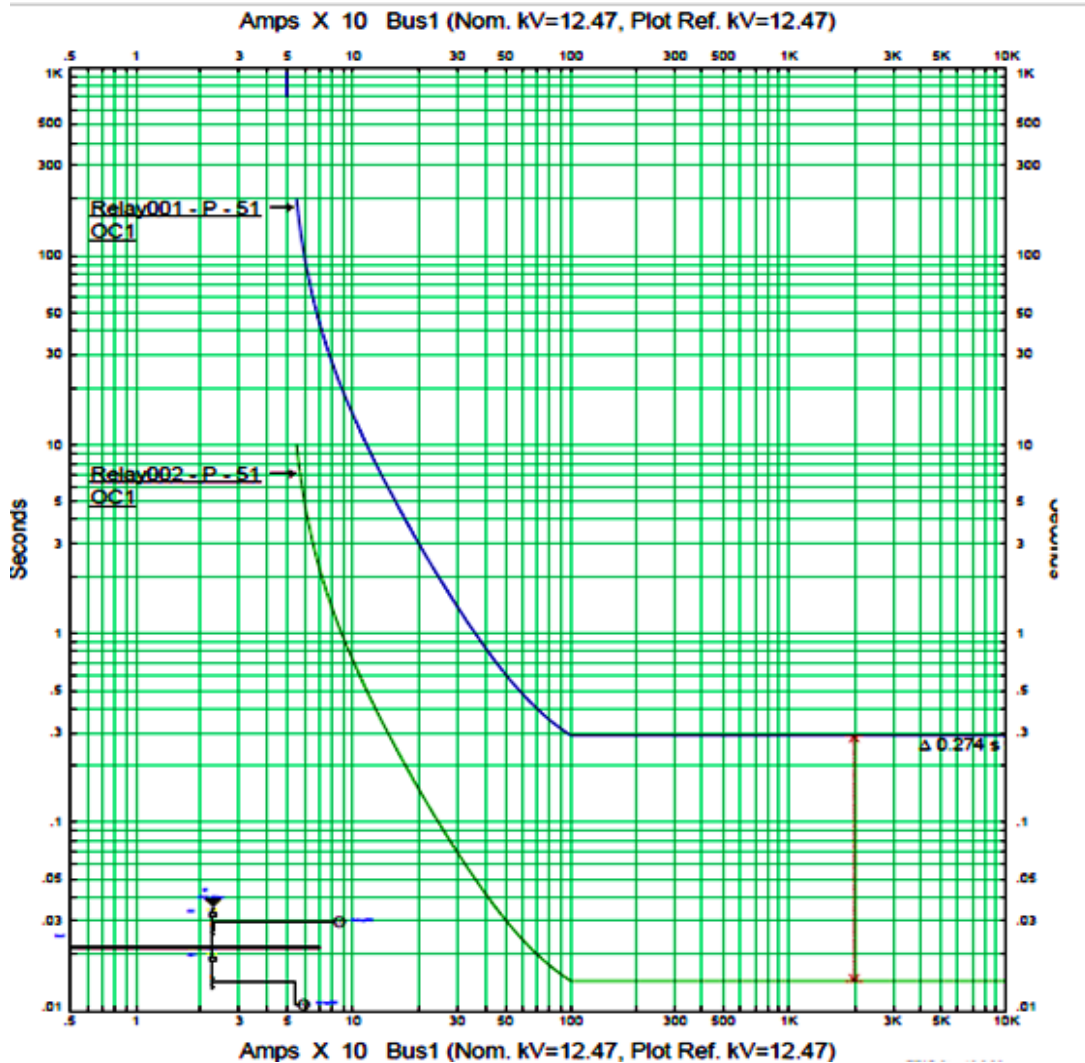


**Fig 6.8. TCC graph for solar connected case (111) with old setting of relay**

The TCC graph for solar connected case (111) with old setting is shown in figure 6.8. It is clear from this plot that for case (111), the CTI constraint is not satisfying when relay setting is the same. The value of CTI in between the relay 1 and 2 for this case is 0.274.

Generally the value of CTI should be higher than or equal to 0.3. This variation in CTI could be due to mal-operation of relays. Thus in such cases the relay co-ordination needs adjustment as per SPP integration. This modification done using PSO technique and identifying the optimized values of TMS/ TDS

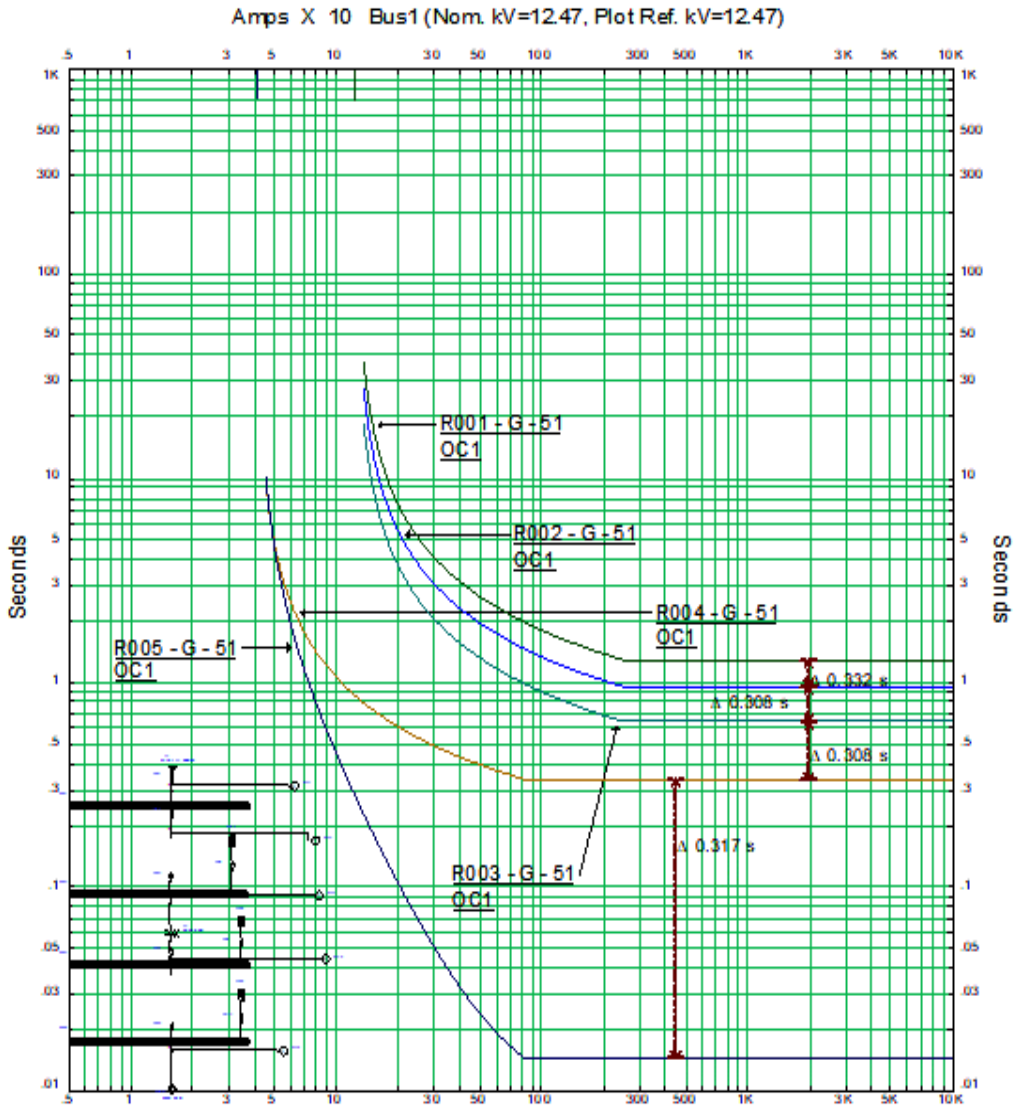


**Fig 6.9. ETAP time current characteristics of relay (TCC) for result validation of TMS**

The plot showing the ETAP time current characteristics of relay (TCC) for result validation of TMS is shown in figure 6.9. It is evident from this plot that for ground fault which occur at load side validates that the result for relay setting, derived through PSO is quite correct. The relay coordination when fault occurs at B location and relay satisfied the CTI (coordination time interval constraint) is shown in figure 6.10. Here the difference between ETAP and MATLAB results for ground fault occurring at location B, has been found to deviate by 10%.



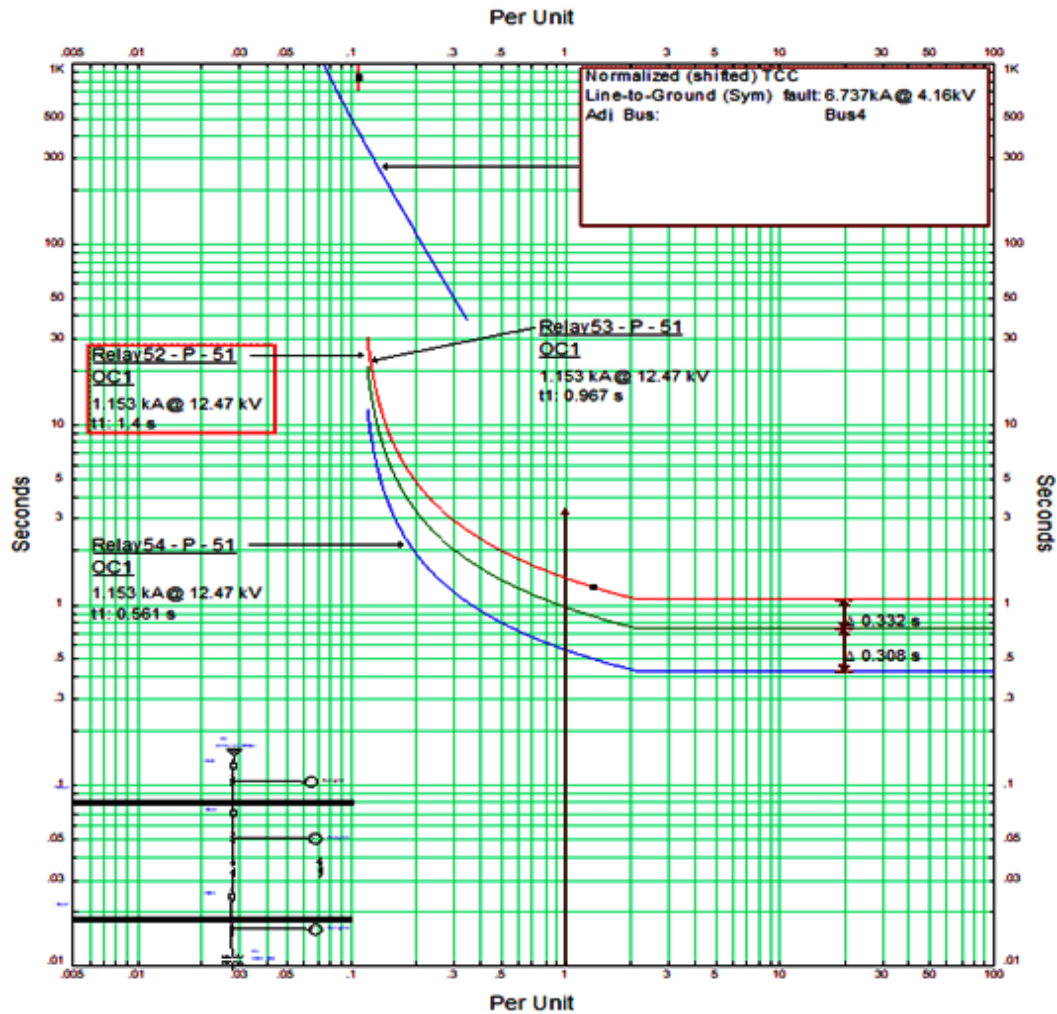


**Fig 6.10. Relay TCC graph and coordination for fault location at B**

The present study shows the simulation of IEEE node test model along with the three solar PV plant. The simulated results are verified by comparing with the ETAP results. It is found that the ETAP results validate the results obtained from MATLAB simulation. The simulated results are found unique and satisfy the permissible limits of variation. The results tabulated in table 6.5 shows that there is a drop in bus voltages when all three SPP contributes for the grid. The variation of voltage regulation in between case number 1 & case number 6 is of the order of 1.149% and current regulation in case of fault is 20.94%. These variation demands a change in the relay setting as per the DG connected in system. The coordination of relays is identified through PSO, GA, SQP and Interior point

algorithms. It is found that SQP takes less time to converge the results. The results shown in table 6.8 proves that PSO is capable to obtain the optimized results for “Optimal relay coordination model”. The result of PSO is validated on electrical transient analysis programming platform through time-coordination curve as shown in figure 6.8.

## **6.2. IEEE node 13**

### **6.2.1 IEEE 13 node grid parameter variation analysis**

Intermittent nature of PV when integrated inside a circulation network, creates the wavering in voltage and voltage unbalance of capricious nature. The significant variation between PV output voltage and bus voltage creates the issues of voltage rise, unbalance loading, flicker in the working system and poor power quality. Therefore in such situation the Distribution System Operator (DSO) plays a vital role to maintain the grid performance, especially when the massive penetration of solar PV get injected into the system [11][13][14][15][16]. Moreover, the extensive integration of PV generators increases the short circuit capacity of the system together with Total Harmonic Distortion (THD). The increase in short circuit current & harmonic variations has a straight impact on the coordination of protection devices. In fact the PV inverters are mainly responsible for an increase in THD, because of semiconductor devices [17][14]. As per IEEE 519 standards [18] [19], the permissible limit of THD in the network is of the order of 20%. If the THD exceeds the permissible value, it can damage the protection device and malfunctioning may occur.

Protection is a vital part of the power system network. This is essential to maintain system healthy. Any rise in short circuit level creates a change in the performance of Directional Overcurrent Relay (DOCR) and leads protection miscoordination [125][126][127]. Many techniques have been developed to bring down the level of short circuit current within the proper functioning limit of the protection scheme [128]. FCL technique is one of them which help to reduce the amount short circuit current. Using this technique the lifespan of gears is also maintained [129] [20][130].

### 6.2.1.1 Load flow

To investigate the load flow, IEEE 13 node feeder network has been considered for investigation. This operates at 4.16 kV line to line voltage [131]. The total associated operating load in the system is 3.4 MW and the reactive load is 2.1 MVAR. The load flow analysis was performed using the ETAP simulation software. The gauss seidel algorithm was used as a reference to examine the results. The solar PV plant is connected to the IEEE 13 node distribution feeder on nodes 680,675 and 634 is shown in Figure 6.11. The solar PV penetration level on three nodes is assumed to be the total load on the IEEE 13 node feeder in the ratio of 1(680):1(675):2(634). The total energy is consumed by the renewable energy source in the network. The six different levels of power injection considered for analysis are as follows:

- Case 1: The contribution from solar PV is zero per cent.
- Case 2: The solar PV contribution is 20% of the active load connected to the system.
- Case 3: The solar PV contribution is 40% of the active load connected to the system.
- Case 4: The solar PV contribution is 60 per cent of the active load connected to the system.
- Case 5: The solar PV contribution is 80 per cent of the active load connected to the system.
- Case 6: The solar PV contribution is 100 per cent of the active load connected to the system.

Case 1 refers to the base case where the solar power contribution is zero. Load flow calculation has been performed at each penetration level on the ETAP platform and the grid performance was calculated. The parameters to be considered are voltage variation, power factor and power loss calculation. Voltage variation in each case is shown in figure 6.12. The voltage of each bus is shown to increase

with an increase in solar PV penetration [17][6][18].

Table 6.11, shows the Solar PV-injected power level in all six cases. The total active and reactive load connected to the system is 3466 kW and 2102 kVAR. Table 6.11 also shows the voltage value in each case for solar PV (PV1, PV2, PV3) which is used as "PV1: PV2: PV3:: 1:1:2" penetration. To have the analyses the realistic conditions for solar PV penetration on distribution gird, 1:1:2 way of penetration is considered.

Systems are assumed to be balanced and thus can be represented through a single line diagram. The solution of load flow needs to build a matrix for admittance (n x n). Here n is the system number, the diagonal elements of the admittance matrix show self-admittance of the bus and the off-diagonal reflects mutual admittance between buses.

$$Y = \begin{bmatrix} Y_{11} & \dots & \dots & \dots & Y_{jk} \\ \dots & \dots & \dots & \dots & \dots \\ \dots & \dots & \dots & \dots & \dots \\ Y_{kj} & \dots & \dots & \dots & Y_{kk} \end{bmatrix} \quad (6.1)$$

Actual and reactive power determined by the initial Gauss Sidle and the specified voltage magnitude and angle of the particular bus. This non-linear equation (Gauss Sidle and Newton Raphson) can be solved by iteration methods. The real and reactive power as calculated using following equations [132][133] :

$$P_K^{c(x)} = \sum_{j=1}^n |V_k| |V_j| |V_{kj}| \cos(\phi_{kj} - \delta_k + \delta_j) \quad (6.2)$$

$$Q_K^{c(x)} = \sum_{j=1}^n |V_k| |V_j| |V_{kj}| \sin(\phi_{kj} - \delta_k + \delta_j) \quad (6.3)$$

The iteration will depend on the tolerance of the power mismatch calculated by their formulas:

$$\Delta P_K^x = P_k^{sc} - P_k^{c(x)} \quad (6.4)$$

$$\Delta Q_K^x = Q_k^{sc} - Q_k^{c(x)} \quad (6.5)$$

It should be noted that the busses are divided into three types : Slack ( $V$  &  $\delta$ ), Produced Bus (P&V) and Load Bus (P&Q constants). In other words, there are two iterations available to solve this problem. First of all, the measured real-and reactive-value requires internal iteration (eq 6.2 & 6.3) if the variables are taken up (at the beginning of the resolution method) and determined (at the beginning of the solution process). Second, external iterations which are necessary to find power inaccuracies intolerance (eq 6.4 & 6.5), i.e. increased precision iteration. Here the first iteration is known as calculation iterations, whereas the second iteration is known as precision iterations.

**Table 6.11. Level of solar PV penetration data for IEEE 13 node**

<b>PV Penetration Level in % &amp; values (All value in kW)</b>						
<b>Total active power load: 3466 kW Total reactive power load: 2102 kVAR</b>						
<b>Cases</b>	<b>1</b>	<b>2</b>	<b>3</b>	<b>4</b>	<b>5</b>	<b>6</b>
<b>Penetration in %</b>	<b>0%</b>	<b>20%</b>	<b>40%</b>	<b>60%</b>	<b>80%</b>	<b>100%</b>
<b>Total PV Power</b>	0	693.20	1386.4	2079.60	2772.80	3466.00
PV 1	0	173.30	346.60	519.90	693.20	866.50
PV 2	0	173.30	346.60	519.90	693.20	866.50
PV 3	0	346.60	693.20	1039.80	1386.40	1733.00

**Table 6.12. Solar PV panel parameters data for IEEE 13 node**

<b>Solar PV Parameters</b>	<b>Values</b>
<b>Module short-circuit current (Isc)</b>	5.96 A
<b>Module open-circuit voltage (Voc)</b>	64.2 V
<b>Module voltage and current at maximum power (Vmp , Imp)</b>	54.7 V, 5.58 A
<b>sun irradiance (MAX)</b>	1000 W/m <sup>2</sup>

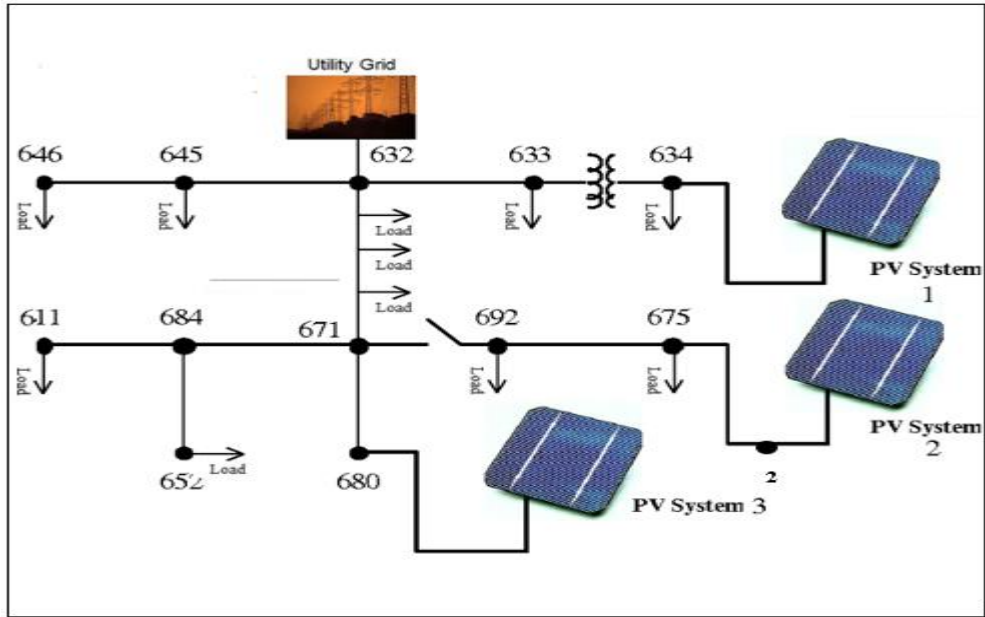


Fig 6.11. Integration of solar PV at node 675,680,634 in IEEE 13 node feeder.

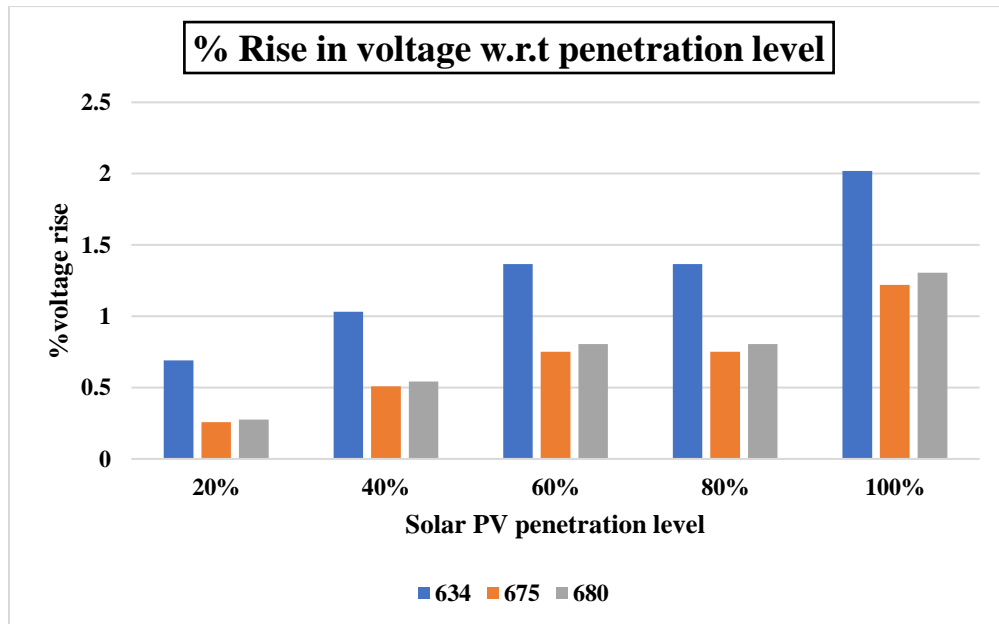


Fig 6.12 Percentage bus voltage rise at bus 634,675,680 when solar PV integrated with the network

### 6.2.1.2 Impact of solar PV DGs on IEEE 13 node distribution grid voltage.

The percentage rise in bus voltage when Solar PV is integrated with the network is calculated through simulation. The variation in bus voltage when the PV is integrated at node 634, 675 and 680 are shown in figure 6.12. It is clear that the variation is different at different level of solar penetration. Maximum variation is observed at node 634 at all level of penetration.

The evaluation was carried out in six different cases including solar photovoltaic for solar penetration inserted at bus 680, 675, 634. The voltage was measured on each bus for all the six cases and the results are shown in Table 1. The solar photovoltaic penetration range is between 0 and 3.4 MW.

The variation in voltage at each solar penetration level is shown in figure 6.12. It is evident that bus voltage varies with increased penetration of the PV and the highest voltage variance is observed at 100% solar penetration level [134].

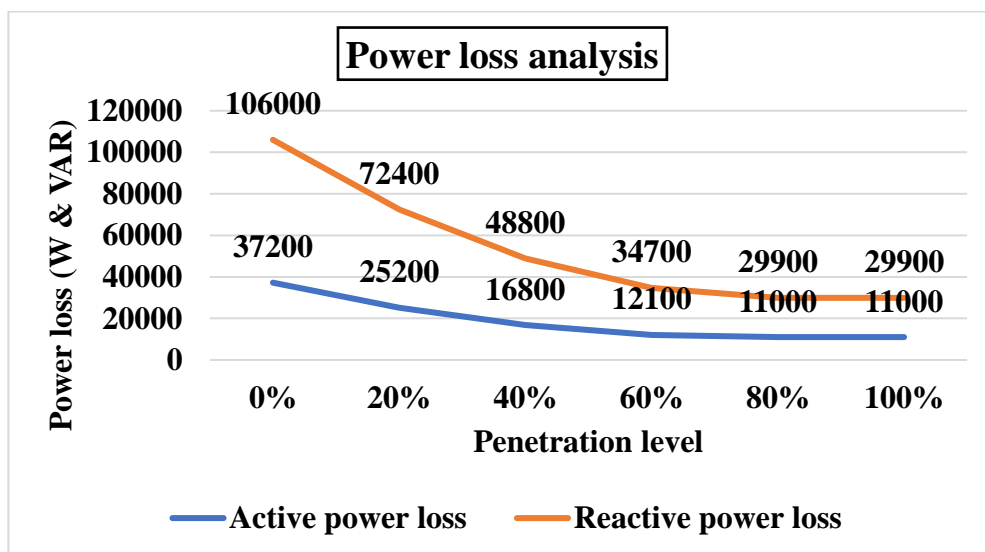


Fig 6. 13.. Active & reactive power losses for each case of solar PV penetration.

### 6.2.1.3 Impact of solar PV plant on distribution grid power losses.

In PV penetration analysis the power loss was calculated at different level of PV penetration and its variation is shown in figure 6.13. It is found that power loss can be classified as active and reactive power loss. It was found to decrease with the increase in PV penetration. In the present investigation, the active power losses decreases by around 32% for case number 2 (20% penetration), and by just about 40% for case number 3 (40% penetration). In case number 4 (60% penetration) the losses in the operating system decreased by approximately 67%. The losses in operating system have reduced by about 70% for the Case number 5 (80 % penetration) & for case number 6 (100 % penetration). In the reactive loss of power, i.e. the MVAR, a similar trend occurs.

**Table 6.13. Voltage at each bus of all six cases**

BUS VOLTAGES (kv)						
BUS NUMBER	Case 1	case 2	case 3	case 4	case 5	case 6
646	4.23	4.23	4.23	4.23	4.23	4.23
645	4.24	4.24	4.24	4.24	4.24	4.24
632	4.27	4.27	4.27	4.27	4.27	4.27
611	2.4	2.41	2.41	2.42	2.42	2.43
684	4.17	4.18	4.19	4.2	4.21	4.21
671	4.18	4.19	4.2	4.21	4.22	4.22
633	4.26	4.23	4.26	4.27	4.27	4.28
634	0.482	0.484	0.486	0.488	0.489	0.491
692	4.18	4.19	4.2	4.27	4.28	4.29
675	4.17	4.18	4.19	4.2	4.21	4.22
680	4.18	4.19	4.2	4.21	4.23	4.24

### 6.2.1.4 Impact on power factor concerning with solar PV.

Most of the PV inverters connected to the grid can only inject power at unit power factor, thereby generating active power only [18]. The power factor and power efficiency of the grid can be influenced by providing only active grid power through solar PV. The present study indicates that the power factor changes as the rate of solar photovoltaic penetration increases (671-632, 675-692) as shown in fig 6.14.. In such situations, many power factors are negative because of the flow of power is the opposite direction.



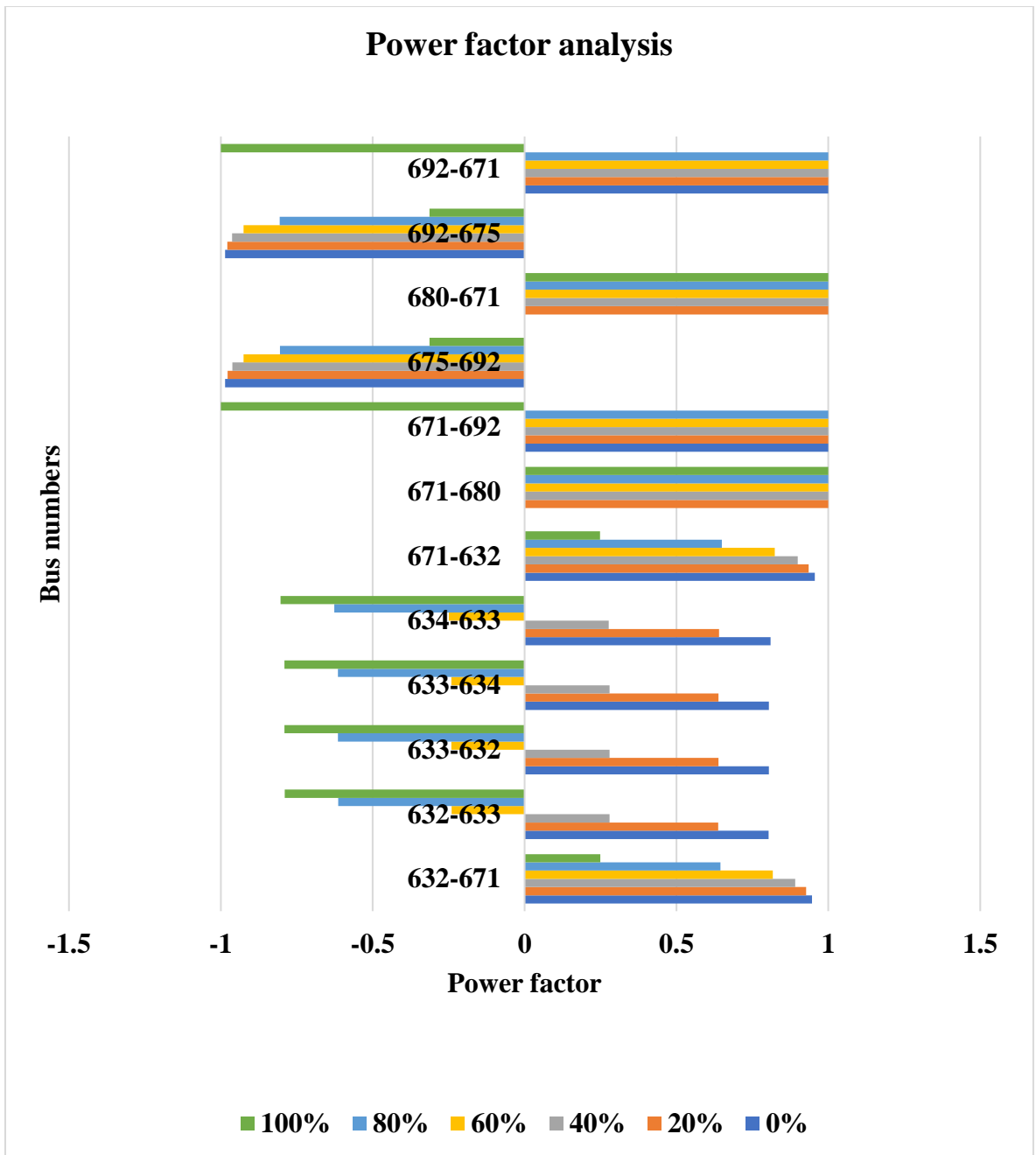


**Fig 6.14. Power factor variation at each line and bus concerning solar PV penetration**

### 6.2.1.5 THD (Total harmonic distortion)

Power quality is a factor for which every customer always shows its concern. The presence of harmonics often results poor quality. These harmonics can affect the electrical equipment and may cause unwanted tripping of relays. The distortions introduced due to the presence of harmonics are referred as

harmonic distortions. When harmonic distortion reaches the system and it is not possible to get rid from them, the capacity of the power system to operate at the optimal level has to be compromised. This causes inefficiency during the operations and causes power consumption. Some precautions must be taken by the power grid service providers to set and consider the tolerance level for maintaining the power quality and preventing power supply interruptions.

Power electronic devices used as power converters creates a problem in power quality such as the distortion of harmonics. The power output of the PV system depends solely on the use of inverters, solar irradiation and temperature that could influence electricity production, voltage and current profile. The PV system must be incorporated into the grid in compliance with the required requirements of the utility company. The standards IEEE 1547, IEC 61727 & EN 61000-3-2 and IEEE Standard 519-1992 define for the power quality. This causes voltage deformity at Common Coupling Point (PCC) in IEEE Standard 519-1992, THD voltage for each harmonic content is limited to 3 per cent and for circuits with an electrically rated 2.3 to 69 kV only 5 per cent THD is permissible. The point of common coupling (PCC) is known as the main point where PV is integrated into the system. It is recommended that, before a distributed resource such as PV is connected to the network, the system voltage distortion should be below 2.5 per cent and current distortion should below 20 per cent. The maximum amount of current injected into the grid is monitored under the standards IEEE 1547 & IEC 61727.

As shown in figure 6.15, the distortions are not available in case number 1, because the contribution of solar PV is zero. The distortion in the sign waveform due to harmonics injected due to solar PV are clearly visible in fig 6.16 To assess the distortions introduced due to the presence of harmonics, harmonics grid parameter needs to be measured. This parameter is expressed as the ratio of the RMS value of the harmonic components to the RMS basic values, and is expressed in per cent. This parameter is a measure of Total Harmonic Distortion (THD). This index is used to calculate variations in standard waveforms that contain harmonics [135][136][137]. The results of THD calculations at different penetration levels are shown in table 6.14, 6.15.

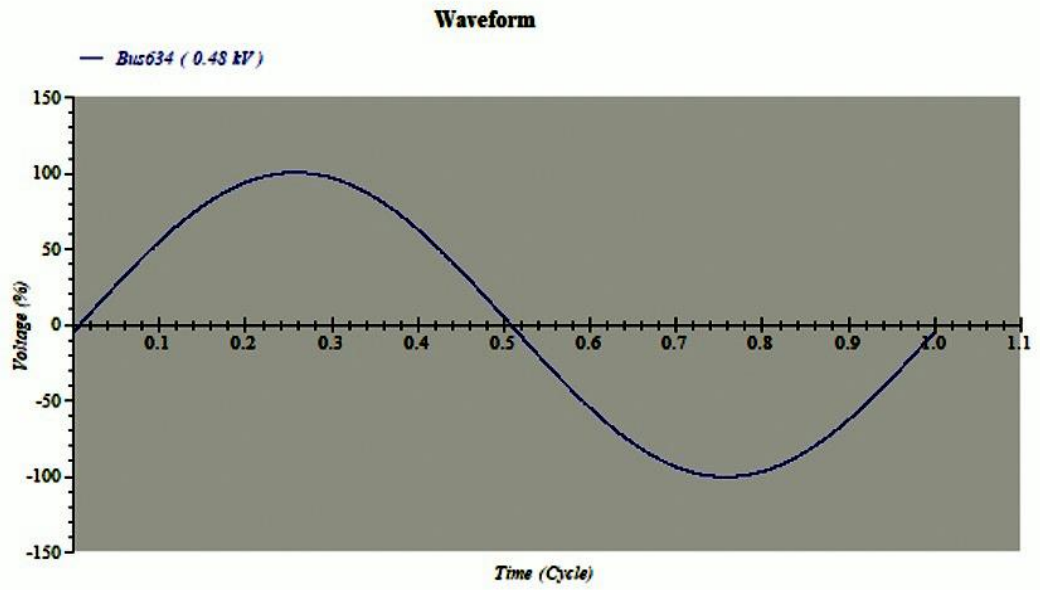


**Fig 6.15. voltage waveform for bus 634 when solar PV contribution is 0%**

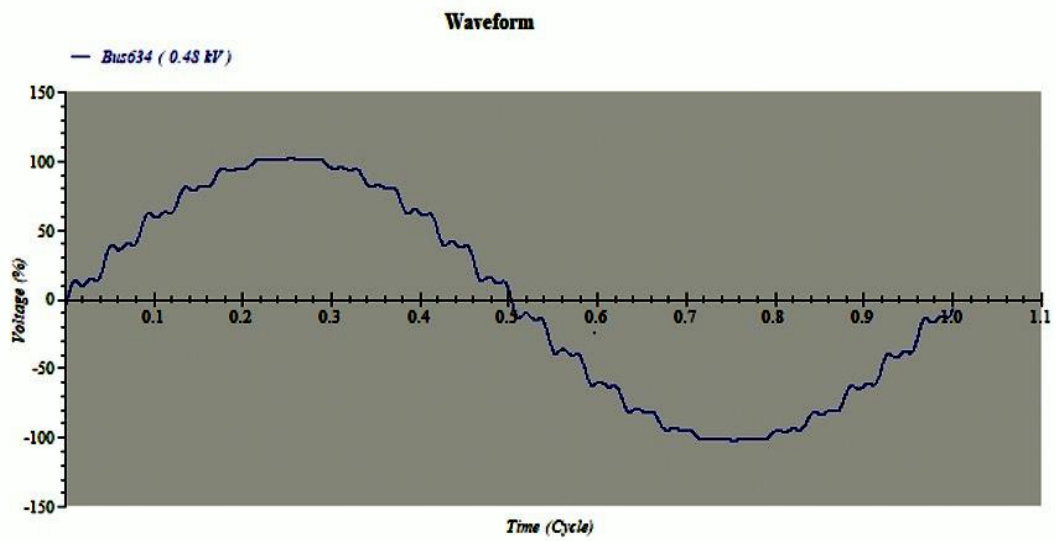


**Fig 6.16. Voltage waveform for bus 634 when solar PV contribution is 80%**

**Table 6.14. Total voltage harmonic distortion (THD) for each level of penetration**

Voltage harmonic distortion						
	Cases					
	C1	C2	C3	C4	C5	C6
<b>Bus</b>	0%	20%	40%	60%	80%	100%
<b>632</b>	0	0.02	0.08	0.10	0.14	0.18
<b>633</b>	0	0.07	0.12	0.19	0.25	0.31
<b>634</b>	0	1.26	2.50	3.72	4.92	6.10
<b>671</b>	0	0.09	0.19	0.28	0.37	0.46
<b>675</b>	0	0.20	0.40	0.60	0.79	0.98
<b>680</b>	0	0.24	0.48	0.72	0.95	1.18
<b>692</b>	0	0.09	0.19	0.28	0.37	0.46

It is clear from table 6.14 and 6.15 that THD is higher than the allowable limits of the standard system IEEE 159. For case number 5 & 6, the prescribed THD limits for current harmonic distortion are 20% and for voltage harmonic distortion this permissible limit is 2.5%.

The results indicate that the current THD on bus 671,675 & 692 for case number 5 & 6 are higher than the THD threshold value. In the THD voltage analysis in bus 634, its value for case number 4 was found to be 3.72% which higher than that of a threshold value, but below the rated value of connected devices. The THD value of case number 5 & 6 is 4.92% & 6.10% respectively, which is greater than that of connected rated devices. This indicates that it is a warning to the service provider. All the THD analysis show that the maximum bearing capacity of PV on the grid is at 60% penetration level. The connection with more than 60% PV penetration are possible only with the implementation of harmonic filters.

The harmonic filter was used mainly for the case number 5 and 6 to minimize the harmonic percentage. Electrical transient analysis software tool was used for filter analysis. The 0.2 Mvar rated harmonic filter was used at bus 634 for reducing the THD voltage. After the implementation filter, THD voltage

was found to be 0.9% for case number 5 and 1.15% for case number 6. After the implementation of filter THD current for bus 671,675 & 692 was reported as 6.55%, 6.91% & 4.91%, respectively.

The analysis of the THD spectrum is shown for both the cases six with filter and without filter. The results without filter are shown in Figure 6.17 whereas with filter they are shown in figure 6.18. The current THD amplitude was found higher for the Case number 5 as shown in figure 6.17. Voltage THD Amplitude with filter is shown in Figure 6.18.

The graphical THD variance analysis is shown in figures 6.17 and 6.18. The maximum harmonic variation in voltage is observed for bus 634, and for bus 671-692, 675-692 maximum harmonic current variation is observed. The analysis shows that when PV penetration increases more by 60 per cent, maximum harmonics occur, which is not permissible in compliance with IEEE and IEC Guidelines.

**Table 6.15. Total current harmonic distortion (THD) for each level of penetration**

Bus numbers		Current harmonic distortion (All values in percentage)					
		Cases					
From bus	To bus	0%	20%	40%	60%	80%	100%
632	671	0	0.17	0.41	0.79	1.41	2.23
	633	0	1.10	2.74	4.14	4.45	4.25
633	632	0	1.10	2.74	4.14	4.45	4.25
	634	0	1.10	2.74	4.14	4.45	4.25
634	633	0	1.10	2.74	4.14	4.45	4.25
671	632	0	0.17	0.41	0.79	1.41	2.23
	680	0	5.66	5.66	5.66	5.66	5.66
	692	0	2.52	6.16	11.93	22.45	47.73
675	692	0	3.03	7.76	16.03	32.71	64.49
680	671	0	5.66	5.66	5.66	5.66	5.66
692	675	0	3.03	7.76	16.03	32.71	64.49
	671	0	2.52	6.16	11.93	22.45	47.73

The graphical THD variance analysis are shown in figures 6.17 and 6.18. The maximum harmonic variation in voltage is observed for bus 634, and for bus 671-692, 675-692 maximum harmonic current variation is observed. The analysis shows that when PV penetration increases by more than 60 per cent,

maximum harmonics occur, which is not permissible in compliance with IEEE and IEC Guidelines.

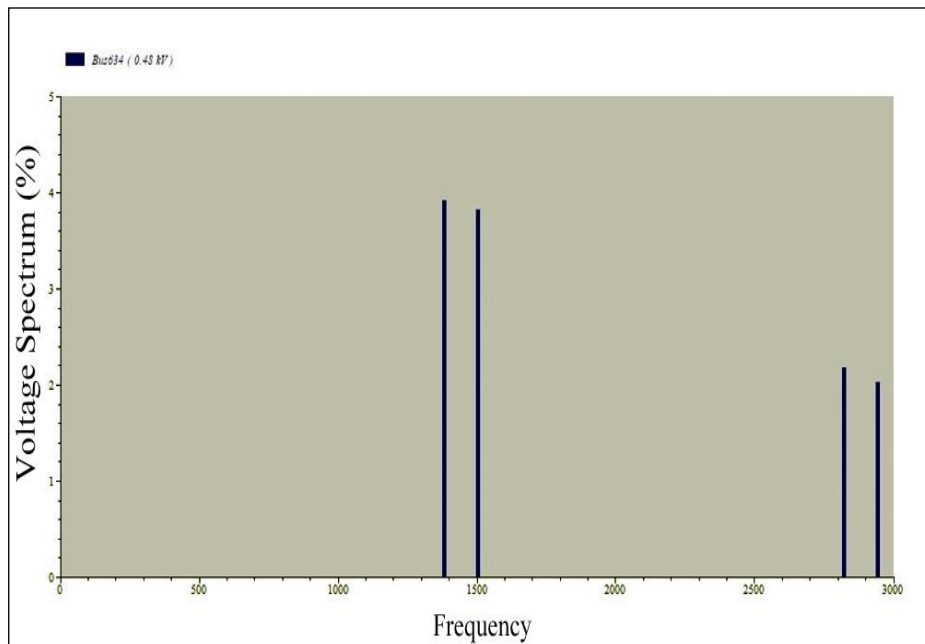


**Fig 6.17. Voltage spectrum showing harmonics at a different frequency for bus 634 without using the filter**

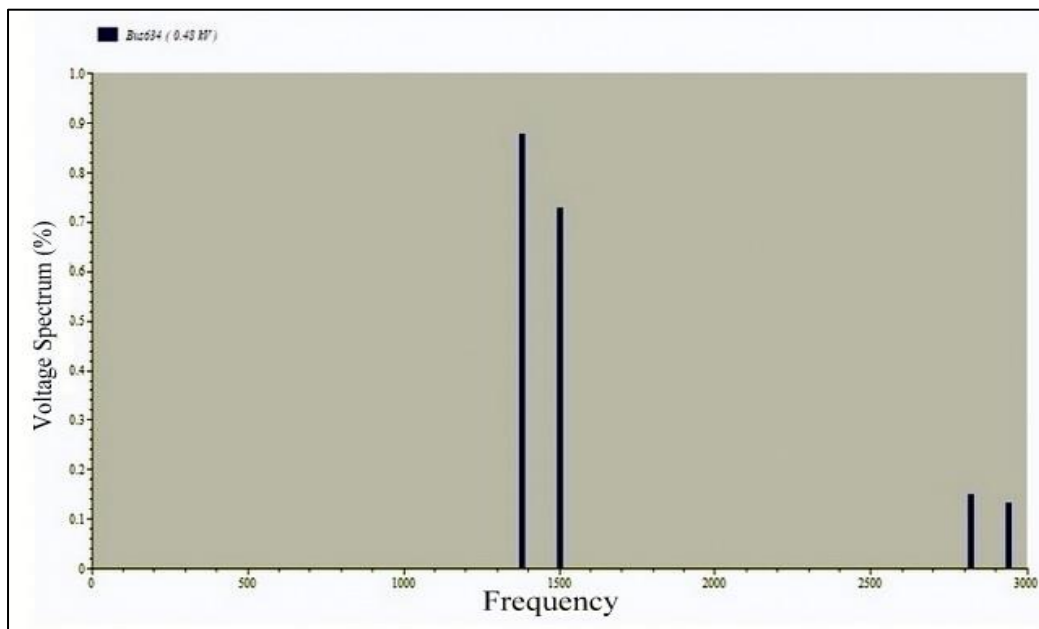


**Fig 6.18. Voltage spectrum after using the filter at bus 634**

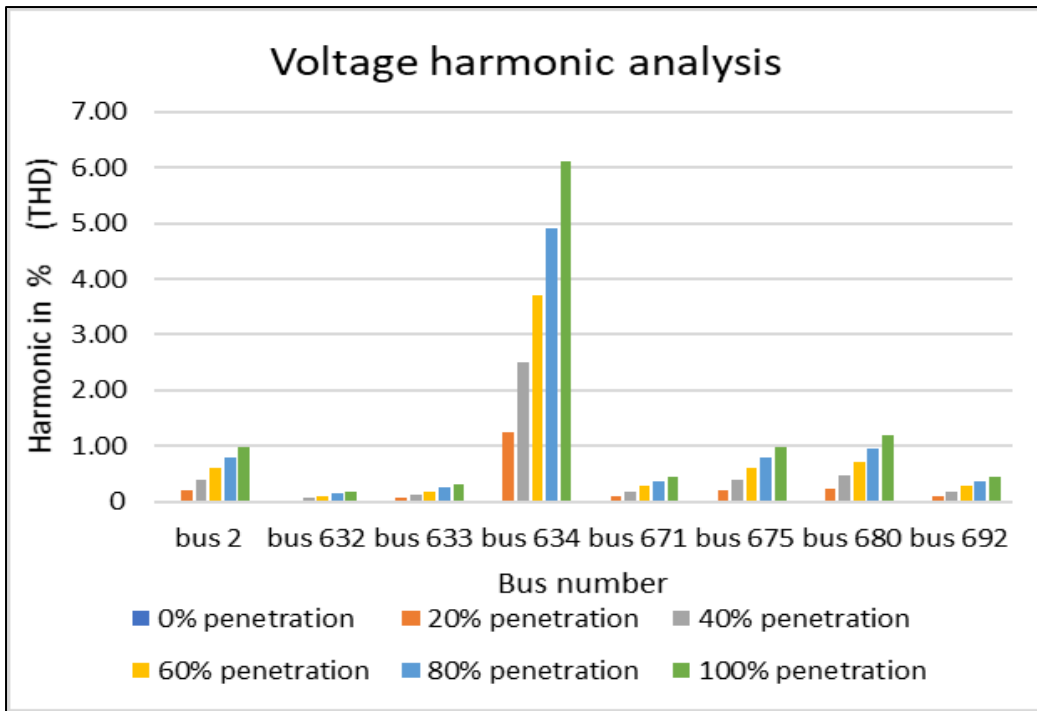


**Fig 6.19. Graphical analysis of voltage THD at every penetration level**

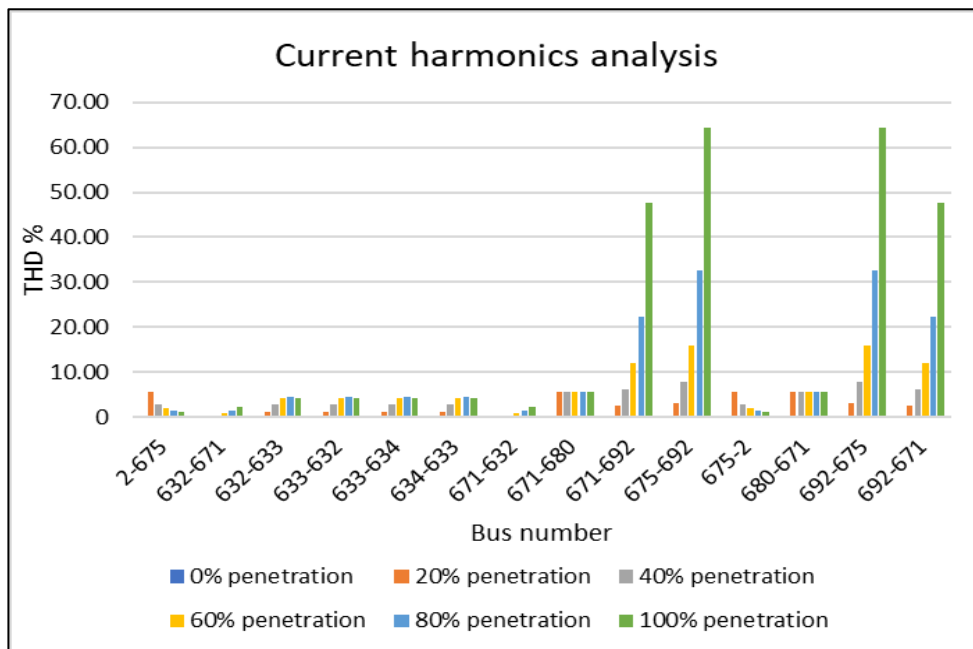


**Fig 6.20. Graphical analysis of current THD at every penetration level**

### 6.2.1.6 Solar PV impact on short circuit current

The big challenge for power distribution is the short circuit (SC) current variability. The security systems are not able to fulfil obligations in time because of SC variation. The three phase short circuit current study is carried out for all penetration situations. The result of this current analysis is given in Table 6.16.

In this study, it is observed an increase in the fault currents when the solar penetration level increases. For the highest level of penetration, the maximum fault current is observed to be 5.77 kA and the lowest fault current. In IEEE 13 node standard system both single-phase line and three-phase line present. For single-phase line, line to ground fault and for two-phase line to line fault was considered for the SC current analysis. For the IEEE 13 node network, the Bus 645,646,611,684,652 contains one phase and two-phase lines. In the present study for these busses, line to ground fault and line to line faults are taken into account.

**Table 6.16. Analysis of fault current for each solar PV penetration case.**

<b>FAULT CURRENT (kA)</b>						
<b>BUS NO.</b>	<b>CASE 1 (0%)</b>	<b>CASE 2 (20%)</b>	<b>CASE 3 (40%)</b>	<b>CASE 4 (60%)</b>	<b>CASE 5 (80%)</b>	<b>CASE 6 (100%)</b>
646	1.551	1.557	1.566	1.578	1.595	1.614
645	1.67	1.68	1.693	1.71	1.73	1.75
632	0.139	0.217	0.341	0.467	0.613	0.75
611	1.59	1.611	1.631	1.659	1.693	1.73
684	1.99	2.004	2.023	2.049	2.079	2.113
671	0.137	0.215	0.338	0.473	0.61	0.784
633	0.138	0.216	0.339	0.471	0.606	0.74
634	1.148	1.773	2.753	3.782	4.796	5.77
692	0.137	0.215	0.338	0.473	0.61	0.748
675	0.137	0.214	0.337	0.469	0.605	0.741
680	0.136	0.213	0.336	0.469	0.606	0.743
652	1.354	1.35	1.354	1.363	1.377	1.394



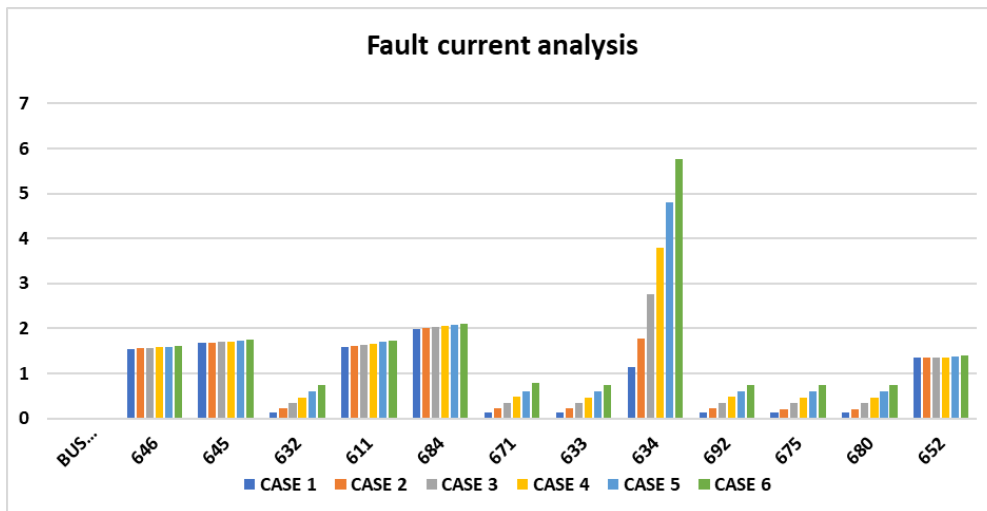


**Fig 6.21. Fault current analysis for IEEE 13 node distribution feeder**

In this section the study is focussed on the solar PV penetration impact on distribution grids. This study examined the detailed effect of solar PV on voltage profiles, voltage imbalances, network stability and the effect of harmonics on grid operation. It is evident from the present study that distribution feeders are starting to experience voltage flickers between 40 to 60 per cent penetration & also witness the maximum THD level after reaching 60% penetration. There is no specific way to estimate the safe degree of solar penetration for distribution systems. Hence for this reason each individual systems must be studied. Safe penetration rates depend on feeder topology, load profile, solar light / cloud patterns and finally on number of harmonics.

The maximum allowed solar share is the point at which voltage increases, flicker problems begin, and the harmonic value exceeds the standard maximum limit (IEEE 519). This study also reveals that increase of solar penetration reduces the power losses of the system which is helpful to cater more consumer demand.

An increased penetration reduces the power losses. On the other hand it increases the short circuit current level, which creates the issue of relay maloperation. However, the increased THD and short circuit current effects can be mitigated through implementation of adaptive & non adaptive protection techniques.

### **6.2.2. Relay coordination solution for IEEE 13 node Solar PV integration distribution grid**

DOCRs are easiest and cheapest, but they are the most difficult to implement. They can quickly reset as the system changes. At the same time, they are mostly implemented in the distribution network, which is the most dynamic part of the entire power system. Any improper operation of these may result in improper actions which affect their sensitivity and selectivity. Since DOCRs are frequently used, to meet the basic requirements of sensitivity, selectivity, reliability and speed [12], Real-time coordination is proposed in this study. An idea is to organize DOCRs online which, as a result, will boost the fulfilment of the basic requirements listed above. The write or built real-time algorithm, firstly the data is updated data from the current system changes, then computes load flow and then perform fault analysis to obtain the input data for the optimization algorithms.

Conventional approaches and optimization strategies commonly used to evaluate relay settings [138]. In the traditional approach all fault currents are predestined for abnormal situations and system contingencies. Standard methods are based on a network topology that requires a graphical selection process, specification of the minimum breakpoint range and linear graph theory [139].

In power grids the synchronization of relays with numerous distributed generators is impossible by traditional techniques [46]. Optimization methods are often designed to reduce the total estimated time of the relays that are subjected to constraints [124]. Such techniques cannot solve complex problems, specifically in the case of large interconnected ring structures, and the results obtained for large networks can be held within local minimum values [140]. The coordination problem is always established as a non - linear programming approach in which the PS and TMS are continuously measured [141]. Several heuristic optimization methods, such as genetic algorithms ( GAs) [44], particle swarm optimization techniques [31], differential evolution algorithms (DEs) [142] and ant colony optimization [61] are reported in literature. These methods are used in the past and produces better results but are time - consuming. The

problem of relay coordination is therefore overcome by adding appropriate penalty functions to large interconnected networks [143][139]. This study introduces a new optimization approach based on GWO-PSO and GWO algorithms. These optimization techniques are used to calculate relay TMS and optimized FCL impedance, which helps to maintain the relay protection strategy.

The solution mainly requires algorithm which provide a solution in a fast and finite time frame that meets the defined requirement of the model. Results for comparative analysis for OCR coordination problem are computed using, WCA, GWO, GWO-PSO, and Interior Point algorithm. Constrained based optimization technique is preferred to solve this kind of problem. In this model, all the constraints are defined for the optimization of the TMS value of overcurrent relay. Relay reaction time is dependent on the TMS value.

#### **6.2.2.1. Impedance Fault current limiter (Zfcl) optimization using GWO & GWO-PSO for IEEE 13 node**

Fault current limiter parameter optimization focused mainly on Z, X, R parameters that play a vital role in limiting the increased fault current. But if the impedance is very high, the system operator's difficulty increases, especially when the grid in operating state.

Table 6.17 shows the optimized value of Zfcl with respect to the increase of the fault current and all the results found to be feasible and satisfied with all the particle limitations of the optimum relay coordination model. The maximum value of Zfcl is 89.5347 ohms, which is higher than the limit of Zfcl max i.e. (60 ohms).

Table 6.18 tabulated the results of the GWO-PSO hybrid optimization and showed that all results met all the practical constraints of the optimal relay coordination model. The maximum value of Zfcl was found to be 89.52467 ohms. In both algorithms, it was found that at case-5 & 6 Zfcl max exceeds the limit. So, for these cases protection switch towards the adaptive protection scheme strategy for optimal relay coordination.

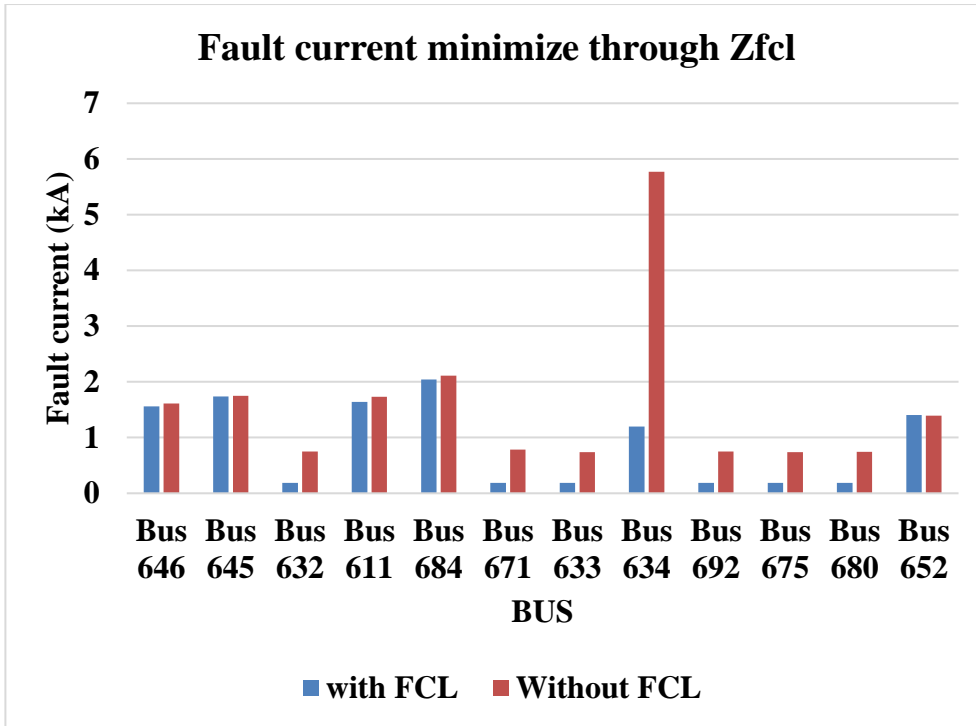


Figure 6.22. Representation of Zfcl fault current minimization for IEEE 13 node

**Table 6.17: Zfcl size optimization for IEEE Node 13 Using GWO for IEEE 13 node**

Zfcl No.	CASE 2			Case 3			Case 4			case 5			Case 6		
	Z	R	X	Z	R	X	Z	R	X	Z	R	X	Z	R	X
<b>1</b>	0.00609	0.00119	0.00597	0.01513	0.00297	0.01483	0.02702	0.0053	0.0265	0.04356	0.00854	0.04272	0.06164	0.01209	0.06045
<b>2</b>	0.00873	0.00171	0.00856	0.01993	0.00391	0.01954	0.03431	0.00673	0.03364	0.05087	0.00998	0.04988	0.06705	0.01315	0.06575
<b>3</b>	6.33388	1.24218	6.21088	10.4383	2.04713	10.2356	12.3763	2.4272	12.136	13.6255	2.67232	13.3609	14.3554	2.81534	14.0766
<b>4</b>	0.02008	0.00394	0.01969	0.03872	0.00759	0.03797	0.06407	0.01257	0.06283	0.09372	0.01838	0.0919	0.12466	0.02445	0.12224
<b>5</b>	0.0086	0.00169	0.00843	0.02008	0.00394	0.01969	0.03544	0.00695	0.03475	0.05269	0.01033	0.05167	0.07165	0.01405	0.07026
<b>6</b>	6.48612	1.27203	6.36016	10.6318	2.08507	10.4254	12.7001	2.49071	12.4535	13.8631	2.71878	13.5939	14.7543	2.89356	14.4677
<b>7</b>	6.40931	1.25697	6.28484	10.5237	2.06387	10.3193	12.5486	2.46099	12.3049	13.707	2.68818	13.4409	14.4389	2.83172	14.1585
<b>8</b>	0.75211	0.1475	0.7375	1.24387	0.24394	1.21972	1.48594	0.29142	1.45709	1.62287	0.31827	1.59135	1.70908	0.33518	1.67589
<b>9</b>	6.48612	1.27203	6.36016	10.6318	2.08508	10.4254	12.7001	2.4907	12.4535	13.8631	2.71885	13.5939	14.6039	2.86407	14.3203
<b>10</b>	6.43289	1.2616	6.30796	10.6103	2.08086	10.4043	12.6559	2.48203	12.4102	13.83	2.71252	13.5613	14.573	2.85799	14.29
<b>11</b>	6.51061	1.27684	6.38418	10.7202	2.1024	10.512	12.7874	2.50782	12.5391	13.9681	2.73936	13.6968	14.7133	2.88553	14.4276
<b>12</b>	0.00134	0.00026	0.00131	0.00134	0.00026	0.00131	0.01194	0.00234	0.01171	0.03022	0.00593	0.02963	0.05191	0.01018	0.0509
$\Sigma$	39.4559	7.73794	38.6896	64.8952	12.727	63.635	77.4271	15.1848	75.9235	84.7507	16.6214	83.1048	89.5247	17.5573	87.7862

**Table 6.18: Optimization of Zfcl parameters using GWO-PSO algorithm for IEEE 13 node**

Zfcl No.	CASE 2			Case 3			Case 4			case 5			Case 6		
	Z	R	X	Z	R	X	Z	R	X	Z	R	X	Z	R	X
1	0.00609	0.00119	0.005967	0.01513	0.00297	0.014833	0.02702	0.0053	0.026496	0.04356	0.00854	0.042718	0.06164	0.01209	0.060445
2	0.00873	0.00171	0.008561	0.01993	0.00391	0.019538	0.03431	0.00673	0.033642	0.05087	0.00998	0.049879	0.06705	0.01315	0.065746
3	6.33388	1.24218	6.210875	10.43834	2.04713	10.23564	12.37632	2.42721	12.13598	13.6255	2.67219	13.3609	14.35537	2.81532	14.0766
4	0.02008	0.00394	0.019691	0.03872	0.00759	0.037972	0.06407	0.01257	0.062826	0.09372	0.01838	0.0919	0.12466	0.02445	0.122241
5	0.0086	0.00169	0.008432	0.02008	0.00394	0.019688	0.03544	0.00695	0.034753	0.05269	0.01033	0.051667	0.07165	0.01405	0.070256
6	6.48613	1.27207	6.360163	10.63184	2.08509	10.42537	12.7001	2.4907	12.45347	13.86309	2.71878	13.59388	14.75425	2.89355	14.46773
7	6.40931	1.25697	6.284844	10.52366	2.06386	10.31929	12.54855	2.46098	12.30487	13.70704	2.68818	13.44085	14.43893	2.83171	14.15854
8	0.75211	0.1475	0.7375	1.24387	0.24394	1.219719	1.48594	0.29142	1.457086	1.62287	0.31827	1.591353	1.70908	0.33518	1.675888
9	6.48613	1.27208	6.360163	10.63184	2.08511	10.42537	12.70009	2.49069	12.45347	13.86309	2.71878	13.59388	14.60389	2.86406	14.32029
10	6.43288	1.26159	6.307962	10.61035	2.08096	10.40428	12.65593	2.48203	12.41016	13.82991	2.71228	13.56134	14.57295	2.858	14.28996
11	6.51061	1.27684	6.384177	10.72016	2.1024	10.51198	12.78739	2.50781	12.53907	13.96805	2.73938	13.6968	14.71331	2.88553	14.42759
12	0.00134	0.00026	0.001309	0.00134	0.00026	0.001309	0.01194	0.00234	0.011713	0.03022	0.00593	0.029628	0.05191	0.01018	0.050899
Σ	39.45589	7.73802	38.68964	64.89526	12.72716	63.635	77.4271	15.18473	75.92352	84.75061	16.62102	83.1048	89.52469	17.55727	87.78617

It is clearly shown in Figure 6.17 that the optimized value of Zfcl is capable of limiting the current under the given constraint. The figure shows all the Zfcl-based fault current with and without FCL. The difference between both currents is seen in graph and also shows that Zfcl is decreasing the fault current level.

**Table 6.19. Relay TMS optimization for IEEE Node 13 Using Interior point algorithm**

Relay no.	Case 1	Case 2	Case 3	Case 4	Case 5	Case 6
<b>R1</b>	0.02521	0.0254	0.02957	0.02356	0.02687	0.02501
<b>R2</b>	0.53369	0.53348	0.621	0.49483	0.56434	0.52514
<b>R3</b>	0.01998	0.01911	0.028	0.02313	0.02285	0.02342
<b>R4</b>	0.41953	0.40137	0.58792	0.48571	0.47976	0.49176
<b>R5</b>	0.27812	0.61768	0.89122	0.9712	0.91776	0.99923
<b>R6</b>	0.15451	0.34353	0.49512	0.53955	0.50987	0.55513
<b>R7</b>	0.0309	0.06871	0.09902	0.10791	0.10197	0.11103
<b>R8</b>	0.1099	0.10443	0.09894	0.09165	0.08177	0.09277
<b>R9</b>	0.13984	0.39606	0.54468	0.5292	0.49637	0.53485
<b>R10</b>	0.37991	0.40973	0.39919	0.34434	0.46188	0.53892
<b>R11</b>	0.47544	0.50673	0.44362	0.39619	0.51021	0.58492
<b>R12</b>	0.64069	0.63676	0.65095	0.58507	0.60769	0.64923
<b>R13</b>	0.12814	0.12735	0.13019	0.11701	0.12154	0.12985
<b>R14</b>	0.61824	0.6195	0.58714	0.57802	0.61559	0.6319
<b>R15</b>	0.12373	0.1239	0.11743	0.1156	0.12312	0.12638
<b>R16</b>	0.0309	0.06871	0.09902	0.10791	0.10197	0.11103
<b>R17</b>	0.15311	0.37247	0.13039	0.39753	0.72801	0.90865
<b>R18</b>	0.08504	0.20693	0.07244	0.22085	0.40767	0.5048
<b>R19</b>	0.01211	0.05408	0.01904	0.04821	0.08302	0.10933
<b>R20</b>	0.01055	0.27042	0.09518	0.24104	0.4151	0.54664
<b>R21</b>	0.11425	0.10062	0.09877	0.09027	0.08523	0.09601
<b>R22</b>	0.15698	0.13774	0.13029	0.11916	0.11082	0.11305
<b>R23</b>	0.09509	0.10135	0.08872	0.07924	0.10204	0.11694

TMS optimized relay values obtained by interior point algorithms are given in Table 6.19. These results are found feasible and met all the practical constraints of the current relay. The TMS relay values are also capable of

maintaining the coordination time interval (CTI) which is essential for a healthy running of the network.

**Table 6.20. Relay TMS optimization for IEEE Node 13 Using GWO algorithm**

TMS optimization using GWO						
Relayno.	Case 1	Case 2	Case 3	Case 4	Case 5	Case 6
<b>R1</b>	0.02541	0.0254	0.02957	0.02356	0.02687	0.02501
<b>R2</b>	0.53369	0.53348	0.621	0.49483	0.56434	0.52514
<b>R3</b>	0.01998	0.01911	0.028	0.02313	0.02285	0.02342
<b>R4</b>	0.41953	0.40137	0.58792	0.48571	0.47976	0.49176
<b>R5</b>	0.27818	0.61799	0.89159	0.97157	0.91798	0.99987
<b>R6</b>	0.15455	0.3437	0.49514	0.53962	0.50993	0.5553
<b>R7</b>	0.0309	0.06871	0.09902	0.10791	0.10197	0.11103
<b>R8</b>	0.1099	0.10443	0.09894	0.09165	0.08177	0.09277
<b>R9</b>	0.13987	0.39625	0.5447	0.52926	0.49643	0.53502
<b>R10</b>	0.38	0.40992	0.3992	0.34439	0.46193	0.5391
<b>R11</b>	0.47556	0.50697	0.44364	0.39624	0.51027	0.5851
<b>R12</b>	0.64084	0.63707	0.65098	0.58515	0.60777	0.64944
<b>R13</b>	0.12814	0.12735	0.13019	0.11701	0.12154	0.12985
<b>R14</b>	0.61839	0.6198	0.58717	0.57808	0.61567	0.63211
<b>R15</b>	0.12373	0.1239	0.11743	0.1156	0.12312	0.12638
<b>R16</b>	0.0309	0.06871	0.09902	0.10791	0.10197	0.11103
<b>R17</b>	0.15311	0.37266	0.13045	0.39768	0.72819	0.90923
<b>R18</b>	0.08504	0.20703	0.07244	0.22088	0.40772	0.50497
<b>R19</b>	0.01211	0.05408	0.01904	0.04821	0.08302	0.10933
<b>R20</b>	0.01055	0.27055	0.09519	0.24107	0.41515	0.54682
<b>R21</b>	0.11425	0.10062	0.09877	0.09027	0.08523	0.09601
<b>R22</b>	0.15698	0.13774	0.13029	0.11916	0.11082	0.11305
<b>R23</b>	0.09509	0.10135	0.08872	0.07924	0.10204	0.11694



**Table 6.21. Relay TDS optimization for IEEE Node 13 Using GWO-PSO algorithm**

<b>TMS optimization using GWO-PSO</b>						
<b>Relay no.</b>	<b>Case 1</b>	<b>Case 2</b>	<b>Case 3</b>	<b>Case 4</b>	<b>Case 5</b>	<b>Case 6</b>
<b>R1</b>	0.02544	0.0254	0.02957	0.02356	0.02687	0.02501
<b>R2</b>	0.53369	0.53348	0.621	0.49483	0.56434	0.52514
<b>R3</b>	0.01998	0.01911	0.028	0.02313	0.02285	0.02342
<b>R4</b>	0.41953	0.40137	0.58792	0.48571	0.47976	0.49176
<b>R5</b>	0.27823	0.61911	0.8913	0.97131	0.91829	0.99991
<b>R6</b>	0.15454	0.34378	0.4952	0.53962	0.51023	0.55557
<b>R7</b>	0.0309	0.06871	0.09902	0.10798	0.10197	0.11103
<b>R8</b>	0.1099	0.10443	0.09894	0.0917	0.08177	0.09277
<b>R9</b>	0.13986	0.39634	0.54477	0.52926	0.49673	0.53528
<b>R10</b>	0.37998	0.41002	0.39925	0.34439	0.46221	0.53935
<b>R11</b>	0.47554	0.50709	0.44369	0.39624	0.51057	0.58538
<b>R12</b>	0.64082	0.63722	0.65106	0.58515	0.60813	0.64975
<b>R13</b>	0.12814	0.12735	0.13019	0.11709	0.12154	0.12985
<b>R14</b>	0.61836	0.61995	0.58724	0.57808	0.61603	0.63241
<b>R15</b>	0.12373	0.1239	0.11743	0.11567	0.12312	0.12638
<b>R16</b>	0.0309	0.06871	0.09902	0.10791	0.10197	0.11103
<b>R17</b>	0.15311	0.37333	0.1304	0.39758	0.72843	0.90927
<b>R18</b>	0.08504	0.20708	0.07245	0.22088	0.40796	0.50521
<b>R19</b>	0.01211	0.05408	0.01904	0.04824	0.08302	0.10933
<b>R20</b>	0.01055	0.27061	0.0952	0.24107	0.41539	0.54708
<b>R21</b>	0.11425	0.10062	0.09877	0.09032	0.08523	0.09601
<b>R22</b>	0.15698	0.13774	0.13029	0.11923	0.11082	0.11305
<b>R23</b>	0.09509	0.10135	0.08872	0.07929	0.10204	0.11694

Similarly Table 6.20 & 6.21 displays the optimized TMS values of GWO and hybrid GWO-PSO algorithms and indicates that all tests are feasible and satisfy all constraints. These findings show that both algorithms can maintain the relay coordination and eliminate the fault efficiently as per the given constraints.

### 6.2.3. Results validation for hybrid protection scheme for IEEE 13 node.

It is clear from all the optimized results that Zfcl max limits is violated for case number 5, as the protection algorithms shift from non-adaptive side to adaptive side. The result validation corresponding to non-adaptive protection is shown in table 6.22.

**Table 6.22: Result validation of non-adaptive protection scheme result.**

IEEE NODE 13 (Non adaptive protection scheme)								
Case No	Relay		Before setting change			After setting change		
	Primary relay	Backup relay	Tp	Tb	CTI	Tp	Tb	CTI
2	R6	R5	0.267	0.132	0.135	0.3029	0.5255	0.2226
3	R18	R17	0.0527	0.0961	0.0434	0.0446	0.2447	0.20013
3	R18	R19	0.0112	0.0667	0.0555	0.0498	0.2505	0.2007
5	R18	R19	0.0296	0.1365	0.1069	0.0509	0.252	0.2011

The validation of results obtained for non-adaptive algorithms by GWO & GWO-PSO are shown in Table 6.22. This table compares the result "after setting change" and "before setting change" and clearly shows that the CTI restriction is violated before setting change (i.e. CTI>0.2sec). After the algorithms have been applied, the result is changed which validates the CTI constraint and reduces the chances of a relay malfunction.

**Table 6.23. Results validation of adaptive protection scheme result.**

IEEE NODE 13 (Adaptive protection scheme)								
	Relay		Before setting change			After setting change		
Case no	Primary relay	Backup relay	Tp	Tb	CTI	Tp	Tb	CTI
2	R6	R5	0.267	0.132	0.135	0.2943	0.5255	0.2312
3	R18	R17	0.0527	0.0961	0.0434	0.0445	0.2449	0.2004
3	R18	R19	0.0112	0.0667	0.0555	0.052	0.2531	0.2011
5	R18	R19	0.0296	0.1365	0.1069	0.0512	0.2541	0.2029

Validation of results obtained by GWO & GWO-PSO, Interior Point Algorithm for Adaptive Algorithms are shown in Table 6.23. This table compares the results for adaptive protection scheme algorithm "after setting change" and "before setting change". The results clearly show that the CTI limitation is violated before setting change (i.e.  $CTI > 0.2\text{sec}$ ). After the application of the adaptive algorithms, the result is changed which validates the CTI constraint and reduces the chances of a relay malfunction.

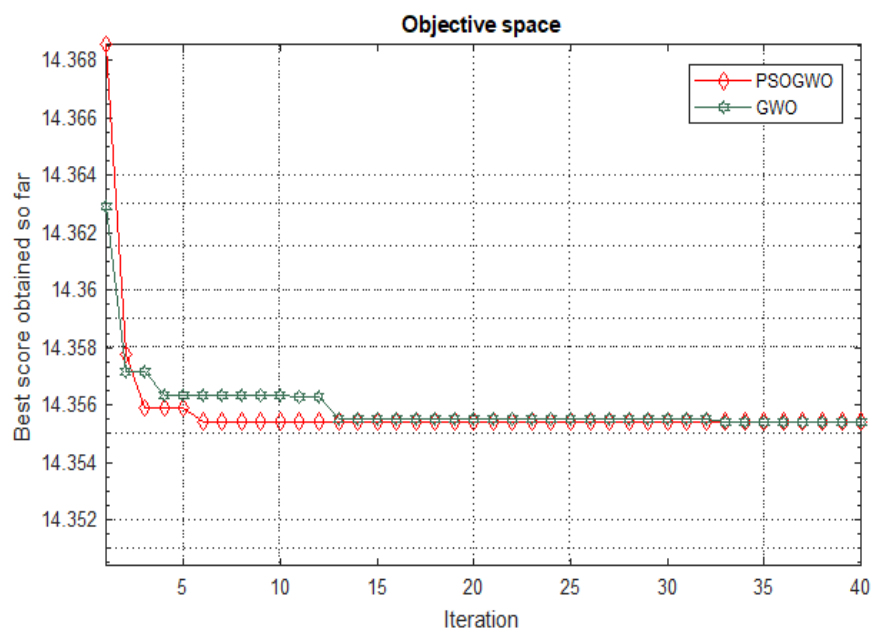


**Fig. 6.23. Zfcl parameter optimization convergence graph for GWO & GWOPSO algorithm (IEEE node 13)**

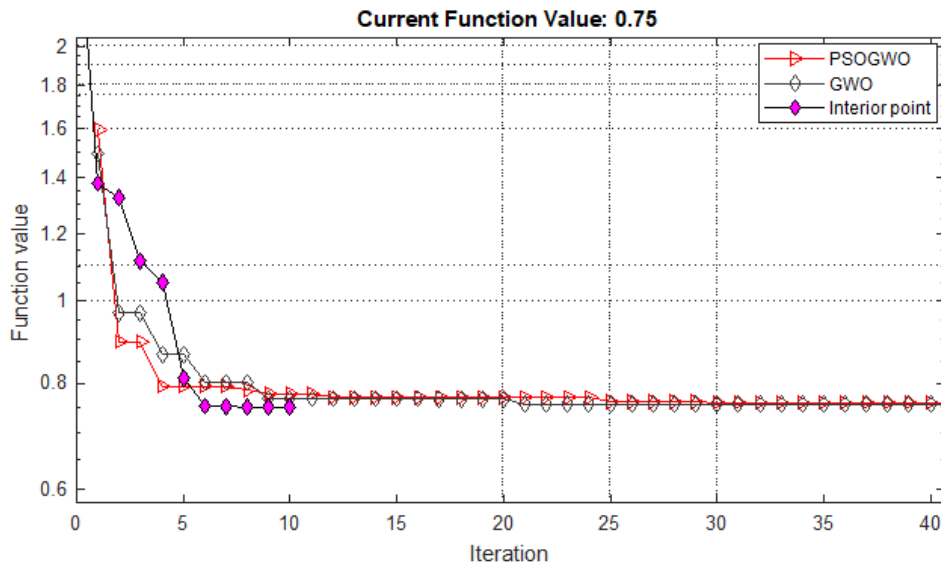


**Fig 6.24. GWO, Interior point & GWO-PSO Convergence graph for TMS optimization (IEEE 13 node)**

$Z_{fel}$  parameter optimization convergence graph for GWO & GWO-PSO algorithm are shown in figure 6.18. These results show that both, GWO, GWO-PSO, algorithms are capable to obtain the feasible results with respect to the given constraint. From the figure, it is also validated that GWO-PSO algorithm takes less iteration as compare with GWO algorithm. GWO algorithms take 0.976 sec to reaches the feasible solution and GWO-PSO take 1.07 sec to reach a feasible solution.

Convergence graph for TMS optimization for GWO, Interior point & GWO-PSO algorithm is shown in figure 6.19. It is clear from the plots that all, GWO, GWO-PSO, Interior point, algorithms are capable to obtain the feasible results with respect to the given constraint. From the figure, it is also validated that Interior point algorithm takes less iteration as compare with GWO & GWO-PSO algorithm. GWO algorithms takes 0.966 second, GWO-PSO takes 1.0286 second and interior-point algorithm take 1.159 seconds to reach the feasible solution.

Thus for IEEE node 13 model, all applied algorithms GWO, GWO-PSO and Interior point, are capable to handle such a complex model. The analysis of the results shows that the Interior point algorithms take less iteration as compared with GWO & GWO- PSO algorithms. However, the calculation time of the interior point algorithm is very high, which is a big disadvantage of this

algorithm. This is due to the fact that for protection purposes, the calculation time of the algorithm plays a vital role to control the response time of the relay. The comparison of algorithm calculation time indicates that, GWO algorithm is much better than other algorithms. This algorithm requires 0.976 seconds to provide results in the adaptive part of the hybrid protection scheme and 0.966 seconds to provide results in the non-adaptive part of the hybrid protection scheme. The results tabulated in tables 6.18 and 6.19 shows that, hybrid protection scheme can deal with the complex grid protection problems.

### 6.3 IEEE 33 node

#### 6.3.1. Impact of solar PV DGs on IEEE 33 node distribution grid

Optimal relay configuration is done in two ways: first, decrease fault current using a fault current limiter and second, dynamically change the relay settings. Here, to test the algorithm, IEEE 33 node network is used to connect five solar PVs to bus No. 18,33,15,23 shows in fig 6.20. Each PV shares 20% of the network penetration.

IEEE 30 node network along with the DG-based solar PV system is shown figure 6.20. R1 to R32 are the relay connection in the 30-node test feeder and Z1 to Z32 are the FCL connected to the IEEE 30 node system.

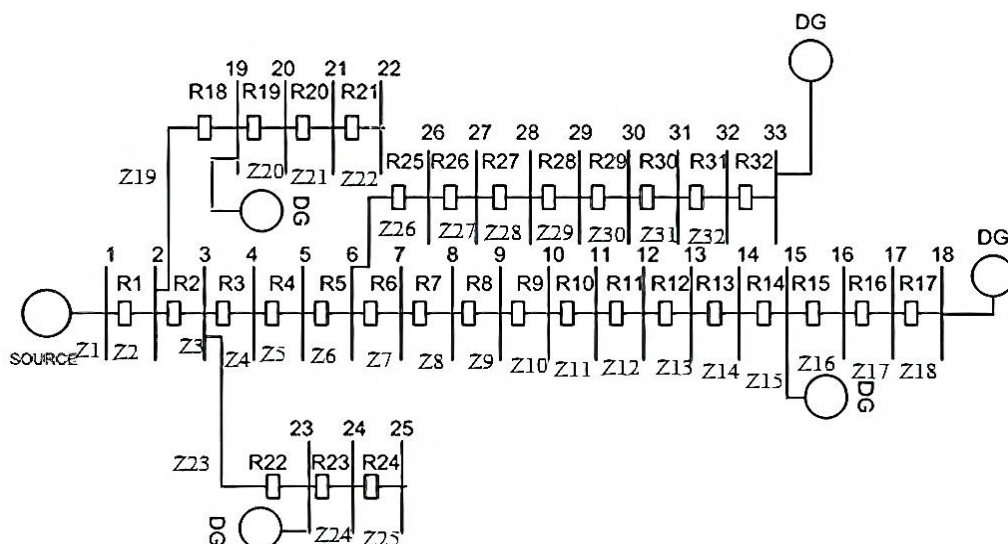


**Fig 6.25. IEEE 33 node model along with Solar DGs & relay location representation.**

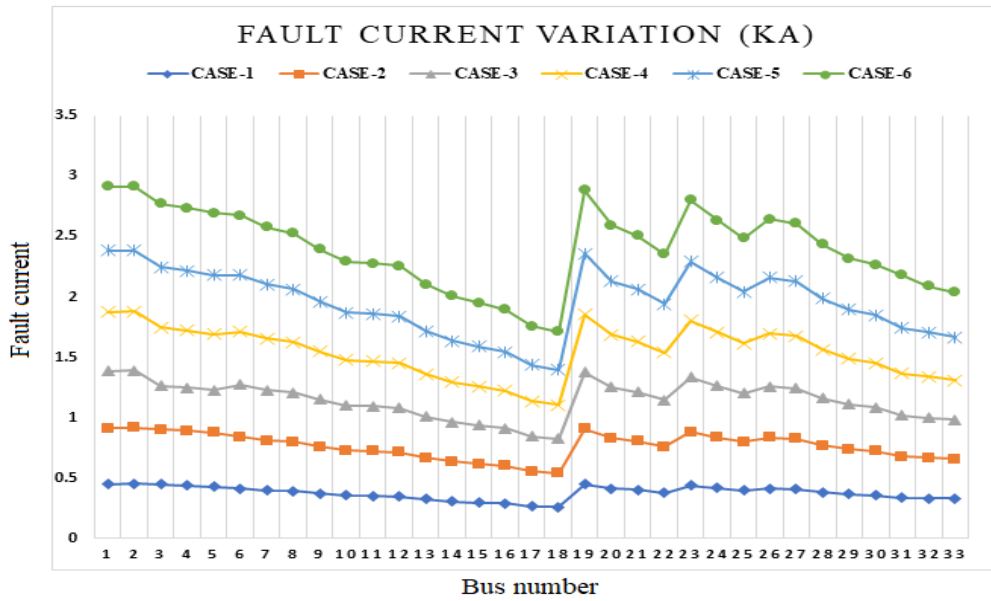


**Fig 6.26. Fault current variation at every bus for each PV penetration case**

### 6.3.1.1. Impact on fault current of IEEE 33 node distribution grid

Fault current variation with respect to solar PV penetration is shown in Figure 6.21. Case 1 represents 0 per cent PV penetration, case 2 represents 20 per cent penetration, case 3 represents 40 per cent penetration, case 4 represents 60 per cent penetration, case 5 represents 80 per cent penetration and case 6 represents 100 per cent penetration. The overall study showed that fault current rises as penetration increases and also noted that maximal fault current rises when penetration reaches to 100% as shown in the chart. This analysis validates the rise in fault current with the amount of penetration.

### 6.3.1.2. Impact on voltage of IEEE 33 node distribution grid

The bus voltage variance is shown in figure 6.22 which shows that the maximum voltage increases at 100% PV penetration. It is also noted that the voltage profile of some busses has improved when the solar PV penetration is increased. All variations are found under the standard grid variation.

### 6.3.2. Relay Coordination solution for IEEE 33 node distribution grid using hybrid protection scheme

In the relay coordination, IEEE 33 node uses a hybrid protection scheme which is a combination of an adaptive and non-adaptive protection schemes. In this segment, the two sections of the protection algorithm are evaluated on the basis of DGs penetration level. This study provides an overview of both adaptive and non-adaptive algorithms and determines the best optimization for each protection algorithm. This study also establish the best performance optimization algorithm that makes the protection scheme more efficient.

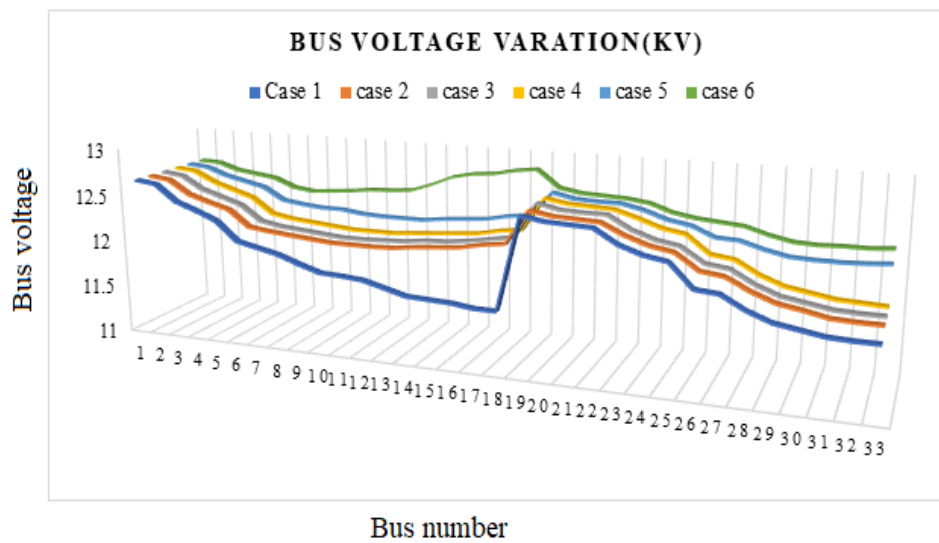


**Fig 6.27. Bus voltage representation for all PV penetration cases**

**Table 6.24. Optimized Zfcl parameters using GWO-PSO algorithm for IEEE 33 node**

Zfcl No.	CASE 2			Case 3			Case 4			case 5			Case 6		
	Z	R	X	Z	R	X	Z	R	X	Z	R	X	Z	R	X
1	0.500	0.098	0.490	0.839	0.164	0.822	1.321	0.259	1.295	1.891	0.371	1.854	2.500	0.490	2.452
2	0.248	0.049	0.243	0.623	0.122	0.611	1.108	0.217	1.086	1.709	0.335	1.676	2.318	0.455	2.273
3	0.367	0.072	0.359	0.614	0.120	0.602	1.216	0.239	1.193	1.864	0.366	1.828	2.515	0.493	2.466
4	0.376	0.074	0.369	0.666	0.131	0.653	1.182	0.232	1.159	1.882	0.369	1.846	2.579	0.506	2.529
5	0.584	0.115	0.573	0.844	0.165	0.827	1.305	0.256	1.279	2.060	0.404	2.020	2.805	0.550	2.750
6	0.507	0.099	0.497	0.710	0.139	0.696	1.141	0.224	1.118	2.043	0.401	2.004	2.885	0.566	2.829
7	0.589	0.116	0.578	0.763	0.150	0.749	1.225	0.240	1.201	2.117	0.415	2.076	3.022	0.593	2.963
8	0.704	0.138	0.691	0.839	0.165	0.823	1.231	0.242	1.207	2.046	0.401	2.006	3.034	0.595	2.975
9	0.826	0.162	0.810	0.925	0.181	0.907	1.262	0.247	1.237	2.033	0.399	1.993	2.823	0.554	2.768
10	1.019	0.200	0.999	1.019	0.200	0.999	1.337	0.262	1.311	2.090	0.410	2.049	3.393	0.665	3.327
11	1.030	0.202	1.010	1.084	0.213	1.063	1.352	0.265	1.325	2.063	0.405	2.023	3.429	0.672	3.362
12	1.109	0.217	1.087	1.109	0.217	1.087	1.382	0.271	1.355	2.059	0.404	2.019	3.501	0.687	3.433
13	1.409	0.276	1.381	1.409	0.276	1.381	1.596	0.313	1.565	2.256	0.442	2.212	3.965	0.778	3.888
14	1.772	0.347	1.737	1.634	0.320	1.602	1.772	0.347	1.737	2.371	0.465	2.325	4.376	0.858	4.291
15	1.876	0.368	1.840	1.739	0.339	1.697	1.876	0.368	1.840	2.510	0.492	2.461	4.620	0.906	4.530
16	2.067	0.405	2.027	1.914	0.375	1.877	1.991	0.390	1.952	2.588	0.508	2.538	4.706	0.923	4.614
17	2.407	0.472	2.361	2.230	0.437	2.187	2.407	0.472	2.361	3.009	0.590	2.951	5.087	0.998	4.988
18	2.645	0.519	2.594	2.459	0.482	2.411	2.552	0.501	2.503	3.188	0.625	3.126	5.228	1.025	5.126
19	0.254	0.050	0.249	0.637	0.125	0.625	1.100	0.216	1.078	1.716	0.337	1.683	2.312	0.453	2.267



<b>20</b>	0.173	0.034	0.170	0.427	0.084	0.418	0.834	0.164	0.817	1.335	0.262	1.309	1.914	0.375	1.877
<b>21</b>	0.138	0.027	0.135	0.364	0.071	0.357	0.756	0.148	0.741	1.254	0.246	1.229	1.800	0.353	1.765
<b>22</b>	0.103	0.020	0.101	0.307	0.060	0.301	0.652	0.128	0.640	1.125	0.221	1.103	1.706	0.335	1.673
<b>23</b>	0.307	0.060	0.301	0.566	0.111	0.555	1.164	0.228	1.141	1.814	0.356	1.779	2.442	0.479	2.394
<b>24</b>	0.213	0.042	0.209	0.462	0.091	0.453	1.016	0.199	0.996	1.572	0.308	1.541	2.193	0.430	2.150
<b>25</b>	0.141	0.028	0.138	0.325	0.064	0.319	0.814	0.160	0.799	1.360	0.267	1.334	1.950	0.382	1.912
<b>26</b>	0.559	0.110	0.548	0.724	0.142	0.710	1.123	0.220	1.101	2.046	0.401	2.007	2.875	0.564	2.819
<b>27</b>	0.484	0.095	0.475	0.654	0.128	0.641	1.065	0.209	1.044	2.013	0.395	1.974	2.830	0.555	2.775
<b>28</b>	0.451	0.089	0.443	0.549	0.108	0.538	0.929	0.182	0.911	2.067	0.405	2.027	2.851	0.559	2.796
<b>29</b>	0.330	0.065	0.324	0.384	0.075	0.377	0.754	0.148	0.740	2.062	0.404	2.022	2.800	0.549	2.746
<b>30</b>	0.287	0.056	0.281	0.343	0.067	0.337	0.621	0.122	0.609	2.045	0.401	2.006	2.816	0.552	2.762
<b>31</b>	0.323	0.063	0.317	0.323	0.063	0.317	0.575	0.113	0.564	2.188	0.429	2.146	5.139	1.008	5.039
<b>32</b>	0.269	0.053	0.264	0.202	0.040	0.198	0.531	0.104	0.521	2.209	0.433	2.166	2.955	0.580	2.898
<b>33</b>	0.201	0.039	0.197	0.201	0.039	0.197	0.464	0.091	0.455	1.572	0.308	1.542	2.360	0.463	2.314
<b>∑</b>	24.2704	4.7599	23.7991	27.8797	5.4677	27.3383	39.6544	7.7769	38.8844	66.1596	12.9750	64.8748	101.7281	19.9506	99.7526

**Table 6.25. Optimized Zfcl parameters using GWO algorithm for IEEE 13 node**

Zfcl	CASE 2			CASE 3			Case 4			case 5			Case 6		
Position No.	Z	R	X	Z	R	X	Z	R	X	Z	R	X	Z	R	X
1	0.49979	0.09802	0.49008	0.83871	0.16448	0.82242	1.32109	0.25909	1.29544	1.89122	0.37090	1.85449	2.5003	0.49035	2.451742
2	0.24822	0.04868	0.24340	0.62343	0.12227	0.61133	1.10783	0.21726	1.08632	1.70919	0.33520	1.67600	2.31827	0.45465	2.273249
3	0.36651	0.07188	0.35940	0.61365	0.12035	0.60174	1.21612	0.23850	1.19251	1.86440	0.36564	1.82820	2.51491	0.49322	2.466073
4	0.37646	0.07383	0.36915	0.66580	0.13057	0.65287	1.18193	0.23180	1.15897	1.88232	0.36915	1.84577	2.57868	0.50572	2.5286
5	0.58432	0.11460	0.57298	0.84373	0.16547	0.82735	1.30478	0.25589	1.27944	2.06030	0.40406	2.02029	2.80467	0.55004	2.750207
6	0.50718	0.09947	0.49733	0.71017	0.13928	0.69638	1.14058	0.22369	1.11843	2.04338	0.40074	2.00370	2.88516	0.56583	2.82913
7	0.58947	0.11561	0.57802	0.76344	0.14972	0.74861	1.22503	0.24025	1.20124	2.11726	0.41523	2.07615	3.02204	0.59267	2.963357
8	0.70433	0.13813	0.69066	0.83900	0.16454	0.82271	1.23140	0.24150	1.20749	2.04568	0.40119	2.00595	3.03383	0.59499	2.974919
9	0.82630	0.16205	0.81025	0.92481	0.18137	0.90686	1.26182	0.24746	1.23731	2.03281	0.39867	1.99333	2.82286	0.55361	2.768038
10	1.01886	0.19982	0.99908	1.01886	0.19982	0.99908	1.33692	0.26219	1.31096	2.08958	0.40980	2.04900	3.39299	0.66542	3.327103
11	1.03019	0.20204	1.01019	1.08449	0.21269	1.06343	1.35167	0.26508	1.32542	2.06332	0.40465	2.02325	3.42852	0.67239	3.361941
12	1.10891	0.21748	1.08738	1.10891	0.21748	1.08738	1.38191	0.27101	1.35507	2.05850	0.40371	2.01853	3.50127	0.68666	3.433282
13	1.40880	0.27629	1.38144	1.40880	0.27629	1.38144	1.59613	0.31303	1.56514	2.25617	0.44247	2.21236	3.96458	0.77752	3.887593
14	1.77160	0.34744	1.73720	1.63387	0.32043	1.60214	1.77160	0.34744	1.73720	2.37128	0.46505	2.32523	4.37557	0.85812	4.290596
15	1.87646	0.36801	1.84002	1.73087	0.33945	1.69726	1.87646	0.36801	1.84002	2.50977	0.49221	2.46103	4.61963	0.90598	4.529915
16	2.06725	0.40542	2.02711	1.91410	0.37539	1.87693	1.99092	0.39045	1.95226	2.58820	0.50759	2.53794	4.70581	0.92289	4.614428
17	2.40744	0.47214	2.36069	2.23017	0.43737	2.18686	2.40744	0.47214	2.36069	3.00914	0.59014	2.95070	5.08718	0.99768	4.988386
18	2.64500	0.51873	2.59363	2.45885	0.48222	2.41110	2.55225	0.50054	2.50269	3.18803	0.62522	3.12612	5.22799	1.0253	5.126461
19	0.25372	0.04976	0.24880	0.63709	0.12494	0.62472	1.09972	0.21567	1.07836	1.71584	0.33650	1.68252	2.31206	0.45343	2.267158

<b>20</b>	0.17313	0.03395	0.16976	0.42668	0.08368	0.41839	0.83365	0.16349	0.81746	1.33542	0.26190	1.30949	1.91423	0.37541	1.877056
<b>21</b>	0.13803	0.02707	0.13535	0.36359	0.07131	0.35653	0.75599	0.14826	0.74131	1.25365	0.24586	1.22930	1.80024	0.35306	1.765282
<b>22</b>	0.10324	0.02025	0.10124	0.30651	0.06011	0.30056	0.65224	0.12792	0.63957	1.12526	0.22068	1.10341	1.7061	0.3346	1.67297
<b>23</b>	0.30665	0.06014	0.30069	0.56606	0.11101	0.55507	1.16382	0.22824	1.14122	1.81386	0.35573	1.77863	2.44152	0.47882	2.394111
<b>24</b>	0.21281	0.04173	0.20867	0.46160	0.09053	0.45263	1.01578	0.19921	0.99605	1.57178	0.30825	1.54126	2.19253	0.42999	2.149955
<b>25</b>	0.14082	0.02762	0.13808	0.32532	0.06380	0.31901	0.81437	0.15971	0.79856	1.35993	0.26670	1.33352	1.94964	0.38237	1.911775
<b>26</b>	0.55874	0.10958	0.54789	0.72381	0.14195	0.70976	1.12328	0.22029	1.10147	2.04629	0.40131	2.00655	2.87454	0.56374	2.818714
<b>27</b>	0.48431	0.09498	0.47490	0.65414	0.12829	0.64144	1.06494	0.20885	1.04426	2.01312	0.39480	1.97402	2.83044	0.5551	2.775476
<b>28</b>	0.45148	0.08854	0.44272	0.54900	0.10767	0.53834	0.92931	0.18225	0.91126	2.06665	0.40530	2.02652	2.8513	0.55919	2.795932
<b>29</b>	0.33027	0.06477	0.32386	0.38428	0.07536	0.37682	0.75437	0.14795	0.73972	2.06231	0.40445	2.02226	2.80017	0.54916	2.745793
<b>30</b>	0.28679	0.05624	0.28122	0.34321	0.06731	0.33654	0.62069	0.12173	0.60863	2.04541	0.40114	2.00569	2.8164	0.55234	2.761708
<b>31</b>	0.32337	0.06342	0.31709	0.32337	0.06342	0.31709	0.57534	0.11283	0.56417	2.18822	0.42915	2.14572	5.1392	1.00789	5.0394
<b>32</b>	0.26889	0.05273	0.26367	0.20227	0.03967	0.19834	0.53144	0.10422	0.52112	2.20901	0.43322	2.16612	2.95534	0.57959	2.897945
<b>33</b>	0.20106	0.03943	0.19716	0.20106	0.03943	0.19716	0.46361	0.09092	0.45460	1.57226	0.30835	1.54172	2.36017	0.46287	2.314332
<b>Total</b>	24.2704	4.75985	23.7991	27.87965	5.46767	27.33827	39.65443	7.77687	38.88436	66.15956	12.97496	64.87475	101.7281	19.9506	99.75263

### 6.3.2.1. Impedance Fault current limiter (Zfcl) optimization using Grey wolf optimization & Hybrid GWO-PSO

Here the fault current limiter parameter optimization focuses mainly on Z, X, R parameters that play a vital role in limiting the increased fault current. When the impedance is very high, the system operator's difficulty increases, especially when the grid is in operating state.

The optimized values of  $Z_{fcl}$  obtained using GWO-PSO hybrid optimization algorithm with respect to the increase in fault current are shown in table 6.24. Here all the results are found feasible and satisfy all the limitations of the optimum relay coordination model. The total value of  $Z_{fcl}$  is also tabulated in table 6.24. It is clear that the maximum value of  $Z_{fcl}$  is 101.7281 ohms, which is higher than the limit of  $Z_{fcl}$  max i.e. (60 ohms).

The results obtained using GWO optimization algorithm are shown in table 6.25. These results shows they met all the practical constraints of the optimal relay coordination model. Here the maximum value of  $Z_{fcl}$  is 101.7279 ohms. Thus for both algorithms, for case-5 & 6,  $Z_{fcl}$  max exceeds the limit.

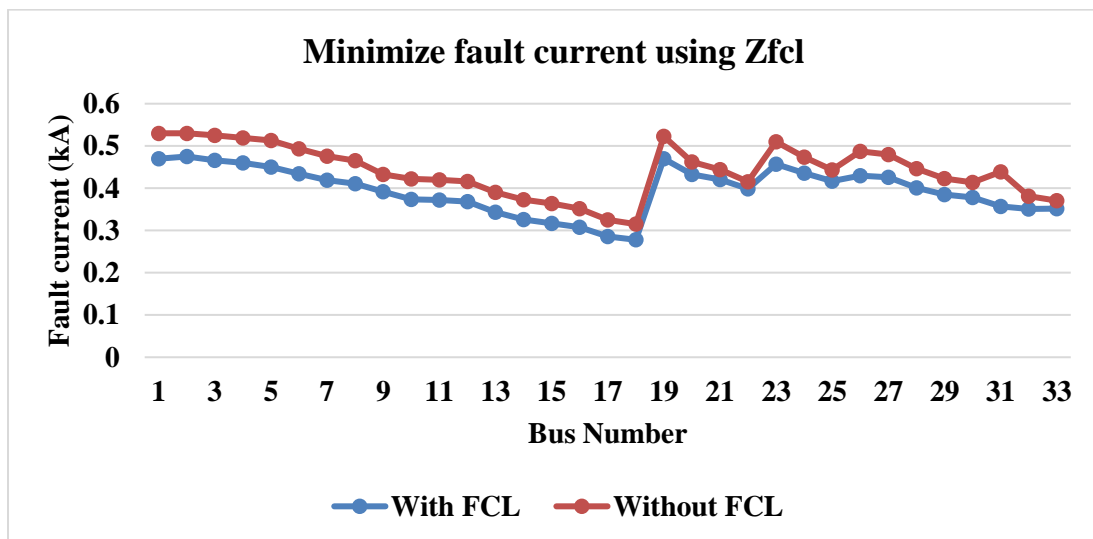


**Fig 6.28. Representation of Zfcl fault current minimization for IEEE 33 node**

$Z_{fd}$  fault current minimization for IEEE 33 node is shown in figure 6.23. Here also the optimized value of  $Z_{fd}$  is capable of limiting the current under the given constraint. This figure clearly shows the variation of  $Z_{fd}$ -based fault current, with and without FCL. The difference between both currents is seen in the graph. Moreover,  $Z_{fd}$  is decreasing the fault current level.

**Table 6.26. Relay TMS parameter optimization using GWO algorithm**

Relay	GWO					
	TMS CASE1	TMS CASE2	TMS case 3	TMS case 4	TMS case5	TDS case 6
1	0.23604	0.2819	0.32488	0.36541	0.39683	0.41635
2	0.01102	0.0127	0.01293	0.01471	0.01619	0.01716
3	0.58011	0.65746	0.57655	0.67207	0.74049	0.77801
4	0.30318	0.34578	0.30424	0.35206	0.38749	0.40473
5	0.01445	0.01646	0.01643	0.0166	0.0184	0.01916
6	0.79849	0.92965	0.93176	0.93515	0.94198	0.97345
7	0.43132	0.50391	0.50466	0.50588	0.50824	0.49588
8	0.02161	0.02512	0.0256	0.02521	0.02532	0.02293
9	0.8951	1.03753	1.03736	1.04015	1.04498	0.91886
10	0.46694	0.53255	0.53266	0.53384	0.53721	0.46398
11	0.02258	0.02553	0.02553	0.0255	0.02575	0.0219
12	0.9613	1.02759	1.02771	1.02976	1.03768	0.85974
13	0.50123	0.51552	0.51538	0.51597	0.52012	0.42857
14	0.02565	0.02355	0.0236	0.02362	0.02376	0.01963
15	1.07091	0.93952	0.93803	0.9396	0.94686	0.97612
16	0.56537	0.46276	0.46203	0.46328	0.46696	0.48149
17	0.02832	0.02141	0.02137	0.02143	0.02164	0.02063
18	0.71013	0.53871	0.53755	0.53899	0.54308	0.5169
19	0.02309	0.02352	0.02398	0.024	0.0241	0.02445
20	0.57452	0.575	0.57578	0.57714	0.57891	0.52802
21	0.02907	0.02908	0.02911	0.02915	0.02922	0.02929
22	0.86045	0.86473	0.86763	1.00986	1.0159	1.02158
23	0.44724	0.44836	0.4499	0.45312	0.4565	0.46071
24	0.02441	0.02437	0.02443	0.0245	0.02475	0.02501
25	0.40761	0.41055	0.41155	0.41432	0.45464	0.45939
26	0.01963	0.01975	0.01981	0.01993	0.02178	0.02201
27	0.80199	0.80545	0.80657	0.81092	0.88658	0.88893
28	0.41143	0.41204	0.41249	0.4145	0.45154	0.45517
29	0.02027	0.02022	0.02023	0.0203	0.02184	0.02196
30	0.97795	0.97856	0.9783	0.97266	1.02856	1.05618
31	0.53539	0.53539	0.53513	0.53643	0.50387	0.50867
32	0.02972	0.02979	0.02967	0.02962	0.02232	0.02261

**Table 6.27. Relay TMS parameter optimization using hybrid GWO-PSO algorithm**

Relay	GWOPSO algorithm results					
	TMS	TMS	TMS	TMS	TMS	TMS
	Case 1	Case 2	case 3	case 4	case5	case 6
1	0.23603	0.28196	0.32492	0.36541	0.39707	0.41655
2	0.01102	0.0127	0.01293	0.01476	0.01619	0.01716
3	0.57994	0.65707	0.5764	0.67776	0.74046	0.7807
4	0.30298	0.34557	0.30424	0.35241	0.38743	0.40492
5	0.01432	0.01635	0.01643	0.0166	0.01836	0.01916
6	0.79874	0.92913	0.93178	0.9351	0.94193	0.98603
7	0.43123	0.50379	0.50483	0.50571	0.50824	0.49652
8	0.02161	0.02512	0.02514	0.02519	0.02532	0.02288
9	0.89477	1.03753	1.03741	1.04053	1.04487	0.9207
10	0.46681	0.5326	0.53264	0.53399	0.53714	0.46411
11	0.02258	0.02545	0.02553	0.0255	0.02565	0.02186
12	0.96064	1.02736	1.02856	1.02971	1.03763	0.85965
13	0.50092	0.51545	0.51545	0.51577	0.52015	0.42846
14	0.02537	0.02355	0.02353	0.02358	0.02381	0.01961
15	1.07282	0.9417	0.93775	0.93946	0.94682	0.97531
16	0.5654	0.4651	0.46194	0.46312	0.467	0.48122
17	0.02832	0.02141	0.02137	0.02141	0.02158	0.02049
18	0.7101	0.53884	0.53762	0.53899	0.5434	0.51715
19	0.02309	0.02352	0.02398	0.02407	0.0241	0.02445
20	0.57452	0.575	0.57578	0.57714	0.57891	0.52802
21	0.02907	0.02908	0.02911	0.02915	0.02922	0.02929
22	0.86037	0.86401	0.86748	1.01001	1.01575	1.02166
23	0.44715	0.44826	0.44983	0.45318	0.45633	0.46041
24	0.02436	0.02437	0.02441	0.02455	0.02462	0.02476
25	0.40761	0.41055	0.41155	0.41432	0.45464	0.45939
26	0.01963	0.01975	0.01981	0.01993	0.02178	0.02201
27	0.80202	0.80754	0.80626	0.81078	0.88636	0.90285
28	0.41122	0.41297	0.41232	0.41445	0.45145	0.45848
29	0.02019	0.02022	0.02023	0.0203	0.02177	0.0224
30	0.97721	0.97921	0.97852	0.97283	1.02859	1.05569
31	0.53501	0.53547	0.53551	0.53669	0.50416	0.50846
32	0.02972	0.02967	0.02967	0.02962	0.02232	0.02254

### 6.3.2.2. Relay TMS optimization using Grey wolf optimization & Hybrid GWO-PSO, Interior point algorithm

TMS optimized relay parameters obtained using GWO algorithms are shown in table 6.26. All the results are found feasible and met all the practical constraints of the current relay. The TMS relay value is also capable of maintaining the coordination time interval (CTI) which is essential for a healthy running of the network.

The optimized TMS values obtained using hybrid GWO-PSO and Interior point algorithms are shown in Table 6.27 & 6.28. These results indicates that all tests are feasible and satisfy all constraints. Thus the results ensures that the used algorithms are capable to maintain the relay coordination and to eliminate the faults efficiently as per the given constraint.

**Table 6.28: Relay TMS parameter optimization using hybrid Interior point algorithm**

Relay	INTERIOR POINT					
	TMS	TMS	TMS	TMS	TMS	TMS
	Case 1	Case 2	Case 3	Case 4	Case 5	Case 6
1	0.23598	0.28176	0.32487	0.36536	0.39678	0.41621
2	0.01102	0.0127	0.01293	0.01471	0.01619	0.01716
3	0.57991	0.65688	0.57638	0.67181	0.74044	0.77778
4	0.30298	0.3455	0.30424	0.35194	0.38743	0.40465
5	0.01432	0.01635	0.01643	0.0166	0.01836	0.01916
6	0.79814	0.92904	0.93094	0.93481	0.94191	0.97317
7	0.43113	0.50379	0.50406	0.50562	0.50824	0.49565
8	0.02161	0.02512	0.02514	0.02519	0.02532	0.02275
9	0.89473	1.03726	1.03726	1.03972	1.04465	0.91848
10	0.46678	0.53242	0.53264	0.53368	0.53704	0.46392
11	0.02258	0.02545	0.02553	0.0255	0.02565	0.02186
12	0.96057	1.02711	1.02711	1.02953	1.03755	0.85959
13	0.5009	0.51523	0.51523	0.51575	0.5201	0.42844
14	0.02537	0.02355	0.02353	0.02358	0.02376	0.01961
15	1.07049	0.93897	0.93773	0.93921	0.94663	0.97529
16	0.56532	0.46265	0.46192	0.46308	0.46687	0.48122
17	0.02832	0.02141	0.02137	0.02141	0.02158	0.02049
18	0.70995	0.53845	0.53753	0.53893	0.54301	0.51674
19	0.02309	0.02352	0.02398	0.024	0.0241	0.02445
20	0.57452	0.575	0.57578	0.57714	0.57891	0.52802
21	0.02907	0.02908	0.02911	0.02915	0.02922	0.02929
22	0.86035	0.86397	0.86748	1.00956	1.01568	1.02106

23	0.44715	0.44824	0.44983	0.4529	0.45633	0.46028
24	0.02436	0.02437	0.02441	0.0245	0.02462	0.02476
25	0.40761	0.41055	0.41155	0.41432	0.45464	0.45939
26	0.01963	0.01975	0.01981	0.01993	0.02178	0.02201
27	0.8014	0.80536	0.80616	0.81076	0.88632	0.88876
28	0.41088	0.41195	0.4123	0.41445	0.45145	0.45515
29	0.02019	0.02022	0.02023	0.0203	0.02177	0.02196
30	0.97716	0.97799	0.97799	0.97221	1.02816	1.05544
31	0.53498	0.53531	0.53508	0.53623	0.50375	0.50836
32	0.02972	0.02967	0.02967	0.02962	0.02232	0.02254

### 6.3.3. Result validation for IEEE 33 node

All the optimized results shown in different tables indicates that the maximum limits of  $Z_{fd}$  is violated for case 5. Thus shifts the protection algorithms from non-adaptive side to adaptive side. The validation of non-adaptive protection scheme for IEEE node 33 is shown in table 6.29.

**Table 6.29: Result validation of non-adaptive protection scheme result.**

IEEE NODE 33 (Non adaptive protection scheme), "CTI=0.2 sec"								
Case no	Relay		Before setting change			After setting change		
	Primary relay	Backup relay	Tp	Tb	CTI	Tp	Tb	CTI
6	R10	R9	0.2021	0.3921	<b>0.19</b>	0.2018	0.4025	<b>0.2007</b>
6	R5	R4	0.1724	0.264	<b>0.14</b>	0.3049	0.6193	<b>0.3144</b>
3	R26	R25	0.009	0.2071	<b>0.1981</b>	0.04	0.244	<b>0.204</b>
5	R23	R22	0.2024	0.359	<b>0.1566</b>	0.2071	0.4232	<b>0.2161</b>

**Table 6.30: Results validation of adaptive protection scheme result.**

IEEE NODE 33 (Adaptive protection scheme) "CTI=0.2 sec"								
Case no	Relay		Before setting change			After setting change		
	Primary relay	Backup relay	Tp	Tb	CTI	Tp	Tb	CTI
6	R10	R9	0.2021	0.3921	0.19	0.2008	0.4025	0.2017
6	R5	R4	0.1724	0.264	0.14	0.3069	0.6193	0.3124
3	R26	R25	0.009	0.2071	0.1981	0.01	0.2140	0.204
5	R23	R22	0.2024	0.3590	0.1566	0.2066	0.4232	0.2166



The validation of results obtained using GWO & GWO-PSO non-adaptive algorithms are shown in table 6.29. In this table the result "after setting change" and "before setting change" are compared. Here it is clear that the CTI restriction is violated before setting change (i.e.  $CTI > 0.2\text{sec}$ ). After the application of algorithms the result is changed which validates the CTI constraint and reduces the chances of a relay malfunction.

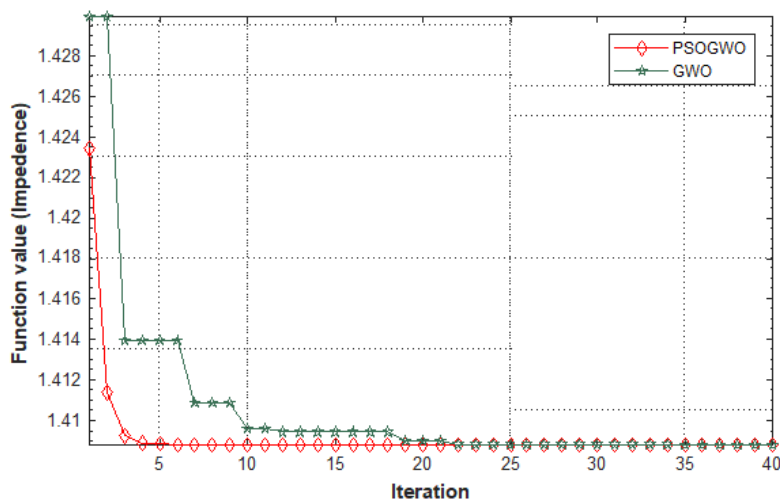


**Figure 6.29. Zfcl parameter optimization convergence graph for GWO & GWOPSO algorithm**

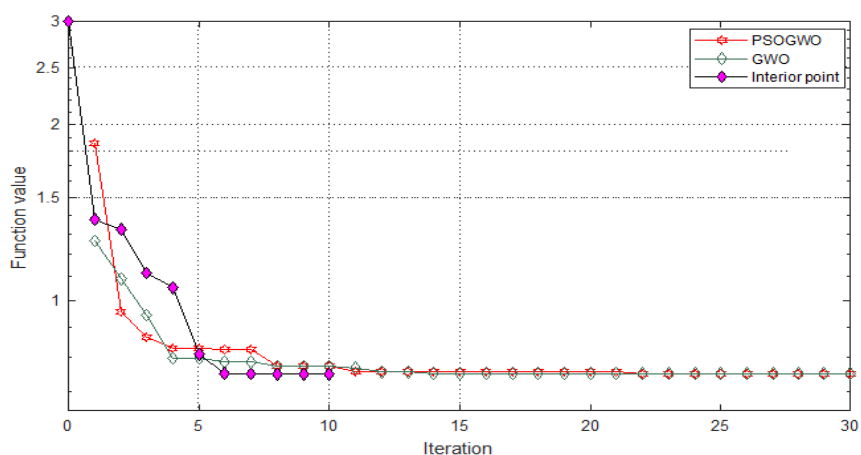


**Figure 6.30: GWO, PSO convergence graph for optimizing relay TMS value**

Validation of results obtained using GWO, GWO-PSO and Interior Point adaptive algorithms are shown in table 6.30. This table compares the result of adaptive protection scheme algorithm "after setting change" and "before setting change". The results clearly show that the CTI limitation is violated before setting change (i.e.  $CTI > 0.2\text{sec}$ ). After the application of the adaptive algorithms, the result is changed which validates the CTI constraint and reduces the chances of a relay malfunction.

Zfcl parameter optimization convergence graph for GWO & GWO-PSO algorithm are shown in figure 6.24. These results further confirm that both the algorithms are capable to obtain the feasible results with respect to the given constraint. The results validates that GWO-PSO algorithm takes less iteration as compare with GWO algorithm. GWO algorithms take 0.956 sec to reaches the feasible solution and GWO-PSO take 1.03 sec to reach a feasible solution.

GWO, PSO & Interior Point convergence graph for optimizing relay TMS value are shown in figure 6.25. The results obtained using GWO, GWO-PSO, Interior point algorithms show that these algorithms are capable to provide the feasible results with respect to the given constraint. It is clear that Interior point algorithm takes less iteration as compare with GWO & GWO-PSO algorithm. GWO algorithms take 0.946 second , GWO-PSO take 1.0266 second and interior-point algorithm take 1.155 sec to reach the feasible solution.

## **CHAPTER 7**

### **CONCLUSION AND RECOMMENDATIONS FOR FUTURE WORK**

#### **7.1 Conclusion**

The optimization techniques based on nature's creation are developed by different scientists. These techniques provides results which are relevant to the performance of the power system. Various bus models are considered for the application of these techniques. It is reported that almost all the techniques gives outcomes, which clear the picture of effect of DGs on distribution grid. The outcome of various optimization techniques applied on different models are given in different tables (2.1 to 2.9). There has been a thorough review of ongoing relay coordination. During past decades, Mathematical tools including Artificial Intelligence and "Nature inspired algorithm"-based optimization methods are developed which seems to be accurate and quick to meet the modern demands. The review presented in the present study confirms that GWO-PSO, GWO, hybrid whale-GWO, GSA-SQP, Water cycle optimization algorithms gives results which are found to be effective in solving the ORC problem. Adaptive protection methods based on nature optimization method are used for solving ORC. In case of DGs, FCL play the vital role but transient effect of FCL can mitigate the relay setting. In the course of present analysis of literature it is identified that FCL based non-adaptive technique is found better as compared with adaptive techniques because this can handle a greater number of DGs can be integrated on a grid with less complexity.

The presented study the results were simulated through MATLAB for IEEE 3 node test model along with three solar PV plant. These simulated results were verified by comparing with the ETAP simulated results. These validated simulated results are found unique and satisfy the permissible limits of variation. It is observed that the bus voltages get dropped when all three SPP contributed for grid. Variation of voltage regulation between case 1 & case 6 is 1.149% and for current regulation in case of fault it is 20.94%. These variation demands that relay setting need to be changed as per DG connected in the

systems. The coordination of relay is identified through the PSO, GA, SQP, Interior point algorithms and found that SQP takes less time to converge. Moreover, PSO is capable in getting optimized results for “Optimal relay coordination model”. The result of PSO validated on electrical transient analysis programming platform through time-coordination curve.

In the analysis of IEEE 33 node distribution grid, it is identified that fault current rises as DGs penetration increases. This rise of penetration into the grid increases the chances of mal-functioning of over current relay.

For IEEE node 33 distribution network, all applied algorithms viz GWO, GWO-PSO, and Interior point algorithm are capable to handle such a complex model. It is found that Interior point algorithms take less iteration as compared with GWO & GWO- PSO algorithms. The calculation time of the interior point algorithm is very high. This is a big disadvantage of this algorithm, because in context of protection purposes the calculation time of the algorithm plays a vital role in controlling the response time of the relay. A comparison of algorithm calculation time shows that GWO is much better than other algorithms. The GWO algorithm requires 0.9468 seconds for IEEE 33 node and to provide results in the adaptive part of the hybrid protection scheme whereas it takes 0.956 seconds to provide results in the non-adaptive part of the hybrid protection scheme. This shows that the hybrid protection scheme can deal with complex grid protection problems.

In the IEEE 13 node study, it is noticed that the fault currents increases when solar penetration level increases. For the highest level of penetration, the maximum fault current is observed (5.77 kA). In IEEE 13 node standard system both single-phase line and three-phase line are present. For the single-phase line the fault may be in between line to ground and in case of two-phase line to line fault may exist. Both cases are considered for the short circuit (SC) current analysis. In IEEE 13 node network, the Bus 645,646,611,684,652 contains one phase and two-phase lines. In the present study for these busses, ground to line and line to line faults are taken into account

Present study also focuses on the penetration impact of solar PV system on distribution grids. In this study the detailed effect of solar PV on voltage

profiles, voltage imbalances, network stability and the effect of harmonics on grid operation was examined. The outcome of this study indicate that the distribution feeders start experience voltage flickers at 40 to 60 per cent penetration & also witness the maximum THD level after reaching 60% penetration. There exist no specific way to estimate the safe degree of solar penetration for distribution systems. Thus for this reason individual systems need to be studied. Safe solar penetration quantity depend upon feeder topology, load profile, solar light / cloud patterns, and number of harmonics.

The maximum allowed solar share is the point at which voltage increases and/or flicker problems begin, and the harmonic value exceeds the standard maximum limit (IEEE 519). The study also reveals that increase solar penetration reduces the power losses of the system which is helpful to cater more consumer demand.

Though an increased penetration reduces the power losses but by such penetration shot circuit current level increases, which creates the issue of relay mal-operation. Such increase of THD and short circuit current effects can be mitigated through the implementation of adaptive & non adaptive protection techniques.

## **7.2. Future scope**

Following points can be included in the hybrid security scheme for future scope:

- 1) THD (Total harmonic distortion) factor can be included as a constraint in the optimal relay coordination model, although THD can also be a reason for relay malfunctioning.
- 2) In the case of a non-adaptive FCL-based security scheme, switching transients may produce and these transient waves may cause over-current relay failure. The attempt can be made to consider this problem by using an FCL-based semiconductor.

## REFERENCES

- [1] Aithal, P. S., and Sridhar Acharya. "Impact of Green Energy on Global Warming-A Changing Scenario." *International Journal of Scientific Research and Modern Education (IJSRME) ISSN (Online)* (2016): 2455-5630.
- [2] H. Javadi, S. M. Ali Mousavi, and M. Khederzadeh, "A novel approach to increase FCL application in preservation of over-current relays coordination in presence of asynchronous DGs," *International Journal of Electrical Power and Energy Systems*, vol. 44, no. 1, pp. 810–815, Jan. 2013.
- [3] S. Ghosh, S. P. Ghoshal, and S. Ghosh, "Optimal sizing and placement of distributed generation in a network system," *International Journal of Electrical Power and Energy Systems*, vol. 32, no. 8, pp. 849–856, 2010.
- [4] P. Mahat, Z. Chen, B. Bak-Jensen, and C. L. Bak, "A simple adaptive overcurrent protection of distribution systems with distributed generation," *IEEE Transactions on Smart Grid*, vol. 2, no. 3, pp. 428–437, Sep. 2011.
- [5] M. S. Javadi, A. E. Nezhad, A. Anvari-Moghadam, and J. M. Guerrero, "Hybrid mixed-integer non-linear programming approach for directional over-current relay coordination," *The Journal of Engineering*, vol. 2019, no. 18, pp. 4743–4747, Jul. 2019.
- [6] H. J. Bahirat and S. A. Khaparde, "Impact on Superconducting Fault Current Limiters on Circuit Breaker Capability."
- [7] S. Kodle, V. Padmini, ... H. B.-2016 I. 6th, and undefined 2016, "Application of Super Conducting fault current limiter in Indian grid," *ieeexplore.ieee.org*.
- [8] L. Wu, X. Chen, J. Liu, K. Yu, S. Xu, and F. Mo, "Calculating the Maximum Penetration Capacity of Distributed Generation Considering Current Protection," vol. 674, pp. 1257–1261, 2014.
- [9] "A Study on Grid Connected PV system," pp. 0–5, 2016.
- [10] S. Mirsaiedi, D. M. Said, and M. R. Miveh, "A Comprehensive Overview

- of Different Protection Schemes in Micro-Grids,” vol. 14, no. 4, pp. 327–332, 2013.
- [11] G. Matkar, D. K. Dheer, A. S. Vijay, and S. Doolla, “A simple mathematical approach to assess the impact of solar PV penetration on voltage profile of distribution network,” *2017 National Power Electronics Conference, NPEC 2017*, vol. 2018-Janua, pp. 209–214, 2018.
- [12] S. Syafii and K. M. N. K. M. Nor, “Renewable Distributed Generation Models in Three-Phase Load Flow Analysis for Smart Grid,” *TELKOMNIKA (Telecommunication Computing Electronics and Control)*, vol. 11, no. 4, p. 661, 2015.
- [13] N. Soni, S. Doolla, and M. C. Chandorkar, “Inertia Design Methods for Islanded Microgrids Having Static and Rotating Energy Sources,” *IEEE Transactions on Industry Applications*, vol. 52, no. 6, pp. 5165–5174, 2016.
- [14] I. M. El-Amin and M. S. Ali, “Impact of PV system on distribution networks,” *2011 IEEE PES Conference on Innovative Smart Grid Technologies - Middle East, ISGT Middle East 2011*, pp. 3–8, 2011.
- [15] D. K. Dheer, N. Soni, and S. Doolla, “Small signal stability in microgrids with high penetration of power electronics interfaced sources,” *IECON Proceedings (Industrial Electronics Conference)*, no. 1, pp. 2272–2278, 2014.
- [16] D. Cheng, B. Mather, R. Seguin, J. Hambrick, and R. P. Broadwater, “PV impact assessment for very high penetration levels,” *2015 IEEE 42nd Photovoltaic Specialist Conference, PVSC 2015*, pp. 1–6, 2015.
- [17] N. El-Naily, S. M. Saad, T. Hussein, and F. A. Mohamed, “A novel constraint and non-standard characteristics for optimal over-current relays coordination to enhance microgrid protection scheme,” *IET Generation, Transmission & Distribution*, vol. 13, no. 6, pp. 780–793, 2019.
- [18] R. Arseneau, G. T. Heydt, and M. J. Kempker, “Application of IEEE Standard 519-1992 harmonic limits for revenue billing meters,” *IEEE*

- Transactions on Power Delivery*, vol. 12, no. 1, pp. 346–352, 1997.
- [19] X. Zong, P. A. Gray, and P. W. Lehn, “New Metric Recommended for IEEE Standard 1547 to Limit Harmonics Injected into Distorted Grids,” *IEEE Transactions on Power Delivery*, vol. 31, no. 3, pp. 963–972, Jun. 2016.
- [20] M. Q. Duong, N. Thien, and N. Tran, “The Impacts of Distributed Generation Penetration into the Power System,” pp. 295–301, 2017.
- [21] A. Elmitwally, E. Gouda, and S. Eladawy, “Optimal allocation of fault current limiters for sustaining overcurrent relays coordination in a power system with distributed generation,” *Alexandria Engineering Journal*, vol. 54, no. 4, pp. 1077–1089, 2015.
- [22] “Adaptive protection scheme for optimally coordinated relay setting using modified PSO algorithm | Atteya | Journal of Power Technologies.” [Online]. Available: <http://www.papers.itc.pw.edu.pl/index.php/JPT/article/view/1278>. [Accessed: 14-Jan-2020].
- [23] S. A. Ahmadi, H. Karami, M. J. Sanjari, H. Tarimoradi, and G. B. Gharehpetian, “Application of hyper-spherical search algorithm for optimal coordination of overcurrent relays considering different relay characteristics,” *International Journal of Electrical Power and Energy Systems*, vol. 83, pp. 443–449, Dec. 2016.
- [24] M. Awaad, S. F. Mekhamer, and A. Y. Abdelaziz, “Design of an adaptive overcurrent protection scheme for microgrids,” *International Journal of Engineering, Science and Technology*, vol. 10, no. 1, p. 1, 2018.
- [25] M. H. Hussain, S. Rafidah, and A. Rahim, “Computational Intelligence Based Technique in Optimal Overcurrent Relay Coordination: A Review DGA-based varrescheduling for transmission loss reduction View project,” 2013.
- [26] A. S. Noghabi, J. Sadeh, and H. R. Mashhadi, “Considering different network topologies in optimal overcurrent relay coordination using a hybrid GA,” *IEEE Transactions on Power Delivery*, vol. 24, no. 4, pp. 1857–1863, 2009.



- [27] A. Y. Hatata and A. Lafi, "Ant Lion Optimizer for Optimal Coordination of DOC Relays in Distribution Systems Containing DGs," *IEEE Access*, vol. 6, pp. 72241–72252, 2018.
- [28] M. Barzegari, S. M. T. Bathaee, and M. Alizadeh, "Optimal coordination of directional overcurrent relays using harmony search algorithm," in *2010 9th Conference on Environment and Electrical Engineering, EEEIC 2010*, 2010, pp. 321–324.
- [29] "Overcurrent relay coordination using MINLP technique - IEEE Conference Publication." [Online]. Available: <https://ieeexplore.ieee.org/abstract/document/5955615>. [Accessed: 14-Jan-2020].
- [30] M. Ezzeddine and R. Kaczmarek, "A novel method for optimal coordination of directional overcurrent relays considering their available discrete settings and several operation characteristics," *Electric Power Systems Research*, vol. 81, no. 7, pp. 1475–1481, Jul. 2011.
- [31] M. M. Mansour, S. F. Mekhamer, and N. E. S. El-Kharbawe, "A modified particle swarm optimizer for the coordination of directional overcurrent relays," *IEEE Transactions on Power Delivery*, vol. 22, no. 3, pp. 1400–1410, 2007.
- [32] D. Birla, R. P. Maheshwari, and H. O. Gupta, "Time-overcurrent relay coordination: A review," *International Journal of Emerging Electric Power Systems*, vol. 2, no. 2. Walter de Gruyter GmbH, 01-Mar-2005.
- [33] M. H. Hussain, I. Musirin, and A. F. Abidin, "Computational Intelligence Based Technique in Optimal Overcurrent Relay Coordination: A Review," *The International Journal of Engineering And Science (IJES)*, vol. 2, no. 1, pp. 1–9, 2013.
- [34] H. A. Smolleck, "A simple method for obtaining feasible computational models for the time-current characteristics of industrial power-system protective devices," *Electric Power Systems Research*, vol. 2, no. 1, pp. 65–69, 1979.
- [35] L. Jenkins, H. Khincha, ... S. S.-I. transactions on, and undefined 1992, "An application of functional dependencies to the topological analysis of

protection schemes,” *ieeexplore.ieee.org*.

- [36] “Nature-inspired Metaheuristic Algorithms - Xin-She Yang - Google Books.” [Online]. Available: [https://books.google.co.in/books?hl=en&lr=&id=iVB\\_ETlh4ogC&oi=fnd&pg=PR5&dq=23\)%09X.S.+Yang,+Nature-Inspired+Meta-Heuristic+Algorithms,+published+by+Luniver+Press,+UK,+2008.&ots=DwhCljGDub&sig=sQkXyMN5riEiY4c1KWKv-31QO6E&redir\\_esc=y#v=onepage&q&f=false](https://books.google.co.in/books?hl=en&lr=&id=iVB_ETlh4ogC&oi=fnd&pg=PR5&dq=23)%09X.S.+Yang,+Nature-Inspired+Meta-Heuristic+Algorithms,+published+by+Luniver+Press,+UK,+2008.&ots=DwhCljGDub&sig=sQkXyMN5riEiY4c1KWKv-31QO6E&redir_esc=y#v=onepage&q&f=false). [Accessed: 14-Jan-2020].
- [37] X. S. Yang, “Firefly algorithms for multimodal optimization,” in *Lecture Notes in Computer Science (including subseries Lecture Notes in Artificial Intelligence and Lecture Notes in Bioinformatics)*, 2009, vol. 5792 LNCS, pp. 169–178.
- [38] X.-S. Yang, “Firefly Algorithm, Stochastic Test Functions and Design Optimisation,” Mar. 2010.
- [39] T. Khurshaid, A. Wadood, S. Gholami Farkoush, C. H. Kim, J. Yu, and S. B. Rhee, “Improved Firefly Algorithm for the Optimal Coordination of Directional Overcurrent Relays,” *IEEE Access*, vol. 7, pp. 78503–78514, 2019.
- [40] R. Benabid, M. Zellagui, A. Chaghi, and M. Boudour, “Application of Firefly Algorithm for Optimal Directional Overcurrent Relays Coordination in the Presence of IFCL,” *International Journal of Intelligent Systems and Applications*, vol. 6, no. 2, pp. 44–53, 2014.
- [41] A. Tjahjono *et al.*, “Adaptive modified firefly algorithm for optimal coordination of overcurrent relays,” *IET Generation, Transmission and Distribution*, vol. 11, no. 10, pp. 2575–2585, Jul. 2017.
- [42] R. L. Haupt and S. E. Haupt, *Practical Genetic Algorithms*. Hoboken, NJ, USA: John Wiley & Sons, Inc., 2003.
- [43] Singiresu S. Rao, *Engineering Optimization: Theory and Practice, Third Edition*, vol. 29, no. 9. 1997.
- [44] P. P. Bedekar and S. R. Bhide, “Optimum coordination of overcurrent

- relay timing using continuous genetic algorithm,” *Expert Systems with Applications*, vol. 38, no. 9, pp. 11286–11292, 2011.
- [45] R. Mohammadi, H. A. Abyaneh, F. Razavi, M. Al-Dabbagh, and S. H. H. Sadeghi, “Optimal relays coordination efficient method in interconnected power systems,” *Journal of Electrical Engineering*, vol. 61, no. 2, pp. 75–83, 2010.
- [46] F. Razavi, H. A. Abyaneh, M. Al-Dabbagh, R. Mohammadi, and H. Torkaman, “A new comprehensive genetic algorithm method for optimal overcurrent relays coordination,” *Electric Power Systems Research*, vol. 78, no. 4, pp. 713–720, 2008.
- [47] M. Singh, B. K. Panigrahi, A. R. Abhyankar, and S. Das, “Optimal coordination of directional over-current relays using informative differential evolution algorithm,” *Journal of Computational Science*, vol. 5, no. 2, pp. 269–276, 2014.
- [48] D. Uthitsunthom and T. Kulworawanichpong, “Optimal overcurrent relay coordination using genetic algorithms,” *2010 International Conference on Advances in Energy Engineering, ICAEE 2010*, pp. 162–165, 2010.
- [49] D. K. Singh and S. Gupta, “Optimal coordination of directional overcurrent relays: A genetic algorithm approach,” *2012 IEEE Students’ Conference on Electrical, Electronics and Computer Science: Innovation for Humanity, SCEECS 2012*, pp. 1–4, 2012.
- [50] C. W. So and K. K. Li, “Time coordination method for power system protection by evolutionary algorithm,” *IEEE Transactions on Industry Applications*, vol. 36, no. 5, pp. 1235–1240, 2000.
- [51] R. Storn and K. Price, “Differential Evolution - A Simple and Efficient Heuristic for Global Optimization over Continuous Spaces,” *Journal of Global Optimization*, vol. 11, no. 4, pp. 341–359, 1997.
- [52] S. Das and P. N. Suganthan, “Differential evolution: A survey of the state-of-the-art,” *IEEE Transactions on Evolutionary Computation*, vol. 15, no. 1, pp. 4–31, Feb. 2011.

- [53] R. Thangaraj, T. R. Chelliah, and M. Pant, "Overcurrent Relay Coordination by Differential Evolution Algorithm," no. December, 2012.
- [54] J. Moirangthem, K. R. Krishnanand, S. S. Dash, and R. Ramaswami, "Adaptive differential evolution algorithm for solving non-linear coordination problem of directional overcurrent relays," *IET Generation, Transmission and Distribution*, vol. 7, no. 4, pp. 329–336, 2013.
- [55] R. Thangaraj, M. Pant, and K. Deep, "Optimal coordination of overcurrent relays using modified differential evolution algorithms," *Engineering Applications of Artificial Intelligence*, vol. 23, no. 5, pp. 820–829, 2010.
- [56] T. R. Chelliah, R. Thangaraj, S. Allamsetty, and M. Pant, "Coordination of directional overcurrent relays using opposition based chaotic differential evolution algorithm," *International Journal of Electrical Power and Energy Systems*, vol. 55, pp. 341–350, 2014.
- [57] H. Yang, F. Wen, and G. Ledwich, "Optimal coordination of overcurrent relays in distribution systems with distributed generators based on differential evolution algorithm," *International Transactions on Electrical Energy Systems*, vol. 23, no. 1, pp. 1–12, Jan. 2013.
- [58] R. Thangaraj, M. Pant, and A. Abraham, "New mutation schemes for differential evolution algorithm and their application to the optimization of directional over-current relay settings," *Applied Mathematics and Computation*, vol. 216, no. 2, pp. 532–544, 2010.
- [59] M. Dorigo and C. Blum, "Ant colony optimization theory: A survey," *Theoretical Computer Science*, vol. 344, no. 2–3, pp. 243–278, Nov. 2005.
- [60] W. K. A. Najy, H. H. Zeineldin, and W. L. Woon, "Optimal protection coordination for microgrids with grid-connected and islanded capability," *IEEE Transactions on Industrial Electronics*, vol. 60, no. 4, pp. 1668–1677, 2013.
- [61] M. Y. Shih, C. A. Castillo Salazar, and A. Conde Enríquez, "Adaptive directional overcurrent relay coordination using ant colony optimisation," *IET Generation, Transmission and Distribution*, vol. 9,

no. 14, pp. 2040–2049, 2015.

- [62] K. I. Tharakan and O. V. G. Swathika, “Optimum coordination of using overcurrent relay using firefly and ant colony optimization algorithm,” in *Proceedings of the International Conference on Computing Methodologies and Communication, ICCMC 2017*, 2018, vol. 2018-January, pp. 617–621.
- [63] M. Y. Shih, A. Conde Enríquez, and L. M. Torres Treviño, “On-line coordination of directional overcurrent relays: Performance evaluation among optimization algorithms,” *Electric Power Systems Research*, vol. 110, pp. 122–132, 2014.
- [64] A. E. Labrador Rivas, L. A. Gallego Pareja, and T. Abrão, “Coordination of distance and directional overcurrent relays using an extended continuous domain ACO algorithm and an hybrid ACO algorithm,” *Electric Power Systems Research*, vol. 170, no. December 2018, pp. 259–272, 2019.
- [65] I. Scharf, A. Subach, and O. Ovadia, “Foraging behaviour and habitat selection in pit-building antlion larvae in constant light or dark conditions,” *Animal Behaviour*, vol. 76, no. 6, pp. 2049–2057, Dec. 2008.
- [66] D. Griffiths, “Pit Construction by Ant-Lion Larvae: A Cost-Benefit Analysis,” *The Journal of Animal Ecology*, vol. 55, no. 1, p. 39, Feb. 1986.
- [67] I. Scharf and O. Ovadia, “Factors influencing site abandonment and site selection in a sit-and-wait predator: A review of pit-building antlion larvae,” *Journal of Insect Behavior*, vol. 19, no. 2. pp. 197–218, Mar-2006.
- [68] G. U. Darji, M. J. Patel, V. N. Rajput, and K. S. Pandya, “A tuned cuckoo search algorithm for optimal coordination of Directional Overcurrent Relays,” *Proceedings of the 2015 IEEE International Conference on Power and Advanced Control Engineering, ICPACE 2015*, no. 1, pp. 162–167, 2015.
- [69] X.-S. Yang and S. Deb, *Cuckoo Search via Lévy Flights*. .

- [70] O. V. Gnana Swathika, S. Mukhopadhyay, Y. Gupta, A. Das, and S. Hemamalini, "Modified cuckoo search algorithm for fittest relay identification in microgrid," in *Advances in Intelligent Systems and Computing*, 2017, vol. 516, pp. 81–87.
- [71] S. S. Gokhale and V. S. Kale, "Time overcurrent relay coordination using the Levy flight Cuckoo search algorithm," *IEEE Region 10 Annual International Conference, Proceedings/TENCON*, vol. 2016-Janua, pp. 1–6, 2016.
- [72] V. N. Rajput, K. S. Pandya, and K. Joshi, "Optimal coordination of Directional Overcurrent Relays using hybrid CSA-FFA method," *ECTI-CON 2015 - 2015 12th International Conference on Electrical Engineering/Electronics, Computer, Telecommunications and Information Technology*, pp. 1–6, 2015.
- [73] A. Ahmarinejad, S. M. Hasanpour, M. Babaei, and M. Tabrizian, "Optimal Overcurrent Relays Coordination in Microgrid Using Cuckoo Algorithm," *Energy Procedia*, vol. 100, no. September, pp. 280–286, 2016.
- [74] T. Nguyen, D. Vo, N. Vu Quynh, and L. Van Dai, "Modified Cuckoo Search Algorithm: A Novel Method to Minimize the Fuel Cost," *Energies*, vol. 11, no. 6, p. 1328, May 2018.
- [75] R. E. Precup, R. C. David, A. I. Stinean, M. B. Radac, and E. M. Petriu, "Adaptive hybrid Particle Swarm Optimization-Gravitational Search Algorithm for fuzzy controller tuning," in *INISTA 2014 - IEEE International Symposium on Innovations in Intelligent Systems and Applications, Proceedings*, 2014, pp. 14–20.
- [76] J. Radosavljević and M. Jevtić, "Hybrid GSA-SQP algorithm for optimal coordination of directional overcurrent relays," *IET Generation, Transmission and Distribution*, vol. 10, no. 8, pp. 1928–1937, 2016.
- [77] A. Srivastava, J. M. Tripathi, R. Krishan, and S. K. Parida, "Optimal Coordination of Overcurrent Relays Using Gravitational Search Algorithm with DG Penetration," *IEEE Transactions on Industry Applications*, vol. 54, no. 2, pp. 1155–1165, 2018.

- [78] A. Chawla, B. R. Bhalja, B. K. Panigrahi, and M. Singh, “Gravitational Search Based Algorithm for Optimal Coordination of Directional Overcurrent Relays Using User Defined Characteristic,” *Electric Power Components and Systems*, vol. 5008, pp. 1–13, 2018.
- [79] M. Singh, “Protection coordination in grid connected & islanded modes of micro-grid operations,” *2013 IEEE Innovative Smart Grid Technologies - Asia, ISGT Asia 2013*, pp. 1–6, 2013.
- [80] A. A. El-Fergany and H. M. Hasanien, “Optimized settings of directional overcurrent relays in meshed power networks using stochastic fractal search algorithm,” *International Transactions on Electrical Energy Systems*, vol. 27, no. 11, pp. 1–17, 2017.
- [81] A. Wadood, T. Khurshaid, S. G. Farkoush, J. Yu, C. H. Kim, and S. B. Rhee, “Nature-inspired whale optimization algorithm for optimal coordination of directional overcurrent relays in power systems,” *Energies*, vol. 12, no. 12, 2019.
- [82] A. Korashy, S. Kamel, F. Jurado, and A. R. Youssef, “Hybrid Whale Optimization Algorithm and Grey Wolf Optimizer Algorithm for Optimal Coordination of Direction Overcurrent Relays,” *Electric Power Components and Systems*, vol. 47, no. 6–7, pp. 644–658, 2019.
- [83] A. A. El-Fergany and H. M. Hasanien, “Water cycle algorithm for optimal overcurrent relays coordination in electric power systems,” *Soft Computing*, vol. 23, no. 23, pp. 12761–12778, 2019.
- [84] A. Korashy, S. Kamel, A. R. Youssef, and F. Jurado, “Modified water cycle algorithm for optimal direction overcurrent relays coordination,” *Applied Soft Computing Journal*, vol. 74, pp. 10–25, 2019.
- [85] A. Sadollah, H. Eskandar, H. M. Lee, D. G. Yoo, and J. H. Kim, “Water cycle algorithm: A detailed standard code,” *SoftwareX*, vol. 5, no. April, pp. 37–43, 2015.
- [86] M. R. Asadi and S. M. Kouhsari, “Optimal overcurrent relays coordination using particle-swarm-optimization algorithm,” *2009 IEEE/PES Power Systems Conference and Exposition, PSCE 2009*, pp. 1–7, 2009.

- [87] “PARTICLE SWARM OPTIMIZATION (PSO).”
- [88] G. Algorithms, “Following a trail of insects as they work together to accomplish a task offers unique possibilities for problem solving.,” *Communications of the ACM*, vol. 45, no. 8, pp. 62–67, 2002.
- [89] H. H. Zeineldin, E. F. El-Saadany, and M. M. A. Salama, “Protective relay coordination for micro-grid operation using particle swarm optimization,” *LESCOPE'06: 2006 Large Engineering Systems Conference on Power Engineering - Conference Proceedings*, pp. 152–157, 2006.
- [90] Y. Damchi, H. R. Mashhadi, J. Sadeh, and M. Bashir, “Optimal coordination of directional overcurrent relays in a microgrid system using a hybrid particle swarm optimization,” *APAP 2011 - Proceedings: 2011 International Conference on Advanced Power System Automation and Protection*, vol. 2, pp. 1135–1138, 2011.
- [91] A. Srivastava, J. M. Tripathi, S. R. Mohanty, and B. Panda, “Optimal over-current relay coordination with distributed generation using hybrid particle swarm optimization-gravitational search algorithm,” *Electric Power Components and Systems*, vol. 44, no. 5, pp. 506–517, 2016.
- [92] D. Vijayakumar and R. K. Nema, “A Novel Optimal Setting for Directional over Current Relay Coordination using Particle Swarm Optimization,” *Engineering and Technology*, vol. 2, no. 5, pp. 980–985, 2008.
- [93] A. Liu and M. T. Yang, “A new hybrid nelder-mead particle swarm optimization for coordination optimization of directional overcurrent relays,” *Mathematical Problems in Engineering*, vol. 2012, 2012.
- [94] S. Louis, J. C. Bansal, and K. Deep, “Swarm Intelligence Symposium Optimization of Directional Overcurrent Relay Times by Particle Swarm,” *2008 Ieee Swarm Intelligence Symposium, St. Louis Mo Usa*, 2008.
- [95] J. Yi and D. Shi, “Parameter Optimization of DOCR and FCL in Microgrids Based on Grey Wolf Optimizer,” *Proceedings - 2018 53rd International Universities Power Engineering Conference, UPEC 2018*,



- pp. 1–5, 2018.
- [96] W. El-Khattam and T. S. Sidhu, “Restoration of directional overcurrent relay coordination in distributed generation systems utilizing fault current limiter,” *IEEE Transactions on Power Delivery*, vol. 23, no. 2, pp. 576–585, 2008.
- [97] W. El-Khattam and T. S. Sidhu, “Resolving the impact of distributed renewable generation on directional overcurrent relay coordination: A case study,” *IET Renewable Power Generation*, vol. 3, no. 4, pp. 415–425, 2009.
- [98] R. M. Chabanloo, H. A. Abyaneh, A. Agheli, and H. Rastegar, “Overcurrent relays coordination considering transient behaviour of fault current limiter and distributed generation in distribution power network,” *IET Generation, Transmission and Distribution*, vol. 5, no. 9, pp. 903–911, 2011.
- [99] M. Y. Shih, A. Conde, C. Angeles-Camacho, E. Fernandez, and Z. M. Leonowicz, “Mitigating the impact of distributed generation and fault current limiter on directional overcurrent relay coordination by adaptive protection scheme,” *Proceedings - 2019 IEEE International Conference on Environment and Electrical Engineering and 2019 IEEE Industrial and Commercial Power Systems Europe, IEEEIC/I and CPS Europe 2019*, no. June, 2019.
- [100] M. A. Jarrahi, M. Mohammadi, and H. Samet, “Optimal Placement and Sizing of Fault Current Limiters in Power Systems with Uncertainties,” *Proceedings - 2019 IEEE International Conference on Environment and Electrical Engineering and 2019 IEEE Industrial and Commercial Power Systems Europe, IEEEIC/I and CPS Europe 2019*, no. June, 2019.
- [101] N. Bayati, “Optimal Placement and Sizing of Fault Current Limiters in Distributed Generation Systems Using a Hybrid Genetic Algorithm,” vol. 7, no. 1, pp. 1329–1333, 2017.
- [102] D. Birla, R. P. Maheshwari, and H. O. Gupta, “A new nonlinear directional overcurrent relay coordination technique, and banes and boons of near-end faults based approach,” *IEEE Transactions on Power*

- Delivery*, vol. 21, no. 3, pp. 1176–1182, 2006.
- [103] B. Muruganantham, R. Gnanadass, and N. P. Padhy, “Challenges with renewable energy sources and storage in practical distribution systems,” *Renewable and Sustainable Energy Reviews*, vol. 73, no. November 2015, pp. 125–134, 2017.
- [104] R. Varier and N. M. Pindoriya, “A novel active anti-islanding protection scheme for grid-interactive roof-top solar PV system,” *2014 18th National Power Systems Conference, NPSC 2014*, 2015.
- [105] G. Hernandez-Gonzalez and R. Iravani, “Current injection for active islanding detection of electronically-interfaced distributed resources,” *IEEE Transactions on Power Delivery*, vol. 21, no. 3, pp. 1698–1705, 2006.
- [106] M. P. Nthontho, S. P. Chowdhury, S. Winberg, and S. Chowdhury, “Protection of domestic solar photovoltaic based microgrid,” *11th IET International Conference on Developments in Power Systems Protection (DPSP 2012)*, pp. P94–P94, 2012.
- [107] D. Solati Alkaran, M. R. Vatani, M. J. Sanjari, G. B. Gharehpetian, and M. S. Naderi, “Optimal Overcurrent Relay Coordination in Interconnected Networks by Using Fuzzy-Based GA Method,” *IEEE Transactions on Smart Grid*, vol. 3053, no. c, pp. 1–1, 2016.
- [108] M. S. Javadi, A. Esmaeel Nezhad, A. Anvari-Moghaddam, and J. M. Guerrero, “Optimal Overcurrent Relay Coordination in Presence of Inverter-based Wind Farms and Electrical Energy Storage Devices,” pp. 1-5 BT-IEEE 18th International Conference on En, 2018.
- [109] C. A. Castillo, A. Conde, and M. Y. Shih, “Improvement of non-standardized directional overcurrent relay coordination by invasive weed optimization,” *Electric Power Systems Research*, vol. 157, pp. 48–58, 2018.
- [110] Y. Damchi, M. Dolatabadi, H. R. Mashhadi, and J. Sadeh, “MILP approach for optimal coordination of directional overcurrent relays in interconnected power systems,” *Electric Power Systems Research*, vol. 158, no. March, pp. 267–274, 2018.

- [111] A. Sharma and B. K. Panigrahi, "Phase Fault Protection Scheme for Reliable Operation of Microgrids," *IEEE Transactions on Industry Applications*, vol. 54, no. 3, pp. 2646–2655, 2018.
- [112] K. P. Anagnostopoulos and G. Mamanis, "The mean-variance cardinality constrained portfolio optimization problem: An experimental evaluation of five multiobjective evolutionary algorithms," *Expert Systems with Applications*, vol. 38, no. 11, pp. 14208–14217, 2011.
- [113] R. K. Verma, B. N. Singh, and S. S. Verma, "Optimal Overcurrent Relay coordination Using GA , FFA , CSA Techniques and Comparison," 2017.
- [114] D. Jitkongchuen, P. Phaidang, and P. Pongtawevirat, "Grey Wolf optimization algorithm with invasion-based migration operation," *2016 IEEE/ACIS 15th International Conference on Computer and Information Science, ICIS 2016 - Proceedings*, pp. 1–5, 2016.
- [115] M. Pradhan, P. K. Roy, and T. Pal, "Oppositional based grey wolf optimization algorithm for economic dispatch problem of power system," *Ain Shams Engineering Journal*, vol. 9, no. 4, pp. 2015–2025, 2018.
- [116] A. Amin, S. Kamel, and M. Ebeed, "Optimal reactive power dispatch considering SSSC using Grey Wolf algorithm," *2016 18th International Middle-East Power Systems Conference, MEPCON 2016 - Proceedings*, pp. 780–785, 2017.
- [117] Z. Darvay and P. R. Rigó, "New Interior-Point Algorithm for Symmetric Optimization Based on a Positive-Asymptotic Barrier Function New Interior-Point Algorithm for Symmetric," *Numerical Functional Analysis and Optimization*, vol. 0, no. 0, pp. 1–22, 2018.
- [118] F. Katiraei, M. R. Iravani, and P. W. Lehn, "Micro-grid autonomous operation during and subsequent to islanding process," *IEEE Transactions on Power Delivery*, vol. 20, no. 1, pp. 248–257, 2005.
- [119] M. A. G. De Brito, L. P. Sampaio, G. Luigi, G. A. E Melo, and C. A. Canesin, "Comparative analysis of MPPT techniques for PV applications," *3rd International Conference on Clean Electrical Power:*

*Renewable Energy Resources Impact, ICCEP 2011*, no. May 2014, pp. 99–104, 2011.

- [120] W. H. Kersting, “Radial distribution test feeders,” in *Power Engineering Society Winter Meeting, 2001. IEEE*, 2001, vol. 2, pp. 908–912.
- [121] H. M. Sharaf, H. H. Zeineldin, D. K. Ibrahim, and E. E. D. A. El-Zahab, “A proposed coordination strategy for meshed distribution systems with DG considering user-defined characteristics of directional inverse time overcurrent relays,” *International Journal of Electrical Power and Energy Systems*, vol. 65, pp. 49–58, 2015.
- [122] A. Sharma and B. K. Panigrahi, “Phase Fault Protection Scheme for Reliable Operation of Microgrids,” *IEEE Transactions on Industry Applications*, vol. 54, no. 3, pp. 2646–2655, 2018.
- [123] C. Li, Y. Liu, A. Zhou, L. Kang, and H. Wang, “A Fast Particle Swarm Optimization Algorithm with Cauchy Mutation and Natural Selection Strategy.”
- [124] M. S. Sachdev and C. S. N. Ow, “An on -line relay coordination algorithm for adaptive protection using linear programming technique,” vol. 11, no. 1, pp. 165–173, 1996.
- [125] T. Zheng, S. Nikolovski, Y. Ngalo, and L. De Marco, “Overcurrent Protection Assessment with High PV Penetration in a Distribution Network,” 2018.
- [126] A. Shrivastava, D. K. Saini, and M. Pandit, “Peer Review of renewable energy-based adaptive protection(s) & relay coordination optimization techniques,” *Recent Advances in Electrical & Electronic Engineering (Formerly Recent Patents on Electrical & Electronic Engineering)*, vol. 13, Apr. 2020.
- [127] K. Sarwagya, P. K. Nayak, and S. Ranjan, “Optimal coordination of directional overcurrent relays in complex distribution networks using sine cosine algorithm,” *Electric Power Systems Research*, vol. 187, no. November 2019, p. 106435, 2020.
- [128] A. Heidari, V. G. Agelidis, H. Zayandehroodi, and M. Hasheminamin,

- “Prevention of overcurrent relays miscoordination in distribution system due to high penetration of distributed generation,” *Proceedings of 2013 International Conference on Renewable Energy Research and Applications, ICRERA 2013*, no. October, pp. 342–346, 2013.
- [129] A. Abbasi, H. K. Karegar, and T. S. Aghdam, “Adaptive protection coordination with setting groups allocation,” *International Journal of Renewable Energy Research*, vol. 9, no. 2, pp. 795–803, 2019.
- [130] S. A. Hosseini, S. H. H. Sadeghi, A. Askarian-Abyaneh, S. H. H. Sadeghi, and A. Nasiri, “Optimal placement and sizing of distributed generation sources considering network parameters and protection issues,” *3rd International Conference on Renewable Energy Research and Applications, ICRERA 2014*, pp. 922–926, 2014.
- [131] H. G. Pinilla, A. J. Aristizábal, and C. A. Forero, “Modeling of Distributed Generators in 13 Nodes IEEE Test Feeder,” *Periodicals of Engineering and Natural Sciences*, vol. 4, no. 2, 2016.
- [132] T. Ramana, V. Ganesh, and S. Sivanagaraju, “Simple and fast load flow solution for electrical power distribution systems,” *International Journal on Electrical Engineering and Informatics*, vol. 5, no. 3, pp. 245–255, 2013.
- [133] S. M. Moghaddas-Tafreshi and E. Mashhour, “Distributed generation modeling for power flow studies and a three-phase unbalanced power flow solution for radial distribution systems considering distributed generation,” *Electric Power Systems Research*, vol. 79, no. 4, pp. 680–686, Apr. 2009.
- [134] I. Song, W. Jung, C. Chu, S. Cho, and H. Kang, “General and Simple Decision Method for DG Penetration,” no. Ldc, pp. 4786–4798, 2013.
- [135] H. Moussa, A. Shahin, J. P. Martin, B. Nahid-Mobarakeh, S. Pierfederici, and N. Moubayed, “Harmonic Power Sharing with Voltage Distortion Compensation of Droop Controlled Islanded Microgrids,” *IEEE Transactions on Smart Grid*, vol. 9, no. 5, pp. 5335–5347, 2018.
- [136] P. Kanjiya, V. Khadkikar, and H. H. Zeineldin, “Optimal control of shunt active power filter to meet IEEE Std. 519 current harmonic constraints

- under nonideal supply condition,” *IEEE Transactions on Industrial Electronics*, vol. 62, no. 2, pp. 724–734, 2015.
- [137] A. Kalair, N. Abas, A. R. Kalair, Z. Saleem, and N. Khan, “Review of harmonic analysis, modeling and mitigation techniques,” *Renewable and Sustainable Energy Reviews*, vol. 78, no. February, pp. 1152–1187, 2017.
- [138] M. Singh, B. K. Panigrahi, and A. R. Abhyankar, “Optimal coordination of directional over-current relays using Teaching Learning-Based Optimization (TLBO) algorithm,” *International Journal of Electrical Power and Energy Systems*, vol. 50, no. 1, pp. 33–41, 2013.
- [139] S. P. George and S. Ashok, “Forecast-based overcurrent relay coordination in wind farms,” *International Journal of Electrical Power and Energy Systems*, vol. 118, no. September 2019, p. 105834, 2020.
- [140] M. Farzinfar, M. Jazaeri, and F. Razavi, “A new approach for optimal coordination of distance and directional over-current relays using multiple embedded crossover PSO,” *International Journal of Electrical Power and Energy Systems*, vol. 61, pp. 620–628, 2014.
- [141] R. Corrêa, G. Cardoso, O. C. B. D. Araújo, and L. Mariotto, “Online coordination of directional overcurrent relays using binary integer programming,” *Electric Power Systems Research*, vol. 127, pp. 118–125, 2015.
- [142] M. Y. Shih, A. Conde Enríquez, T. Y. Hsiao, and L. M. Torres Treviño, “Enhanced differential evolution algorithm for coordination of directional overcurrent relays,” *Electric Power Systems Research*, vol. 143, pp. 365–375, 2017.
- [143] M. N. Alam, B. Das, and V. Pant, “An interior point method based protection coordination scheme for directional overcurrent relays in meshed networks,” *International Journal of Electrical Power and Energy Systems*, vol. 81, pp. 153–164, Oct. 2016.
- [144] S. Nie *et al.*, “Analysis of the impact of DG on distribution network reconfiguration using OpenDSS,” in *2012 IEEE Innovative Smart Grid Technologies - Asia, ISGT Asia 2012*, 2012, pp. 1–5.

## LIST OF PUBLICATIONS

- 1) A. Shrivastava, D. K. Saini, and M. Pandit, “Relay co-ordination optimization for integrated solar photo-voltaic power distribution grid,” Cogent Engineering, vol. 6, no. 1, Apr. 2019.
- 2) A. Shrivastava, D. K. Saini, and M. Pandit, “Peer Review of renewable energy-based adaptive protection(s) & relay coordination optimization techniques,” Recent Advances in Electrical & Electronic Engineering (Formerly Recent Patents on Electrical & Electronic Engineering), vol. 13, Apr. 2020.
- 3) A. Shrivastava, D. K. Saini, and M. Pandit , “Distribution grid parameter variation due to Solar PV power integration in distribution grid, International Journal of Renewable Energy Research (IJRER), 10(3), Sep 2020.
- 4) M. Pandit, A. Shrivastava, D. K. Saini, “Relay coordination optimization for solar PV integrated Grid using the Water cycle optimization algorithm” Book chapter accepted in entitled book “Applied Soft Computing and Embedded System Applications in Solar Energy” (CRC Press) 2020.

## Author CV

Name: Aayush Shrivastava      Father's Name: A K Shrivastava

Address: 137 Saraswati Nagar, Gwalior, Madhya Pradesh, India,  
474011

Mobile No. 9806944007

Email: mr.aayushshrivastava@gmail.com

Aadhaar No. 942543058296



Academic Qualifications (Please mention in chronological order starting  
from class X)

Qualification	Year	College/ Board/ University	%Marks/CGP A	Division
M. E	2014	Madhav Institute of Technology & Science, Gwalior	8.5 (CGPA)	First
B. E	2012	Laxmi Narayan Institute of Technology	72%	First
12 <sup>th</sup>	2008	Miss Hill School (M P Board)	62%	Fisrt
10 <sup>th</sup>	2006	Miss Hill School (M P Board)	60%	First

### Experience

Position Held	Name of Organization	From (DD/MM/Y Y)	To (DD/MM/YY)	Total Experience (Y-M)
<i>Doctoral Research fellow</i>	<i>University of petroleum &amp; energy studies, Dehradun</i>	<i>30/09/2015</i>	<i>30/07/2020</i>	<i>4-10</i>
<i>Assistant professor</i>	<i>Global institute of technology</i>	<i>15/7/2015</i>	<i>15/9/2015</i>	<i>0-3</i>



## PLAGIARISM CERTIFICATE

- 1) We **Devender Kumar Saini** , **Manjaree Pandit** certify that the Thesis titled Protection Schemes & Optimal Relay Co-ordination for RE Integrated Power Distribution Grid submitted by Scholar Mr. Aayush Shrivastava having SAP ID 500049145 has been run through a Plagiarism Check Software and the Plagiarism Percentage is reported to be 9 %.
- 2) Plagiarism Report generated by the Plagiarism Software is attached .

**Signature of the Internal Guide**

**Signature of External Guide/ Co Guide**

**Signature of the Scholar**

**CORPORATE OFFICE:** 210, 2<sup>nd</sup> Floor,  
Okhla Industrial Estate, Phase III,  
New Delhi - 110 020, India.  
T: +91 11 41730151/53, 46022691/5  
F: +91 11 41730154













**ENERGY ACRES:** Bidholi Via  
Prem Nagar, Dehradun - 248 007  
(Uttarakhand), India.  
T: +91 135 2770137, 2776053/54/91, 2776201  
F: +91 135 2776090/95

**KNOWLEDGE ACRES:** Kandoli Via  
Prem Nagar, Dehradun - 248 007  
(Uttarakhand), India.  
T: +91 8171979021/2/3, 7060111775

## Document Information

<b>Analyzed document</b>	CHAPTERs.pdf (D80483310)
<b>Submitted</b>	10/2/2020 11:11:00 AM
<b>Submitted by</b>	Debajyoti Bose
<b>Submitter email</b>	debajyoti@shooliniuniversity.com
<b>Similarity</b>	9%
<b>Analysis address</b>	debajyoti.subam@analysis.urkund.com

## Sources included in the report

<b>W</b>	URL: <a href="https://link.springer.com/article/10.1186/s41601-017-0061-1">https://link.springer.com/article/10.1186/s41601-017-0061-1</a> Fetched: 10/5/2019 7:54:06 AM	 <b>12</b>
<b>W</b>	URL: <a href="https://www.researchgate.net/publication/256970663_Optimal_coordination_of_directi...">https://www.researchgate.net/publication/256970663_Optimal_coordination_of_directi ...</a> Fetched: 12/20/2019 5:33:25 PM	 <b>3</b>
<b>W</b>	URL: <a href="https://docplayer.net/155408664-Nature-inspired-whale-optimization-algorithm-for-o...">https://docplayer.net/155408664-Nature-inspired-whale-optimization-algorithm-for-o ...</a> Fetched: 12/20/2019 2:44:59 PM	 <b>3</b>
<b>J</b>	<b>Hybrid Whale Optimization Algorithm and Grey Wolf Optimizer Algorithm for Optimal Coordination of Direction Overcurrent Relays</b> URL: 06ab08b3-da89-4c1b-9317-b2962fdb69d3 Fetched: 12/11/2019 4:57:25 PM	 <b>7</b>
<b>SA</b>	<b>Report of sagar kathad for DP2.pdf</b> Document Report of sagar kathad for DP2.pdf (D75340994)	 <b>1</b>
<b>SA</b>	<b>6PAPER_ELSEVIER_COMPUTATIONAL SCIENCE_DOCR_SCA_SARWAGYA_12.11.2019.docx</b> Document 6PAPER_ELSEVIER_COMPUTATIONAL SCIENCE_DOCR_SCA_SARWAGYA_12.11.2019.docx (D58741704)	 <b>13</b>
<b>SA</b>	<b>Hannah-thesis-ver1.docx</b> Document Hannah-thesis-ver1.docx (D61538116)	 <b>6</b>
<b>SA</b>	<b>1423379721-TS.pdf</b> Document 1423379721-TS.pdf (D61729142)	 <b>3</b>
<b>W</b>	URL: <a href="https://www.researchgate.net/publication/3275836_A_Modified_Particle_Swarm_Optimiz...">https://www.researchgate.net/publication/3275836_A_Modified_Particle_Swarm_Optimiz ...</a> Fetched: 11/12/2019 5:38:04 PM	 <b>6</b>
<b>W</b>	URL: <a href="http://www.papers.itc.pw.edu.pl/index.php/JPT/article/view/1278">http://www.papers.itc.pw.edu.pl/index.php/JPT/article/view/1278</a> . Fetched: 10/2/2020 11:15:00 AM	 <b>1</b>
<b>SA</b>	<b>Hannah Lalitha - 1 - 1423379721.pdf</b> Document Hannah Lalitha - 1 - 1423379721.pdf (D54808091)	 <b>2</b>
<b>SA</b>	<b>Chapter-2_Literature Review.docx</b> Document Chapter-2_Literature Review.docx (D45071705)	 <b>9</b>